CONTACT ANALYSIS FOR MODIFIED SPUR GEARS

A THESIS SUBMITTED TO
THE GRADUATE SCHOOL OF NATURAL AND APPLIED SCIENCES
OF
MIDDLE EAST TECHNICAL UNIVERSITY

BY

BURAK OCAK

IN PARTIAL FULFILLMENT OF THE REQUIREMENTS
FOR
THE DEGREE OF MASTER OF SCIENCE
IN
ENGINEERING SCIENCES

AUGUST 2020

Approval of the thesis:

CONTACT ANALYSIS FOR MODIFIED SPUR GEARS

submitted by **BURAK OCAK** in partial fulfillment of the requirements for the degree of **Master of Science in Engineering Sciences, Middle East Technical University** by,

Prof. Dr. Halil Kalıpçılar
Dean, Graduate School of **Natural and Applied Sciences**

Prof. Dr. Murat Dicleli
Head of Department, **Engineering Sciences**

Prof. Dr. Zafer Evis
Supervisor, **Engineering Sciences, METU**

Examining Committee Members:

Prof. Dr. Mehmet Kadri Aydınol
Metallurgical and Materials Engineering, METU

Prof. Dr. Zafer Evis
Engineering Sciences, METU

Prof. Dr. Fahrettin Öztürk
Mechanical Engineering, Ankara Yıldırım Beyazıt Uni.

Prof. Dr. Sadettin Orhan
Mechanical Engineering, Ankara Yıldırım Beyazıt Uni.

Prof. Dr. Ömer Keleş
Mechanical Engineering, Gazi University

Date: 25.08.2020

I hereby declare that all information in this document has been obtained and presented in accordance with academic rules and ethical conduct. I also declare that, as required by these rules and conduct, I have fully cited and referenced all material and results that are not original to this work.

Name, Surname: Burak Ocak

Signature :

ABSTRACT

CONTACT ANALYSIS FOR MODIFIED SPUR GEARS

Ocak, Burak
M.S., Department of Engineering Sciences
Supervisor: Prof. Dr. Zafer Evis

August 2020, 112 pages

Gears are subjected to high speed and high power especially in critical applications. It is known that these high power gears are mostly subjected to main failure modes due to contact stress, bending stress, and fatigue. In this thesis, a new analytical model is developed for contact stress in selected gear pairs. The new analytical method is built by combining the Weber Banaschek Method with the Sainsot Method for mesh stiffness and gear foundation stiffness, respectively. Results obtained from the newly developed method are compared to the results obtained from available transmission tools (MASTA and KISSsoft).

Combination of these two analytical methods yielded accurate results. It is also seen that the analytical solutions are more close to KISSsoft results than the MASTA solutions. The contact stress calculations according to the new method resulted close to ISO standard and compared to the FEM module of MASTA.

The results obtained from the new analytical method are close to experimental results by 96%. The MASTA Programme tends to give higher results on contact pressure compared to KISSsoft solutions. Finally, calculations according to AGMA 2001-C95 standard yielded in lower safety factors compared to the ISO 6336 standard.

Keywords: Gear Analysis, Weber-Banaschek Formulation, Mesh Stiffness, Gear Materials, Profile Modifications, Hertzian Contact Theory.

ÖZ

MODIFIKASYON YAPILMIŞ DÜZ DİŞLİLER İÇİN KONTAK ANALİZİ

Ocak, Burak
Yüksek Lisans, Mühendislik Bilimleri Bölümü
Tez Danışmanı: Prof. Dr. Zafer Evis

Ağustos 2020, 112 sayfa

Dişliler özellikle kritik uygulamalarda yüksek hız ve yüksek güce maruz kalırlar. Bu yüksek güç dişlilerinin kontak gerilmesi, eğilme gerilmesi ve yorulma kaynaklı temel arıza durumlarına maruz kaldığı bilinmektedir. Bu tezde, seçilen dişli çiftlerinde kontak gerilmesi için yeni bir analitik metot geliştirilmiştir. Yeni analitik metot Weber Banaschek ve Sainsot metotları birleştirilerek sırasıyla dişli rijitliği ve gövde rijitliği için oluşturulmuştur. Yeni geliştirilen metottan elde edilen sonuçlar transmisyon programları (MASTA ve KISSsoft) ile karşılaştırılmıştır.

İki analitik metodun birleştirilmesi, kesin sonuçların elde edildiğini göstermiştir. Analitik çözümlerin MASTA çözümlerinden ziyade, KISSsoft sonuçlarına daha yakın olduğu görülmüştür. Yeni metoda göre yapılan kontak gerilme hesapları ISO standardına yakın bulunmuş ve MASTA'nın sonlu elemanlar modülü ile karşılaştırılmıştır.

Yeni analitik metottan elde edilen sonuçlar deneysel sonuçlara %96 yakınlıktadır. MASTA programı kontak basıncında KISSsoft çözümlerine göre yüksek sonuç verme eğilimindedir. Son olarak, AGMA 2001-C95 standardına göre yapılan hesaplamalar ISO 6336 standardına göre daha düşük güvenlik katsayısı vermiştir.

Anahtar Kelimeler: Dişli Analizi, Weber-Banaschek Formülasyonu, Kontak Rijitliği, Dişli Malzemeleri, Profil Modifikasyonları, Hertzian Kontak Teorisi

To My Family

ACKNOWLEDGEMENTS

I would like to thank my supervisor Prof. Dr. Zafer Evis for his supervision, help, and guidance from beginning to the end of this dissertation. Without his endless support and trust through my master's years at METU, this thesis would not have been possible.

I want to thank the Presidency of Defence Industries, Turkey for funding they have provided for the SAYP project (Project Number: DDDKA1) in cooperation with Turkish Aerospace.

My sincere thanks go to my fellow teammates at Turkish Aerospace for their support and encouragement. Special thanks to Prof. Dr. Fahrettin Ozturk at Turkish Aerospace for his suggestions, editing, and help.

My deepest appreciation goes to my family, Mehmet Ocak, Hüma Ocak, and Banu Ocak for their endless lifelong support.

TABLE OF CONTENTS

LIST OF TABLES

TABLES

LIST OF FIGURES

FIGURES

ABBREVIATIONS

ABBREVIATIONS

AGMA	American Gear Manufacturers Association
ISO	International Organization for Standardization
FEM	Finite element method
SAP	Start of active profile
EAP	End of active profile
HPSTC	Highest point of single tooth contact
LPSTC	Lowest point of single tooth contact
RPM	Revolution per unit
TVMS	Time variable mesh stiffness
r_b	Base radius
P_B	Base pitch
r_{any}	Any radius on contact line
ϕ_1	Roll angle from the tooth center to the tangent of the base circle
ϕ_2	Roll angle from the start of involute to the tooth center
$d_{i1,2}$	Inner diameter of pinion and wheel
S_f	Length of arc in the tooth root
$d_{b1,2}$	Base diameter of pinion and wheel

u_f	Tooth height at the line of action
$d_{f1,2}$	Root diameter of pinion and Wheel
$d_{b1,2}$	Base diameter of pinion and wheel
F	Total mesh force
E	Elastic modulus
ν	Poisson’s ratio

CHAPTER 1

INTRODUCTION

Gears are important machine elements of powertrain systems widely used in different industries. Gears are mostly used to transmit power from one side of the system to another side. These elements range from small to large sizes according to their application areas. For example, Gears in medical applications science are small, whereas gears used in marine applications tend to be larger.

For aviation gearboxes, it could be said that gears are subjected to high speed and high power. Therefore, the design of aviation gearboxes is highly challenging due to higher loads at high speeds. High power applications at high speeds yield in contact problems during gear meshes through powertrain.

Optimization of gear contact stress and transmission error is crucial in such high power applications. To accomplish this goal, micro modifications are applied efficiently on gear geometries.

In that scope, stiffness calculations should be carried out to calculate contact stress and transmission error. However, stiffness calculation of gear meshes by the finite element method (FEM) is not very accurate. Therefore, an analytical solution approach to find mesh stiffness was taken into account in this thesis. The results obtained from the FEM and analytical method were compared.

Calculating the contact pressure based on computed stiffness of the gears were also part of this thesis. Micro modification effects on transmission error and contact pressure were also investigated. Moreover, material selections for the gears were analyzed for selected cases.

Calculation of contact pressure values for gears are subjected to change for different standards. Different transmission design tools also yield different results for the same powertrain. Therefore, solutions from the analytical method and these transmission tools were also compared.

CHAPTER 2

LITERATURE REVIEW

Gears are the most critical elements in mechanical transmission systems. The application of the gears takes place in different areas such as aerospace, automotive, buildings, medicine, etc. Choosing the correct type of gear is highly dependent on the application in which different power and speed parameters are available. In literature, for gear contact calculations, different studies were carried out as shown in Table 2.1.

Table 2.1 *Literature Review on Gear Contact.*

Study on Gear Contact	Details	References
Mesh Stiffness	FEM, analytical methods, FEM and analytical combined methods and experimental methods are used in these studies.	Wu et al., 2012; Li, 2007a; Ma et al., 2013; Ma et al., 2015; Li et al., 2004; Wang et al., 2018; Wan et al., 2018; Liang et al., 2014; Chen and Shao, 2011; Ma et al., 2014; Fernandez del Rincon et al., 2013; Chang et al., 2015; Pedersen and Jørgensen, 2014; Pandya and Parey, 2013; Raghuwanshi and Parey, 2018
Contact Pressure	FEM and analytical methods are used in these studies.	Hwang et al., 2013; Mehta et al., 2018; Li, 2007b; Jyothirmai et al., 2014; Patil et al., 2014a; Qin and Guan, 2014; Lin et al., 2007; Perez and Aznar, 2017; Patil et al., 2014b; Sirichai et al., 1997; Shinde et al., 2009; Perez et al., 2011; Mao, 2007
Transmission Error	Static and dynamic transmission errors and effects of micro geometry modifications are studied.	Shweiki et al., 2019; Bruyere et al., 2015; Bozca, 2018; Ma et al., 2016; Fernandez del Rincon et al., 2013, Chang et al., 2015, Pedersen and Jørgensen, 2014 Sanchez, et al., 2019
Material Effects	Alloy effects are studied in materials.	Tobie et al., 2017

2.1 Gear Types and Gears in Aviation

Spur gears are widely used in high speed and high power aviation gearboxes especially in fixed-wing aircraft. Evolvent profile is typically used to create proper gear geometry. Aerospace gears are mainly subjected to high contact loading as shown in Figure 2.1. Therefore, main fatigue failure modes occur as pitting and micro pitting in case of high contact loadings (Figure 2.2). Therefore, in this research, contact loadings are focused since those are more critical for high speed and high power applications in aviation gearboxes.

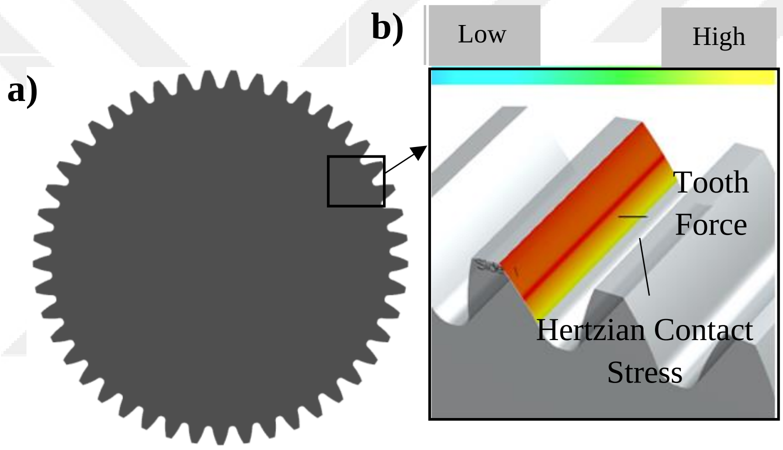

Figure 2.1 *Contact Stress on Gear Flank:* ***a)*** *Gear;* ***b)*** *Hertzian Contact Stress.*

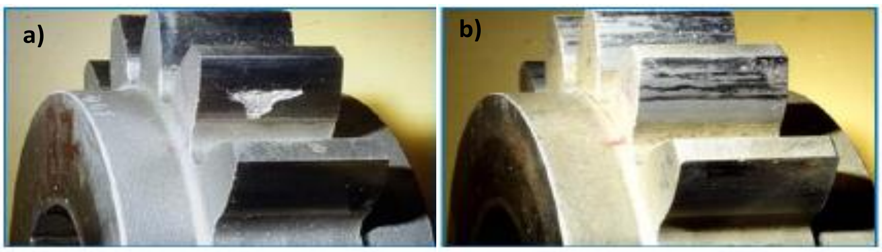

Figure 2.2 *Common Gear Failure Modes in Aviation:* ***a)*** *Pitting;* ***b)*** *Micro Pitting (Tobie et al., 2017).*

2.2 Gear Materials

The strength of gears is also investigated based on different gear materials in this thesis. The major parameter affecting the strength is different alloying elements in gear materials. In a study, effect of different elements in alloys was investigated for gears (Table 2.2). It is seen that Mo containing alloys in gears have a more significant effect on gear strength than Ni containing alloy gears (Tobie et al., 2017).

Table 2.2 *Gear Materials and their Compositions Modified from (Tobie et al., 2017).*

Steel	Standard	Alloy Weight %									
		C	**Si**	**Mn**	**P**	**S**	**Cr**	**Mo**	**Ni**	**Fe**	**Region**
20MnCr5	EN 10084 (1.7147)	0.22	0.40	1.4	0.035	0.035	1.3	-	-	93.01	West Europe
18CrNiMo7-6	EN 10084 (1.6587)	0.21	0.40	0.90	0.025	0.035	1.8	0.35	1.7	94.58	
15CrNi6	EN 10084 (1.5919)	0.19	0.40	0.60	0.035	0.035	1.7	-	1.7	95.34	France, Germany
17NiCrMo6-5	EN 10084 (1.6566)	0.20	0.40	0.90	0.025	0.035	1.1	0.25	1.5	95.59	Italy, France
SAE 8620	SAE J1249	0.23	0.35	0.90	0.030	0.040	0.60	0.25	0.70	96.9	North America
SAE 9310	SAE J1249	0.13	0.35	0.65	0.025	0.040	1.4	0.15	3.5	93.75	
20CrMnTi	GB T 3077-1999	0.23	0.37	1.1	0.035	0.035	1.3	0.15	0.30	96.48	China
20CrMnMo	GB T 3077-1999	0.23	0.37	1.2	0.025	0.035	1.4	0.30	0.30	96.14	
SCM420	JIS	0.23	0.35	0.85	0.030	0.030	1.2	0.30	-	97.01	Japan

In Table 2.2, it is seen that amounts of C, P, S do not differ too much for different gear materials. However, Mo and Ni contents vary for different materials, and this results in different strength values (Table 2.3). It is seen that higher amount of Ni element results in dramatically higher strength just as SAE9310 material that is commonly used in aerospace gears. Effects of elements in gear materials are stated in Table 2.3.

Table 2.3 *Elements in Gears and their Effects.*

Element	Effects
Carbon (C)	Increase tensile strength, hardness, abrasion, and wear resistance.
	Decrease roughness and ductility.
Chromium (Cr)	Increase tensile strength, hardness, hardenability, toughness, resistance to wear and abrasion, resistance to corrosion, and scaling at elevated temperatures.
Manganese (Mn)	Increase tensile strength, hardenability, and resistant to wear.
	Enable steel to increase strength at a slower quench rate.
Phosphorus (P)	Increase strength and hardness and improves machinability.
	Also, increase brittleness to steel.
Sulfur (S)	Increase machinability.
	Decreases weldability, impact toughness, and ductility.
Silicon (Si)	Increase tensile and yield strength, hardness, forgeability, and magnetic permeability.
Nickel (Ni)	Increase strength and hardness without a decrease in ductility and toughness.
	Increase resistance to corrosion and scaling at elevated temperatures when introduced in suitable quantities in high chromium (stainless) steels.
Molybdenum (Mo)	Increase strength, hardness, hardenability, and toughness, as well as creep resistance and strength at elevated temperatures.
	Also, increase machinability and resistance to corrosion.

2.3 Mesh Stiffness Foundation

There are different studies present in literature to determine gear mesh stiffness. These different types of studies could be divided into 4 main subdivisions:

- Finite Element Methods (Wu et al., 2012; Li, 2007b; Ma et al., 2013; Ma et al., 2015; Li et al., 2004)
- Analytical Methods (Wang et al., 2018; Wan et al., 2018; Liang et al., 2014; Chen and Shao, 2011; Ma et al., 2014)
- Analytical and Finite Element Methods (Fernandez del Rincon et al., 2013; Chang et al., 2015; Pedersen and Jørgensen, 2014)
- Experimental Methods (Pandya and Parey, 2013)

To find mesh stiffness analytically, there are important parameters that need to be considered during calculations. In a study by Kim et al., 2020, macro geometry of helical gears is studied for optimization based on weight, efficiency, and noise. Since gear noise requires complex and time-consuming calculations, they reduce static transmission error by microgeometry modifications in their study. Also in a study by Kim et al., 2020, bending (k_b), shear (k_s), axial (k_a), gear foundation (k_f) and Hertzian contact stiffness k_h parameters are covered to find out mesh stiffness.

In a study by Wang and Zhang, 2017, helical gears are analyzed to find mesh stiffness and contact pressure values based on the slice approach as shown in Figure 2.3 (a). Stiffness values are found analytically by considering geometry in Figure 2.3 (b) and derived values are used to find contact stress values.

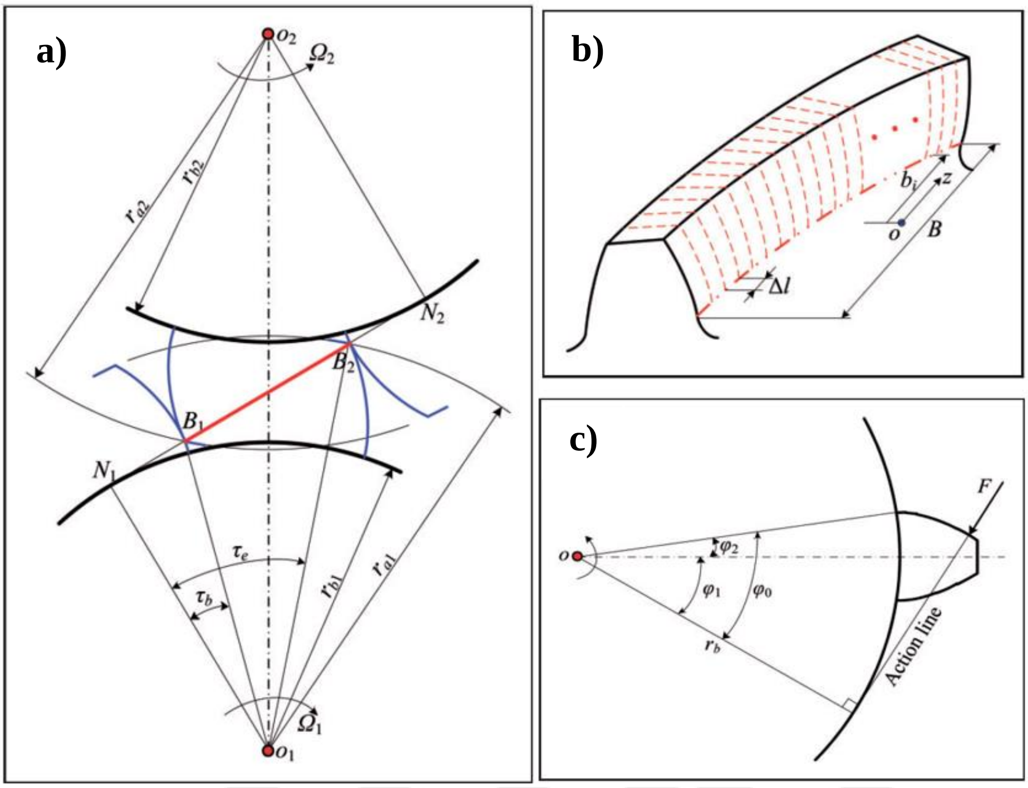

Figure 2.3 a) *Gear Model -Sliced Approach;* ***b)*** *Gear Stiffness Geometry;* ***c)*** *Line of Action (Wang and Zhang, 2017).*

In Figure 2.3 (c), it is seen that for the gears in mesh pressure angle between the gears shall be between τ_e and τ_b. Those values could be written as in Equations 2.1 – 2.2.

$$\tau_b = \text{arc tan } (|N_1 B_1| / |r_{b1}|) \tag{2.1}$$

$$\tau_e = \text{arc tan } (|N_1 B_1| + |B_1 B_2| / |r_{b1}|) \tag{2.2}$$

2.4 Contact Stress Analysis

There are many studies present to calculate contact stress for gears in literature. However, FEM is commonly used in the studies of contact stress (Hwang et al., 2013; Mehta et al., 2018; Li, 2007b; Jyothirmai et al., 2014; Patil et al., 2014b; Qin and Guan, 2014; Lin et al., 2007; Perez and Aznar, 2017; Sirichai et al., 1997; Shinde et al., 2009; Perez et al., 2011; Mao, 2007).

Three different cases were investigated to determine the effects on contact stress and transmission error for helical gears (Shehata et al., 2019). These cases include:

- Micro geometry modifications
- Misalignment
- Micro geometry modifications and misalignment

For these cases above, contact stress, root stress, and transmission error are determined. Results are compared between LDP, KISSsoft, and ABAQUS. In this study, it is found that gear tools give higher stress values than FEM software. It is also seen that microgeometry modifications and misalignment of the gears have crucial effects on transmission error. In the case of misalignment, the peak to peak transmission error is higher than the other cases.

However, proper micro modifications on gear geometry could yield a decrease in transmission error values. Also, results obtained from only microgeometry modifications and micro modifications with misalignment are compared. It is seen that transmission error values for these two cases are very close to each other. Additionally, KISSsoft gives higher contact stress results than LDP and ABAQUS. An example of gear contact analysis is given in Figure 2.4. It was seen that the analytical approach gives more accurate results than FEM to determine gear contact stress. Therefore, the analytical approach is used based on gear geometry calculations (Dudley, 1984; Litvin and Fuentes, 2004) in this thesis.

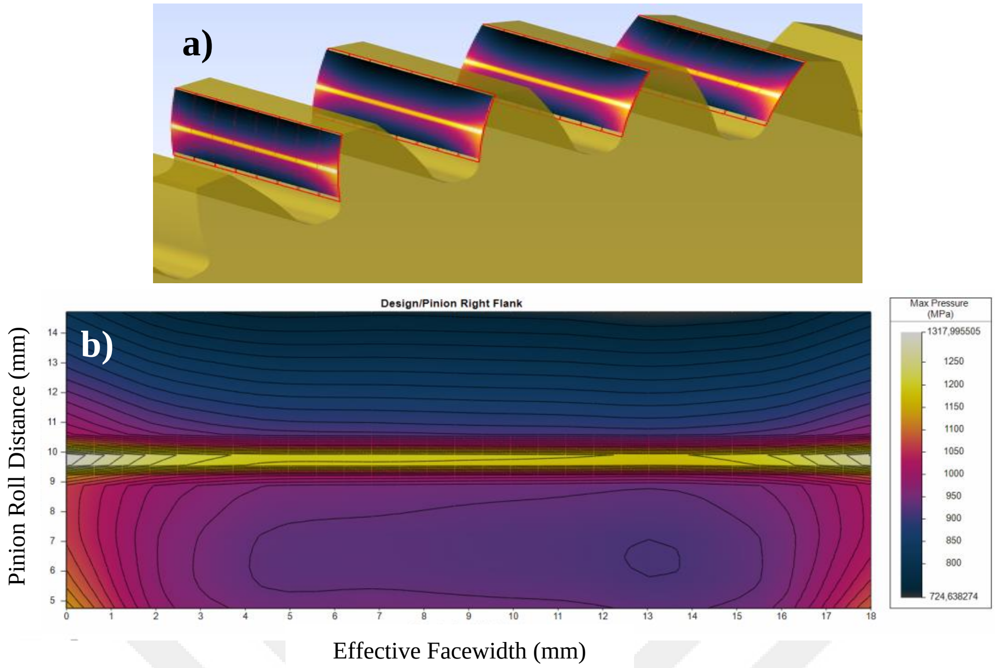

Figure 2.4 *Gear Contact Analysis:* ***a)*** *Gear Contact Pressure;* ***b)*** *Flank Contact Pressure.*

2.5 Gear Profile Modification Effects

Micro modifications are carried out on gear profile to optimize tooth contact stress and transmission error. Micro modifications could be divided into two main subdivisions as tip relief and crowning. There are many studies on gear crowning present in literature (Guan et al., 2018; Ye and Tsai, 2016; Bruyere et al., 2019; Guan et al., 2019; Jia and Fang, 2019; Seol and Kim, 1998; Tran et al. 2014, Wu and Tran, 2016).

However, tip relief modifications are more common in aviation gearboxes. Tip relief usually starts from the Highest Point of Single Tooth Contact (HPSTC) and continues to the tip diameter of the gear. This modification could be either linear or parabolic. In the case of tip relief modification to driver gear, the tooth contact point is delayed on contact line hence transmission error is tried to be minimized (Sánchez et al., 2019).

Moreover, there are many studies to investigate tip relief modification effects on gear contact stress by using an analytical approach. Profile modifications are also a crucial part of structural optimization of the gears. In a study, the analytical method is proposed to calculate non-Hertzian contact pressures for the gears with tip relief by Wen et al., 2019. The results of the study are based on the profile modification effects on different loading applications. Comparison is also made between the results obtained from the analytical approach and finite element method. Results showed that tip relief modifications have a crucial role to define the location of maximum contact pressure on the gear profile (Wen et al., 2019).

2.5.1 Transmission Error

To minimize static transmission error (Figure 2.5), it is important to identify the amount of tip relief modification on gear geometry. There are many studies to minimize static transmission error in powertrain systems. In those studies, FEM, analytical methods, and finite-analytical methods are carried out to minimize transmission errors (Shweiki et al., 2019; Bruyere et al., 2015; Bozca, 2018). In a study by Ma et al., 2016, the effect of flexibility of the gears on gear mesh stiffness is investigated. Additionally, different torque, size, and profile modifications are used. Results obtained from the analytical method, FEM (Figure 2.6), and finite element-analytical combined method (Fernandez del Rincon et al., 2013, Chang et al., 2015, Pedersen and Jørgensen, 2014) are all compared.

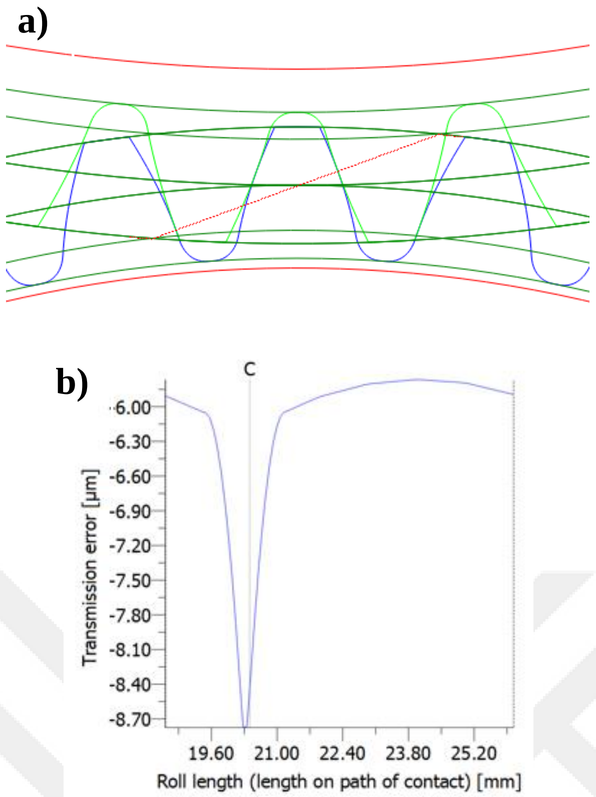

Figure 2.5 *Transmission Error Sample:* ***a)*** *Gear Mesh 2D;* ***b)*** *Transmission Error.*

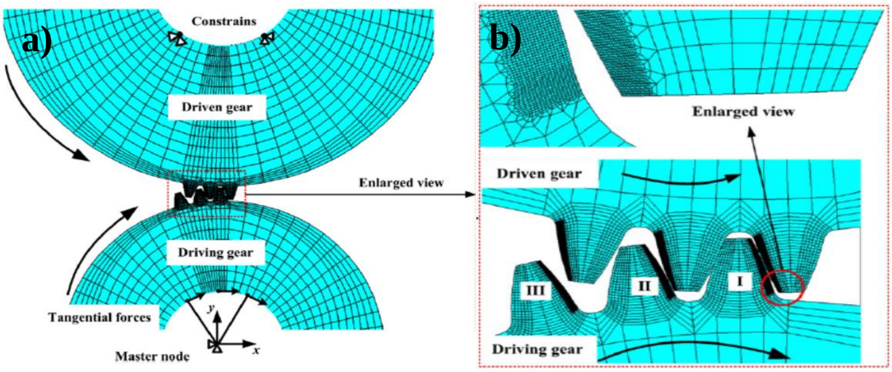

Figure 2.6 *Finite Element Models:* ***a)*** *Gear Pair;* ***b)*** *Contact Area (Ma et al., 2016).*

In this study, non-linear Hertzian mesh stiffness, fillet foundation stiffness, and profile modification effects are also investigated. Moreover, modifying factors are used effectively for analytical calculations. Modifying Factors λ (Figure 2.7) for fillet foundation are obtained by using the finite element method.

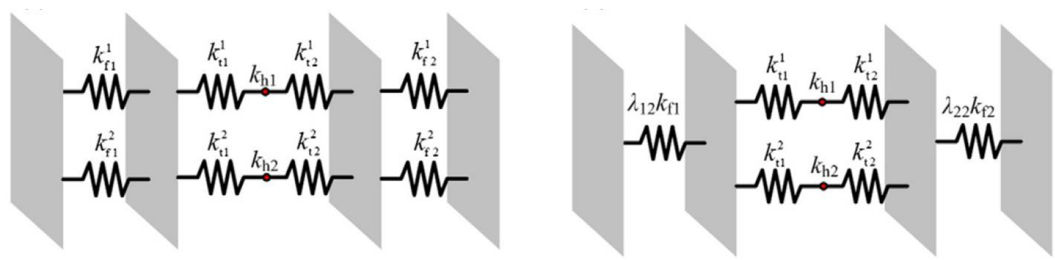

Figure 2.7 *Gear Mesh Stiffness Modifying Factors λ (Ma et al., 2016).*

Results obtained for gear mesh stiffness values are compared based on the approaches: analytical solution and analytical-finite element combined solution. In a study by Ma et al., 2016, it is observed that the purposed analytical model gives accurate results by comparing FEM solutions.

In another study, by Sanchez et al., 2019, profile modification effects on load distribution and transmission error are investigated for different types of modifications. In this study, also analytical approach is proposed to find out mesh stiffness values to investigate static transmission errors. Additionally, in a study by Sheweiki, 2019 lightweight gears are analyzed to investigate transmission errors and deformation quantities by using finite element and analytical methods. By using this method, high accuracy in results is obtained within the relatively less time.

2.6 Aim of The Thesis

Gears are subjected to high speed and high power in aerospace applications. Accurate calculation methods are needed to determine mesh stiffness and contact pressure for such high-power gears. The purpose of the thesis is to propose a newly developed method to calculate gear mesh stiffness. The method is a combination of two different methods used in mesh stiffness calculations, namely Weber-Banaschek and Sainsot’s Methods. By combining these two methods effects of gear foundation is considered based on experimental data studied in Sainsot’s Method. The results obtained from the newly developped method are compared with transmission tools (MASTA and KISSsoft). The differences between the results obtained from well-known transmission tools (MASTA and KISSsoft) are also discussed for the first time in literature.

First, gear geometries were created by using evolvent profile approach and mesh stiffness values were determined analytically. Afterwards, contact pressure values were obtained by using analytical approach. Profile modifications were added to minimize transmission errors for related gear pairs. Results of the analytical model were compared with KISSsoft and MASTA (FEM Based) which are common transmission design tools. Effects of the material selection for related gear pairs were also investigated and results of the calculations according to ISO 6336 and AGMA 2001- C95 standards were compared in this thesis.

CHAPTER 3

CONTACT ANALYSIS FOR MODIFIED SPUR GEARS

3.1 Proposed Analytical Method for Mesh Stiffness

In order to calculate mesh stiffness for gear pairs, there are five different types of mesh stiffness considered in calculations which are:

- Bending Stifness (by Weber-Banaschek Method)
- Shear Stiffness (by Weber-Banaschek Method)
- Compression Stifness (by Weber-Banaschek Method)
- Hertzian Stiffness (by Weber-Banaschek Method)
- Gear body Stiffness (by Sainsot Method)

The proposed method was illustrated in Figure 3.1 in detail. In the method, bending, shear, compression, and hertzian stiffness were calculated by Weber-Banaschek formulations. Calculations according to the Weber-Banaschek formulations were carried out based on involute gear profile as explained in Section 3.2. For gear body stiffness, the Sainsot's Method was used as explained. Deformations obtained from each method for given slice of gear pairs were combined. After combining deformations on the slices of the gear pairs, stiffness values for these points were found. These stiffness values were sum up according to the points where single or double teeth pair in contact through gear mesh. Effects of these five different types of mesh stiffness can be seen in deformation quantitites. Deformations during the mesh of gear pair were calculated based on bending deformation (δ_z), gear body deformation (δ_{RK}), hertzian flattening (δ_H).

For gear body deformation, the Saintsot Method that is based on experimental data was used and combined with the Weber-Banaschek Method.

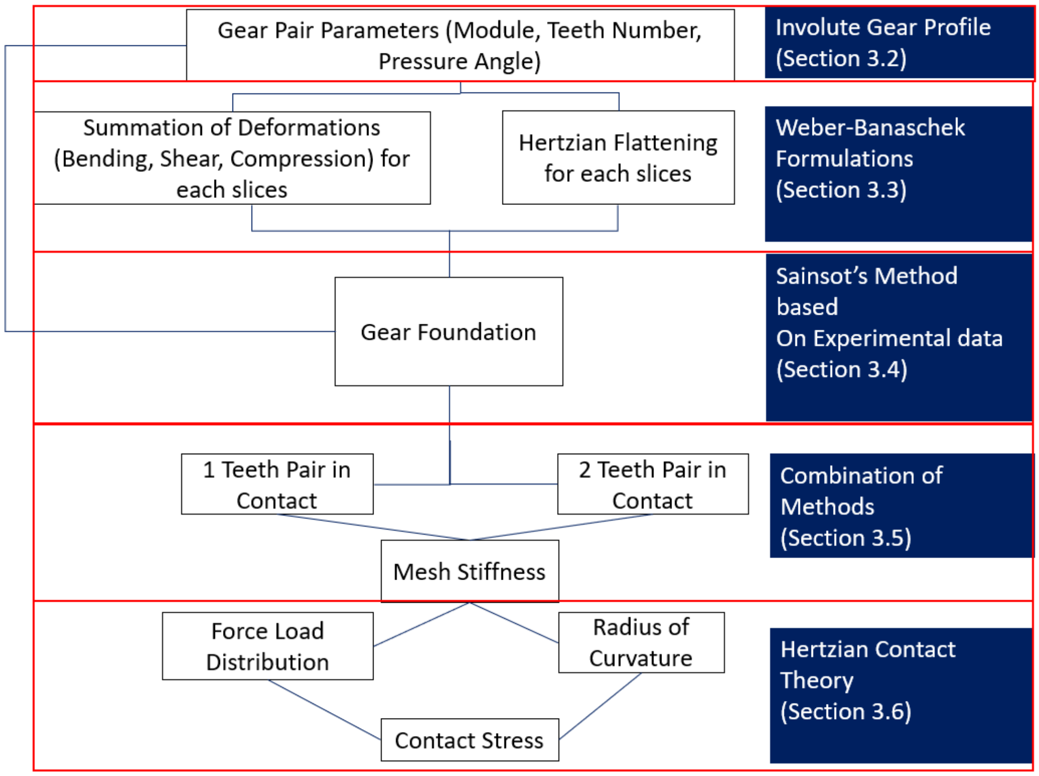

Figure 3.1 *Proposed Analytical Method.*

3.2 Involute Gear Profile

In order to prepare input datas to the Weber-Banaschek and the Saintsot's Methods, gear geometry calculations were carried out based on involute gear profile. Prepared MATLAB GUI and involute profile of gears are given in Figure 3.2. Detailed excel sheet was prepared as shown in Table 3.1 and Table 3.2. The excel sheets give results of gear output parameters including pitch radius, any radius on contact line for gear and pinion, contact ratios, sliding velocities etc.

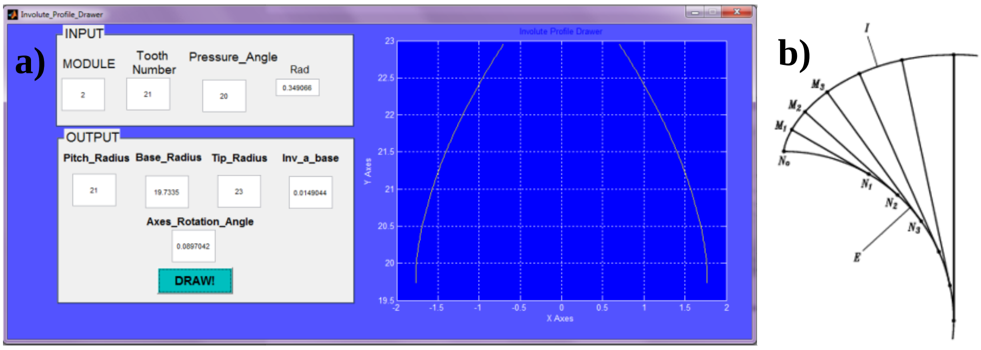

Figure 3.2 *Gear Profile: a) MATLAB GUI; b) Involute Profile.*

Table 3.1 *Gear Parameters Calculation Sheet - Gear Pair Sample.*

	Pinion	**Gear**
Module	2	2
Teeth Number	45	63
Pressure Angle (α)	20	20
Gear Width (mm)	13	14
v	0.3	0.3
E (N/m^2)	200000	200000
Base Output		
Base Radius (mm)	42.2	59.2
Addendum Factor	1	1
Dedendum Factor	1.25	1.25
Pitch Radius [Reference Radius] (mm)	45	63
Tip Radius (mm)	47	65
Root Radius (mm)	42.5	60.5
Center Distance of Gear Pair (mm)	108	
Working Pressure Angle	20	20
Length of Theoretical Line of Action (mm)	36.9	
Length of Actual Line of Action (mm)	10.4	
Contract Ratio [Ɛ]	**1.76**	

Table 3.2 *Gear Parameters Calculation- Gear Pair Sample.*

CONTACT LENGTH																		
Pinion (r_{any}) (mm)	**Pinion Pressure Angle (Degree)**	**Curvature Radius Pinion (mm)**	**Pinion θany (Roll Angle) (Degree)**	**V pinion (m/s)**	**V base pinion (m/s)**	**V tangential pinion (m/s)**	**V relative sliding pinion (m/s)**	**Specific Sliding - Pinion**	**Gear (r_{any}) (mm)**	**Gear Pressure Angle (Degree)**	**Curvature Radius Gear (mm)**	**Gear θany (Roll Angle) (Degree)**	**V gear (m/s)**	**V base gear (m/s)**	**V tangenti al gear (m/s)**	**V relative sliding gear (m/s)**	**Specific Sliding - Gear**	**Length Path of Contact (mm)**
47.00	25.88	20.52	0.49	72.85	65.54	31.80	13.62	0.43	61.44	15.50	16.42	0.28	68.02	65.54	18.18	-13.62	-0.75	20.52
46.91	25.65	20.30	0.48	72.70	65.54	31.47	13.05	0.41	61.49	15.70	16.64	0.28	68.08	65.54	18.42	-13.05	-0.71	20.30
46.82	25.41	20.09	0.48	72.56	65.54	31.14	12.49	0.40	61.55	15.89	16.85	0.28	68.14	65.54	18.65	-12.49	-0.67	20.09
46.73	25.18	19.88	0.47	72.42	65.54	30.81	11.92	0.39	61.61	16.08	17.06	0.29	68.21	65.54	18.89	-11.92	-0.63	19.88
46.64	24.94	19.67	0.47	72.28	65.54	30.48	11.36	0.37	61.67	16.27	17.27	0.29	68.27	65.54	19.12	-11.36	-0.59	19.67
46.55	24.70	19.45	0.46	72.14	65.54	30.15	10.79	0.36	61.73	16.46	17.49	0.30	68.34	65.54	19.36	-10.79	-0.56	19.45
46.46	24.47	19.24	0.45	72.01	65.54	29.82	10.23	0.34	61.79	16.64	17.70	0.30	68.41	65.54	19.59	-10.23	-0.52	19.24
46.37	24.23	19.03	0.45	71.87	65.54	29.49	9.66	0.33	61.85	16.83	17.91	0.30	68.48	65.54	19.83	-9.66	-0.49	19.03
46.28	23.99	18.81	0.44	71.74	65.54	29.16	9.10	0.31	61.91	17.02	18.12	0.31	68.54	65.54	20.06	-9.10	-0.45	18.81
46.20	23.75	18.60	0.44	71.60	65.54	28.83	8.53	0.30	61.98	17.21	18.34	0.31	68.61	65.54	20.30	-8.53	-0.42	18.60
46.11	23.50	18.39	0.43	71.47	65.54	28.50	7.97	0.28	62.04	17.40	18.55	0.31	68.68	65.54	20.54	-7.97	-0.39	18.39
46.03	23.26	18.18	0.43	71.34	65.54	28.17	7.40	0.26	62.10	17.58	18.76	0.32	68.75	65.54	20.77	-7.40	-0.36	18.18
45.94	23.02	17.96	0.42	71.21	65.54	27.84	6.84	0.25	62.17	17.77	18.97	0.32	68.83	65.54	21.01	-6.84	-0.33	17.96
45.86	22.77	17.75	0.42	71.08	65.54	27.52	6.27	0.23	62.23	17.96	19.19	0.32	68.90	65.54	21.24	-6.27	-0.30	17.75
45.78	22.53	17.54	0.41	70.96	65.54	27.19	5.71	0.21	62.30	18.14	19.40	0.33	68.97	65.54	21.48	-5.71	-0.27	17.54
45.70	22.28	17.33	0.41	70.83	65.54	26.86	5.14	0.19	62.36	18.33	19.61	0.33	69.04	65.54	21.71	-5.14	-0.24	17.33
45.62	22.03	17.11	0.40	70.71	65.54	26.53	4.58	0.17	62.43	18.51	19.82	0.33	69.12	65.54	21.95	-4.58	-0.21	17.11
45.54	21.79	16.90	0.40	70.58	65.54	26.20	4.01	0.15	62.50	18.70	20.04	0.34	69.19	65.54	22.18	-4.01	-0.18	16.90
45.46	21.54	16.69	0.39	70.46	65.54	25.87	3.45	0.13	62.57	18.88	20.25	0.34	69.27	65.54	22.42	-3.45	-0.15	16.69
45.38	21.29	16.48	0.39	70.34	65.54	25.54	2.89	0.11	62.64	19.07	20.46	0.35	69.35	65.54	22.65	-2.89	-0.13	16.48
45.31	21.04	16.26	0.38	70.22	65.54	25.21	2.32	0.09	62.71	19.25	20.67	0.35	69.42	65.54	22.89	-2.32	-0.10	16.26
45.23	20.79	16.05	0.38	70.10	65.54	24.88	1.76	0.07	62.78	19.43	20.89	0.35	69.50	65.54	23.12	-1.76	-0.08	16.05
45.16	20.53	15.84	0.37	69.99	65.54	24.55	1.19	0.05	62.85	19.62	21.10	0.36	69.58	65.54	23.36	-1.19	-0.05	15.84
45.08	20.28	15.63	0.37	69.87	65.54	24.22	0.63	0.03	62.92	19.80	21.31	0.36	69.66	65.54	23.59	-0.63	-0.03	15.63
45.01	20.03	15.41	0.36	69.76	65.54	23.89	0.06	0.00	62.99	19.98	21.52	0.36	69.74	65.54	23.83	-0.06	0.00	15.41
44.94	19.77	15.20	0.36	69.65	65.54	23.56	-0.50	-0.02	63.07	20.16	21.74	0.37	69.82	65.54	24.07	0.50	0.02	15.20
44.86	19.52	14.99	0.35	69.54	65.54	23.23	-1.07	-0.05	63.14	20.34	21.95	0.37	69.90	65.54	24.30	1.07	0.04	14.99
44.79	19.26	14.78	0.35	69.43	65.54	22.90	-1.63	-0.07	63.21	20.52	22.16	0.37	69.98	65.54	24.54	1.63	0.07	14.78
44.72	19.00	14.56	0.34	69.32	65.54	22.57	-2.20	-0.10	63.29	20.70	22.37	0.38	70.07	65.54	24.77	2.20	0.09	14.56
44.66	18.75	14.35	0.34	69.21	65.54	22.24	-2.76	-0.12	63.36	20.88	22.59	0.38	70.15	65.54	25.01	2.76	0.11	14.35
44.59	18.49	14.14	0.33	69.11	65.54	21.91	-3.33	-0.15	63.44	21.06	22.80	0.39	70.23	65.54	25.24	3.33	0.13	14.14
44.52	18.23	13.93	0.33	69.00	65.54	21.58	-3.89	-0.18	63.52	21.24	23.01	0.39	70.32	65.54	25.48	3.89	0.15	13.93
44.45	17.97	13.71	0.32	68.90	65.54	21.26	-4.46	-0.21	63.59	21.42	23.22	0.39	70.40	65.54	25.71	4.46	0.17	13.71
44.39	17.71	13.50	0.32	68.80	65.54	20.93	-5.02	-0.24	63.67	21.60	23.44	0.40	70.49	65.54	25.95	5.02	0.19	13.50
44.32	17.45	13.29	0.31	68.70	65.54	20.60	-5.59	-0.27	63.75	21.78	23.65	0.40	70.58	65.54	26.18	5.59	0.21	13.29
44.26	17.18	13.08	0.31	68.60	65.54	20.27	-6.15	-0.30	63.83	21.95	23.86	0.40	70.67	65.54	26.42	6.15	0.23	13.08
44.20	16.92	12.86	0.30	68.51	65.54	19.94	-6.72	-0.34	63.91	22.13	24.07	0.41	70.75	65.54	26.65	6.72	0.25	12.86
44.14	16.66	12.65	0.30	68.41	65.54	19.61	-7.28	-0.37	63.99	22.31	24.29	0.41	70.84	65.54	26.89	7.28	0.27	12.65
44.08	16.39	12.44	0.29	68.32	65.54	19.28	-7.85	-0.41	64.07	22.48	24.50	0.41	70.93	65.54	27.12	7.85	0.29	12.44
44.02	16.13	12.23	0.29	68.23	65.54	18.95	-8.41	-0.44	64.15	22.66	24.71	0.42	71.02	65.54	27.36	8.41	0.31	12.23
43.96	15.86	12.01	0.28	68.14	65.54	18.62	-8.98	-0.48	64.23	22.83	24.93	0.42	71.11	65.54	27.59	8.98	0.33	12.01
43.90	15.59	11.80	0.28	68.05	65.54	18.29	-9.54	-0.52	64.32	23.01	25.14	0.42	71.21	65.54	27.83	9.54	0.34	11.80
43.85	15.32	11.59	0.27	67.96	65.54	17.96	-10.10	-0.56	64.40	23.18	25.35	0.43	71.30	65.54	28.07	10.10	0.36	11.59
43.79	15.06	11.38	0.27	67.87	65.54	17.63	-10.67	-0.61	64.48	23.35	25.56	0.43	71.39	65.54	28.30	10.67	0.38	11.38
43.73	14.79	11.16	0.26	67.79	65.54	17.30	-11.23	-0.65	64.57	23.53	25.78	0.44	71.48	65.54	28.54	11.23	0.39	11.16
43.68	14.52	10.95	0.26	67.70	65.54	16.97	-11.80	-0.70	64.65	23.70	25.99	0.44	71.58	65.54	28.77	11.80	0.41	10.95
43.63	14.25	10.74	0.25	67.62	65.54	16.64	-12.36	-0.74	64.74	23.87	26.20	0.44	71.67	65.54	29.01	12.36	0.43	10.74
43.58	13.98	10.53	0.25	67.54	65.54	16.31	-12.93	-0.79	64.83	24.04	26.41	0.45	71.77	65.54	29.24	12.93	0.44	10.53
43.53	13.71	10.31	0.24	67.46	65.54	15.98	-13.49	-0.84	64.91	24.22	26.63	0.45	71.87	65.54	29.48	13.49	0.46	10.31
43.48	13.43	10.10	0.24	67.39	65.54	15.65	-14.06	-0.90	65.00	24.39	26.84	0.45	71.96	65.54	29.71	14.06	0.47	10.10

3.3 Weber-Banaschek Formulations

After obtaining outputs for gear mesh, in order to find out effect of bending, shear, axial, and hertzian deformation on mesh stiffness, the Weber-Banaschek formulations were used as shown in Figure 3.3.

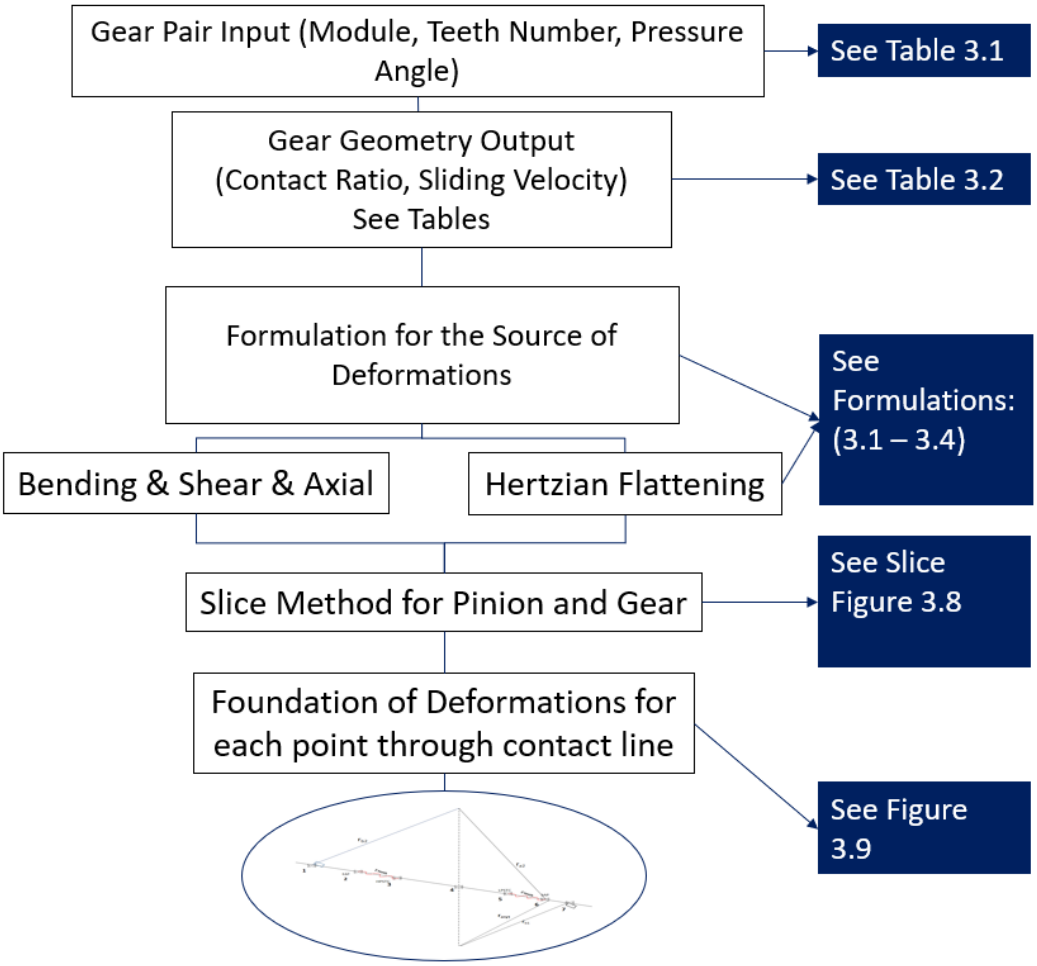

Figure 3.3 *Flow Chart to use Weber-Banaschek Formulations.*

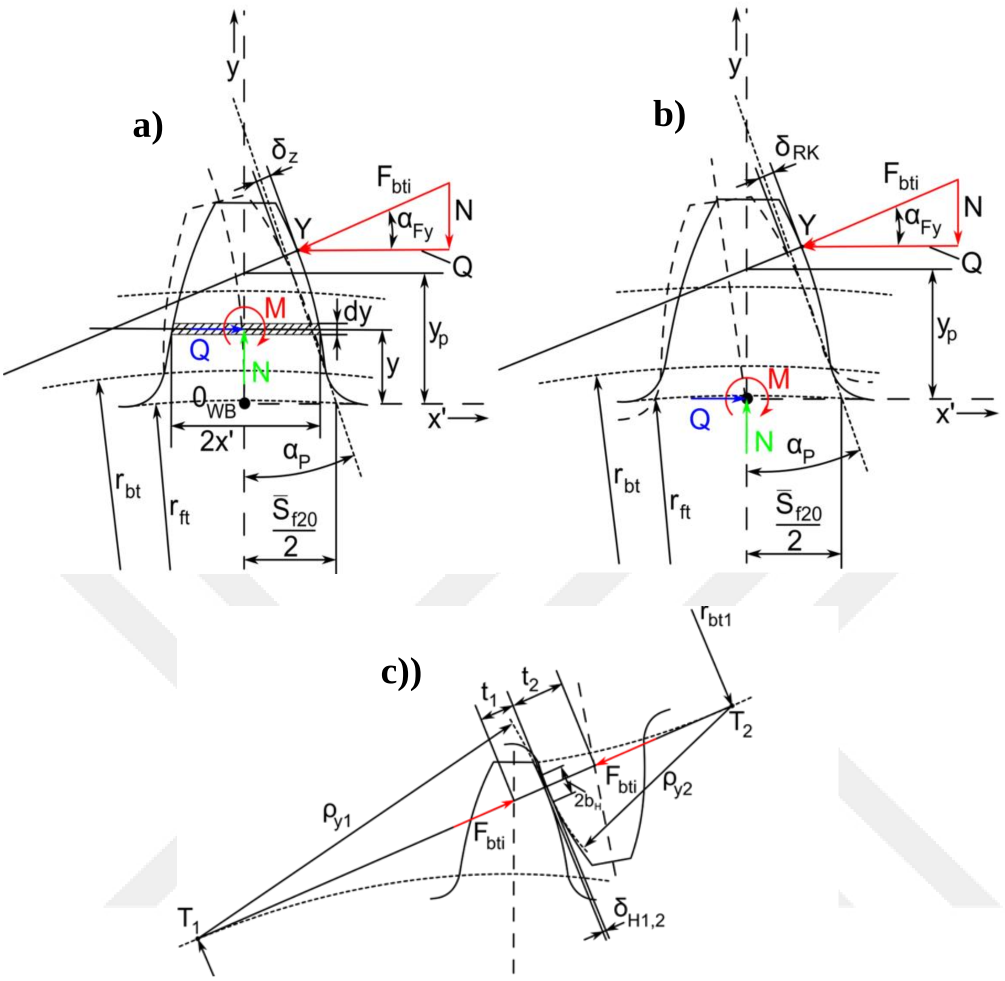

Figure 3.4 *Gear Deformation according to Weber/Banaschek a) Bending, Shear and Axial Deformation b) Gear Body Deformation c) Hertzian Flattening.*

$$\delta_Z = \frac{F_{bti}}{b}\ (\cos\alpha_{Fy})^2\ \frac{1-\nu^2}{E}\ \left[12\int_0^{y_p}\frac{(y_p-y)^2}{(2x')^3}\ dy + \left(\frac{2.4}{1-\nu} + \left(\tan\alpha_{any}\right)^2\right)\int_0^{y_p}\frac{dy}{2x'}\right] \tag{3.1}$$

$$\delta_{RK} = \frac{F_{bti}}{b}\ (\cos\alpha_{Fy})^2\ \frac{1-\nu^2}{E}\ \left[\frac{18}{\pi}\frac{y_p^2}{s^2{}_{f20}} + \frac{2(1-2\nu)}{1-\nu}\frac{y_p}{s_{f20}} + \frac{4.8}{\pi}\left(1 + \frac{1-\nu}{2.4}\left(\tan\alpha_{any}\right)^2\right)\right] \tag{3.2}$$

$$\delta_{H1,2} = \frac{F_{bti}}{\pi b_g}\left[\frac{1-\nu_1^2}{E_1}\ln\left(\frac{b_H^2}{4t_1^2}\right) + \frac{\nu_1(1+\nu_1)}{E_1} + \frac{1-\nu_2^2}{E_2}\ln\left(\frac{b_H^2}{4t_2^2}\right) + \frac{\nu_2(1+\nu_2)}{E_2}\right] \tag{3.3}$$

where

y_p refers to distance from direction of force to gear root, that is subjected to change

a_{any} refers to a_{F_y}

$b_{1,2}$ refers to gear and pinion thickness respectively

δ_Z refers to deformation due to bending, shear and axial compression

δ_{RK} refers to deformation due to gear body

$\delta_{H1,2}$ refers to Hertzian deformation

ν refers to Poisson's Ratio

E refers to Elastic Modulus

Total deformation obtained from Weber-Banaschek could be rewritten as:

$$\delta_{total} = \delta_{Z1} + \delta_{RK1} + \delta_{RK2} + \delta_{H1,2} + \delta_{Z2} \tag{3.4}$$

3.4 Sainsot Method

In order to calculate the stiffness of foundation, the method proposed by Sainsot is considered (Sainsot et al., 2004). Gear pair outputs were found as explained in Section 3.2. These outputs were given into the Sainsot Method as shown in Figure 3.5. Gear pair parameters and gear coefficients were given by user in MATLAB code as explained in Section 3.2.

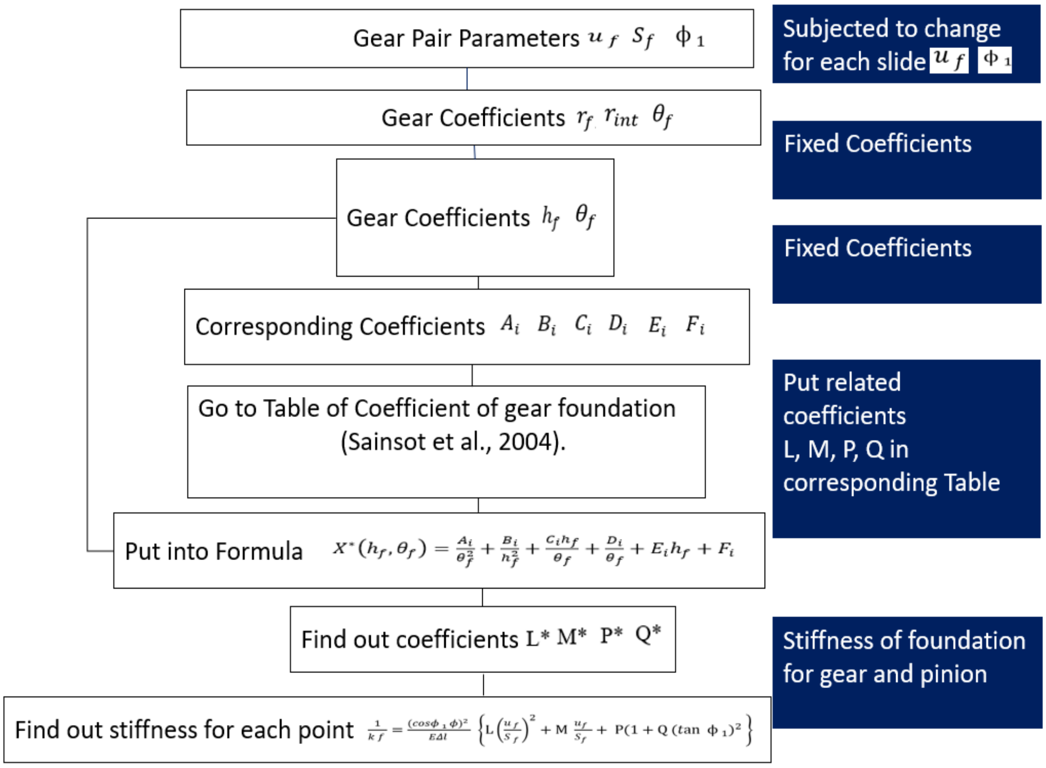

Figure 3.5 *The Use of Sainsot Method in Stiffness Foundation.*

Parameters of gear foundation are shown in Figure 3.6.

Here;

s_f refers to 1.05 * ltt_{max}

ltt_{max} refers to maximum lineer tooth thickness and given as:

$$ltt_{max} = r_{any} - \sin\left(\frac{\frac{S_{wany}}{r_{any}}}{2}\right) \tag{3.5}$$

S_{wany} and r_{any} refers to tooth thickness and radius from center to the point in slice.

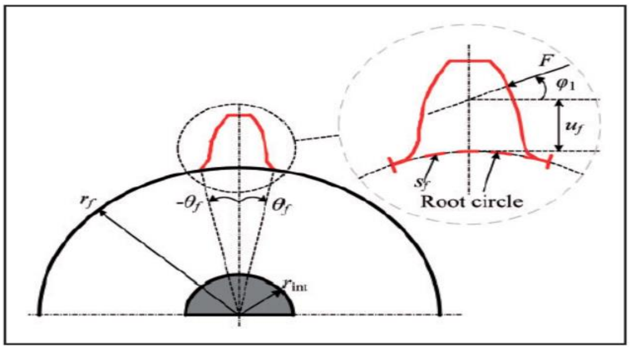

Figure 3.6 *Gear Foundation Parameters (Wang and Zhang, 2017).*

To calculate the coefficient of *L*, *M*, *P*, *Q* stated in Equation 3.6, Table 3.3 is used as stated in the work by Sainsot et al., 2004.

$$\frac{1}{k\,f} = \frac{(cos\phi_{\,1}\,\phi)^2}{E\Delta l}\left\{\mathrm{L}\left(\frac{u_f}{S_f}\right)^2 + \mathrm{M}\,\frac{u_f}{S_f} + \mathrm{P}(1 + \mathrm{Q}\,(tan\ \phi_{\,1})^2\right\} \tag{3.6}$$

$$X^*(h_f, \theta_f) = \frac{A_i}{\theta_f^2} + \frac{B_i}{h_f^2} + \frac{C_i h_f}{\theta_f} + \frac{D_i}{\theta_f} + E_i h_f + F_i \tag{3.7}$$

$$h_f = r_f / \, r_{int} \tag{3.8}$$

Table 3.3 *Coefficients of Gear Foundation (Sainsot et al., 2004).*

	A_i	B_i	C_i	D_i	E_i	F_i
L *	-5.574 x 10^{-5}	-1.9986 x 10^{-3}	-2.3015 x 10^{-4}	4.7702 x 10^{-3}	0.0271	6.8045
M *	60.11 x 10^{-5}	28.1 x 10^{-3}	-83.431 x 10^{-4}	-9.9256 x 10^{-3}	0.1654	0.9086
P *	-50.952 x 10^{-5}	185.5 x 10^{-3}	0.0538 x 10^{-4}	53.3 x 10^{-3}	0.2895	0.9236
Q *	-6.2042 x 10^{-5}	9.0889 x 10^{-3}	-4.0964 x 10^{-4}	7.8297 x 10^{-3}	0.1472	0.6904

3.5 Combination of Methods

After obtaining deformations from the Weber-Banaschek and the Saintsot methods, the deformations were sum up for corresponding gear slices which are given in Figure 3.8. Slices on gear and corresponing pinion were shown for illustration only. In calculations, slices were started from start of active profile to end of active profile through contact line as shown in Figure 4.4. Combination of methods are given in Figure 3.7.

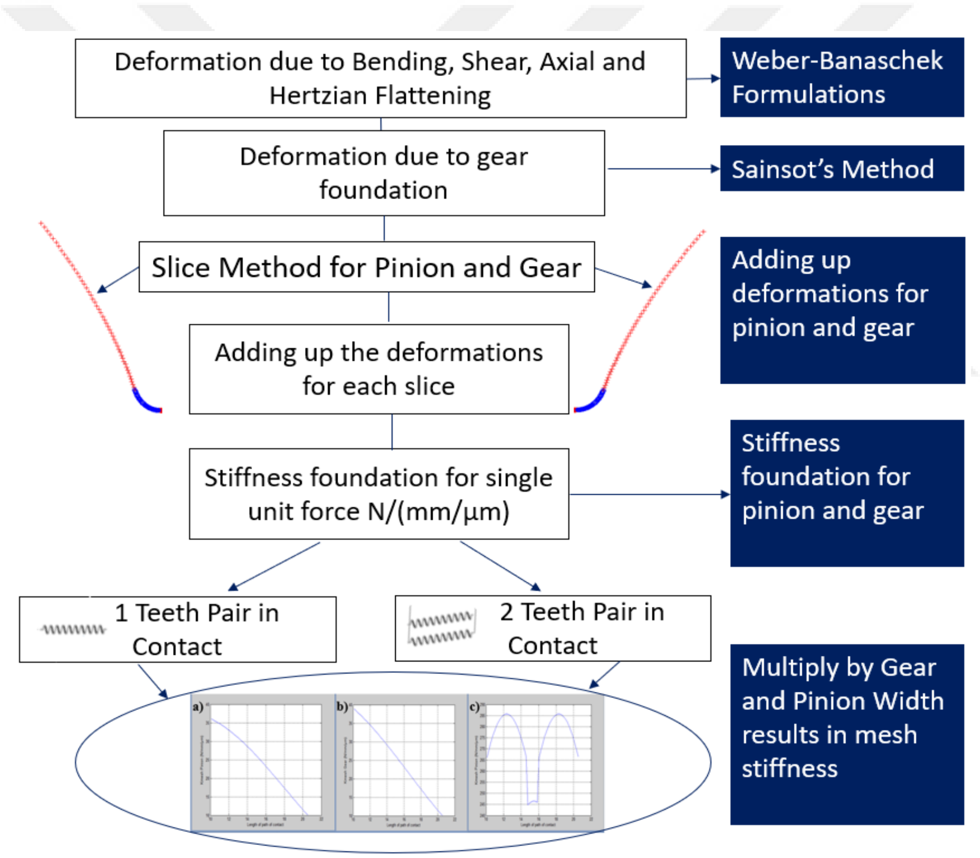

***Figure 3.7** Combination of Two Methods (Weber Banaschek and Sainsot Methods).*

After obtaining total deformations for given slices on gear and pinion, stiffness for a given contact point was calculated for single unit force N/(mm/μm).

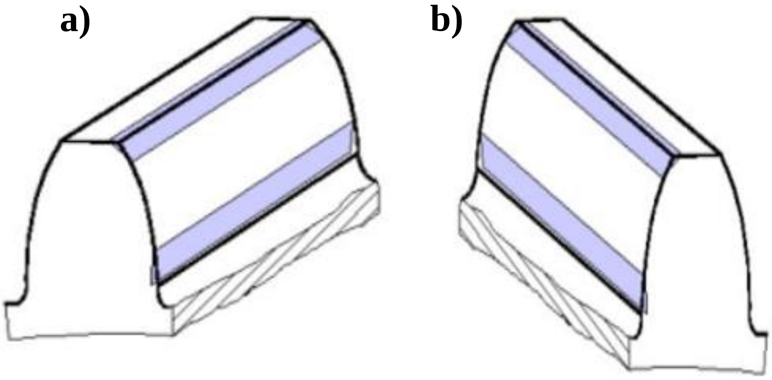

Figure 3.8 *Gear Slice Method for Gear Pair: a) Gear; b) Pinion (from KISSsoft).*

There are two main region through gear mesh as shown in Figure 3.9. Then mesh stiffness turned to

$$\frac{1}{k_{1\ teeth\ pair}} = \frac{1}{\frac{1}{k_{1\ pinion}}} + \frac{1}{\frac{1}{k_{1\ gear}}} \quad (3.9)$$

$$\frac{1}{k_{2\ teeth\ pair}} = \frac{1}{\frac{1}{k_{2\ pinion}}} + \frac{1}{\frac{1}{k_{2\ gear}}} \quad (3.10)$$

For the region where only single teeth pair in contact, mesh stiffness turned into:

$$\frac{1}{k_{mesh\ for\ single\ teeth\ pair\ in\ contact}} = k_{2\ teeth\ pair} \quad (3.11)$$

For the region where two teeth pair in contact, mesh stiffness turned into:

$$\frac{1}{k_{mesh\ for\ double\ teeth\ pair\ in\ contact}} = k_{1\ teeth\ pair} + k_{2\ teeth\ pair} \quad (3.12)$$

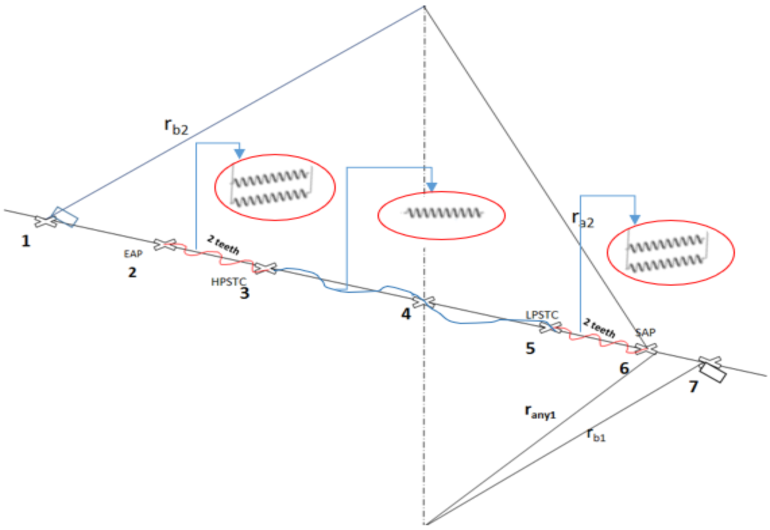

Figure 3.9 *Teeth Pairs in Contact Through Gear Mesh.*

Then total mesh stiffness was drawn through contact line as shown in Figure 3.10. Stiffness values tend to decrease where only single teeth pair in contact during mesh.

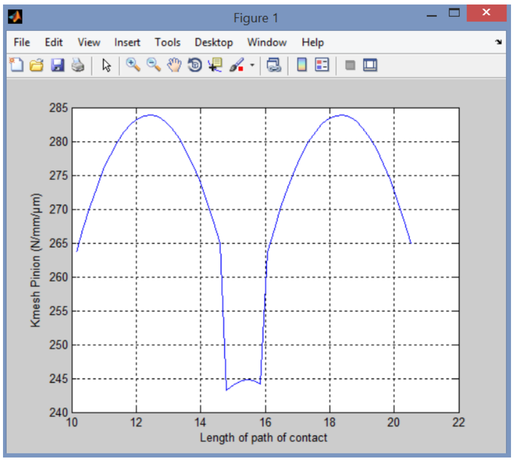

Figure 3.10 *Calculation Output for Sample Gear Pair (Teeth Numbers: 45/63, Module:2 mm, Pressure Angle:20 degree) .*

3.6 Hertzian Contact Theory

In this thesis, contact stress for mating gears was calculated by the Hertzian contact theorem. The equation could be stated as seen in Equation 3.13 (Wang and Zhang, 2017).

$$\sigma_c = \sqrt{\frac{F_i}{\pi \Delta l} \frac{\frac{1}{\rho_1}+\frac{1}{\rho_2}}{\frac{1-v_1{}^2}{E_1}+\frac{1-v_2{}^2}{E_2}}} \tag{3.13}$$

Here ρ_1 and ρ_2 are radius of curvatures for mating gears as shown in Figure 3.4.c crespectively, ρ_{y1} and ρ_{y1}. E_1 and E_2 are Young's modulus of gears. Also, Δl corresponds to width of slice on gear and pinion. Additionally, v_1 and v_2 denote Poisson's ratios of the gear pairs. F_i is the load at contact points. After obtaining mesh stiffness, radius of curvature for mating gear pairs, F_i was calculated for slices of gear and pinion. Obtained load distribution and contact stress through contact line for sample gear pair is given in Figure 3.11

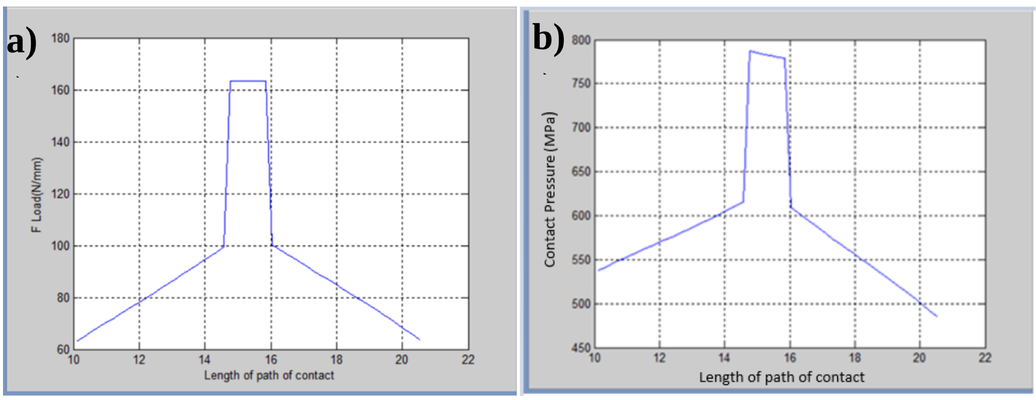

Figure 3.11 *Calculation Output for Sample Gear Pair (Teeth Numbers: 45/63, Module:2 mm, Pressure Angle:20 degree): a) Load Distribution b) Contact Stress*

3.7 Gear Material Allowable Specifications

Common gear material allowable specifications are summurized in Table 3.4.

Table 3.4 *Gear material specifications (KISSsoft).*

Material	Type	Surface Hardness	Contact Stress Allowable (MPa)
20MnCr5	Case-hardening steel	60 HRC	1500
16MnCr5	Case-hardening steel	59 HRC	1500
16MnCr5	Case-hardening steel (Nitrided)	710 HV	1000
18CrNiMo7-6	Case-hardening steel	61 HRC	1500
15CrNi6	Case-hardening steel	60 HRC	1500
17NiCrMo6-5	Case-hardening steel	60 HRC	1500
SAE 8620 (20NiCrMo)	Case-hardening steel	60 HRC	1500
SAE 9310	Case-hardening steel	60 HRC	1893

In this thesis, effects of given gear materials were compared based on fatigue life. Materials to be compared are 16MnCr5, 18CrNiMo7-6 and SAE9310, respectively.

3.8 AGMA Standard

AGMA (AGMA 2001 - D04) contact stress number for gears in mesh can be calculated from the Equation 3.14. Calculated number refers to maximum contact pressure in which occur at the highest point of single tooth contact (HPSTC) in gear mesh.

$$s_c = Z_E \sqrt{W_t\, K_O\, K_V\, K_s\, \frac{K_H}{2 r_1 W Z_1}} \tag{3.14}$$

Contact stress formulation includes factors as:

s_c : Contact stress number

Z_E : Elastic coefficient

W_t : Transmitted tangential load

K_O : Overload factor

K_V : Dynamic factor

K_s : Size factor

K_H: Load distribution factor

r_1 : Pitch radius of pinion

W : Face width

Z_1 : Geometry factor for pitting resistance

3.9 Profile Modifications

Tip relief modifications (Figure 3.12) are commonly applied on gears to compensate transmission errors (TE). TE is defined as the difference between ideal and real positions of the output shaft with reference to input shaft. Ideal position represents the condition of a consisting perfectly aligned shaft within the gearbox. TE could be commonly explained in two ways: angular displacement or linear displacement on the line of action. Minimization of TE results in minimization of noise in a practical way. Related tip relief parameters were used in Equations 3.15 - 3.23. Tip relief modification commonly starts from HPSTC.

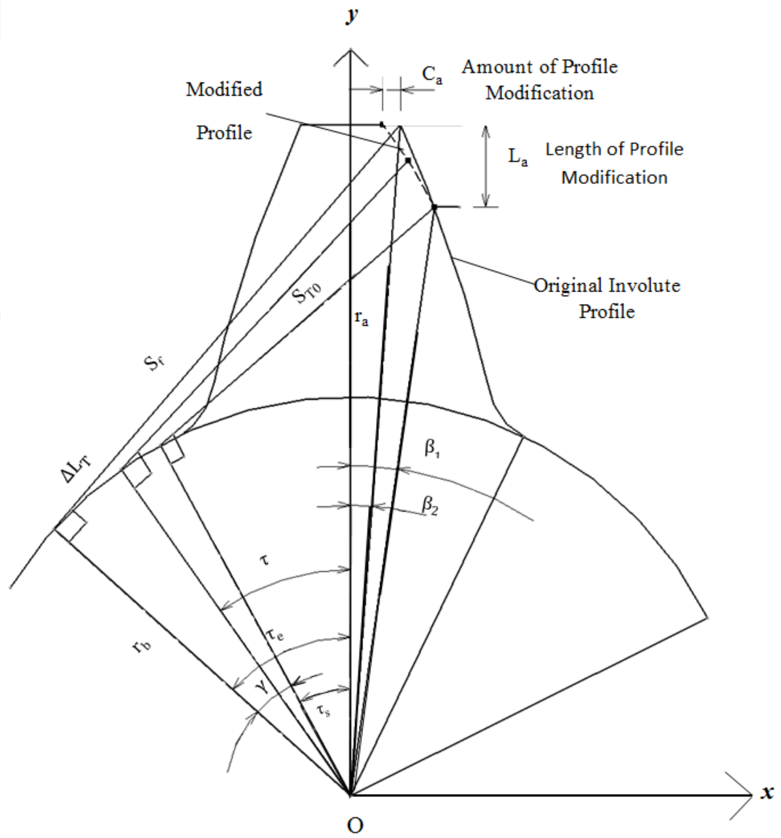

Figure 3.12 *Micro Geometry Modification (Tip relief) Modified from (Ma et al., 2016).*

Related parameters shown in Figure 3.12 are presented in Equation 3.15:

$$C= C_a(\frac{\tau-\tau_s}{\tau_e-\tau_s}) \quad (3.15)$$

C : Material removal amount

C_a: Profile modification amount

τ : Angle for for arbitrary point

τ_s : Angle for starting point

τ_e : Angle for ending point

By using geometrical relationship in Figure 3.12, L_a , β_1, β_2 could be defined as follows.

$$L_a= r_a \cos\beta_1 -r_{T0} \cos\beta_2 \quad (3.16)$$

$$\beta_1=\arctan\frac{S_f}{r_b} -\tau_e \quad (3.17)$$

$$\beta_2=\arctan\frac{S_{T0}}{r_b}-\tau_s \quad (3.18)$$

$$S_f=\sqrt{r_a^2-r_b^2} \quad (3.19)$$

$$S_{T0} = S_f - \Delta L_T \quad (3.20)$$

$$\tau_s = \tau_e- \gamma \quad (3.21)$$

$$\gamma=\frac{\Delta L_T}{r_b} \quad (3.22)$$

$$\tau_e=\frac{S_f}{r_b} - \theta_b \quad (3.23)$$

CHAPTER 4

CASE STUDY

Case study was carried out based on the powertrain as seen in Figure 4.1. The powertrain consists of 1 input and 2 output shafts. There were also 2 idler gears which are not used for power extraction. Analysis was carried out with respect to power split given in Figure 4.2. In Figure 4.2, it is seen that power is supplied from input shaft and splitted into 2 output shafts.

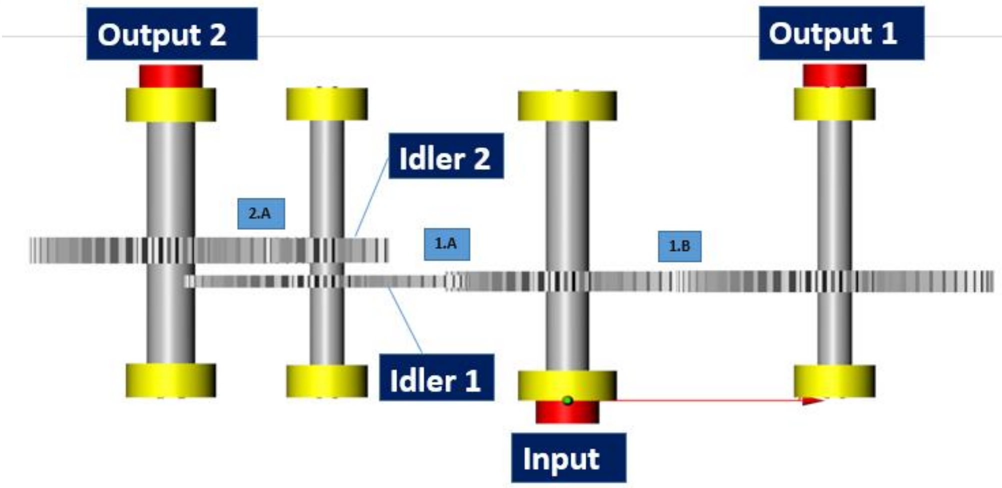

Figure 4.1 *Powertrain Case Study.*

Powertrain properties are summarised in Table 4.1. Powertrain in this case study consists of 5 gears and 3 gear meshes in total. Input shaft has 45 teeth and two output shafts have 57 and 49 teeth. Both output shafts were subjected to power extraction of 100 kW. Input rpm value is 10000 and related rpm values for output shaft 1 and output shaft 2 are 7894 and 4227, respectively.

Face width values are 14 mm and 19 mm for output shafts. Since output shaft 2 is subjected to the same power with lower rpm, it has higher load on its gear teeth. Therefore, face width is arranged by considering required safey factor. Gear ratios were derived from teeth numbers divisons and used to find out regarding rpm values. These rpm and torque values are considered in contact analysis calculations. Pitch diameters and pitch radiues values were calculated based on module 2 and stated in Table 4.1. Idler gears were used to transmit to torque not for power extraction in this thesis. Idler gears were subjected to 7142 rpm as stated in Table 4.1.

Table 4.1 *Powertrain System Properties.*

POWERTRAIN							OPERATION CASE
	Teeth Number	**Face Width (mm)**	**Pitch Diameter (mm)**	**Pitch Radius (mm)**	**Material**	**Gear Ratio**	**INPUT RPM: 10000 INPUT POWER: 200 kW**
Output1	57	14	114	57	Steel, Grade 3-Case Carburized	1.27	7894
Input	45	13	90	45	Steel, Grade 3-Case Carburized	1.00	10000
Idler1	63	10	126	63	Steel, Grade 3-Case Carburized	1.4	7142
Idler2	29	18	58	29	Steel, Grade 3-Case Carburized	1.4	7142
Output2	49	19	98	49	Steel, Grade 3-Case Carburized	2.37	4227

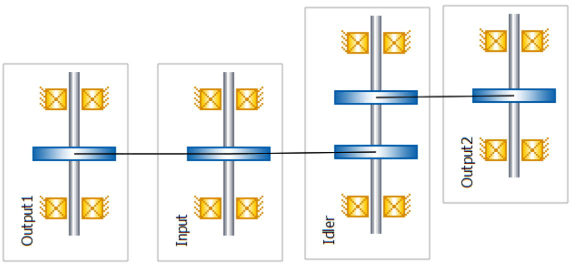

Figure 4.2 *Powertrain Power Split.*

4.1 Gear Parameters Selection

For the first gear pair of 45/63, gear parameters were stated in terms of gear macro and microgeometry properties. For pinion and gear, these properties are given in Table 4.2. Gear module was taken as 2, power extraction was 100 kW.

Table 4.2 *Pinion and Gear Parameters of Teeth Numbers of 45 and 63.*

	Pinion	**Gear**
Module	2	2
Teeth Number	45	63
Pressure Angle (α)	20	20
Gear Width (mm)	13	14
v	0.3	0.3
E (N/m^2)	200000	200000
Base Output		
Base Radius (mm)	42.2	59.2
Addendum Factor	1	1
Dedendum Factor	1.25	1.25
Pitch Radius [Reference Radius] (mm)	45	63
Tip Radius (mm)	47	65
Root Radius (mm)	42.5	60.5
Center Distance of Gear Pair (mm)	108	
Working Pressure Angle	20	20
Length of Theoretical Line of Action (mm)	36.9	
Length of Actual Line of Action (mm)	10.4	
Contact Ratio [Ɛ]	**1.76**	

Length of contact lines in gear mesh is calculated based on involute gear geometry by using excel GUI specially created for this purpose (Figure 4.3). Inputs of excel GUI are module, teeth number, and pressure angle. Outputs of excel GUI are pitch radius, base radius and tip radius.

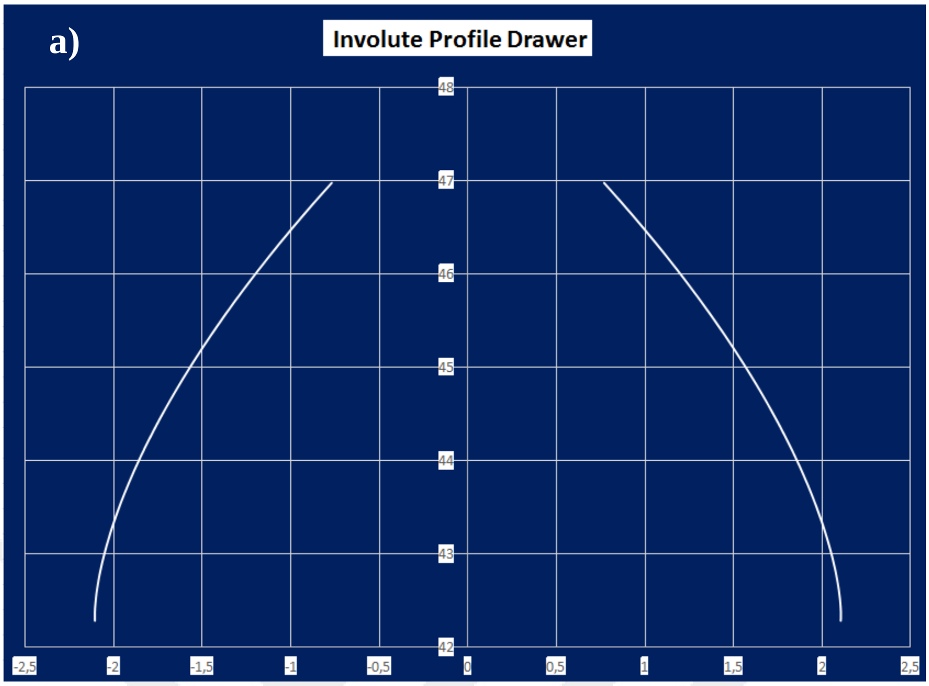

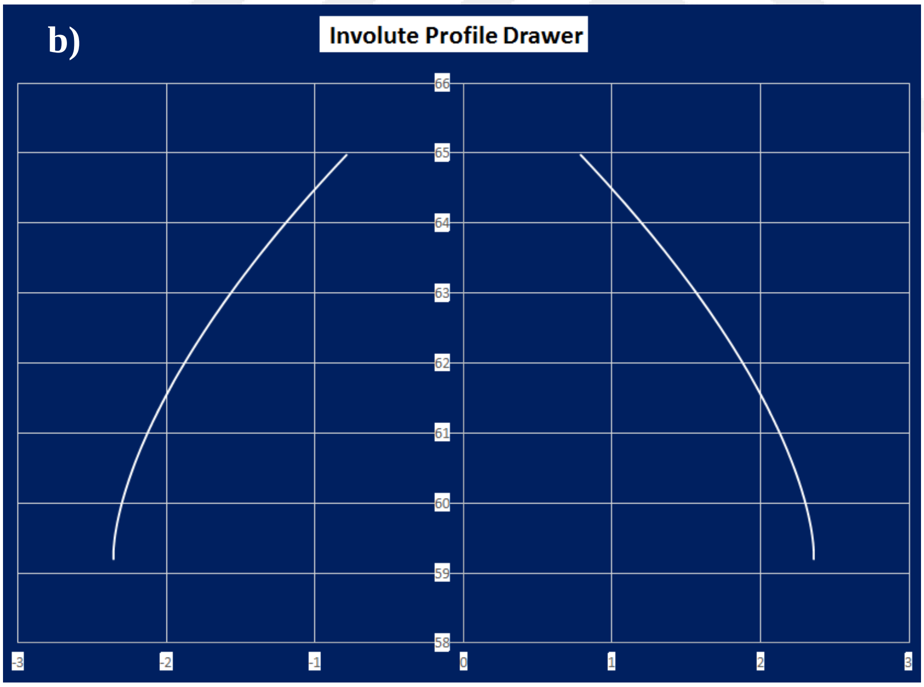

Figure 4.3 *Excel GUI* ***a)*** *Involute Profile for Pinion;* ***b)*** *Involute Profile for Gear.*

Geometrical values for gear mesh of teeth numbers 45 and 63 are shown in Table 4.3 and diagram is shown in Figure 4.4.

Table 4.3 *Geometrical Values of Gear Mesh of Teeth Numbers of 45 and 63.*

[1-7] : Length of Theroretical Line of Action	36.94
[1-6]	26.84
[6-7]	10.10
[2-7]	20.52
[1-2]	16.42
[2-6]	10.42
P_B = [3-6]=[2-5]	5.90
[5-6]	4.51
[2-3]	4.51
[1-5]	22.33
$r_{SAP1\ pinion}$	43.48
$r_{EAP1\ -\ pinion}$	47.00
$r_{SAP2\ -\ gear}$	65.00
$r_{EAP2\ -\ gear}$	61.44
$r_{HPSTC1\ -\ pinion}$	45.21
$r_{LPSTC1\ -\ pinion}$	44.74
$r_{HPSTC2\ -\ gear}$	63.27
$r_{LPSTC2\ -\ gear}$	62.79

In Figure 4.4, [1-7] line refers to theoretical line of action. In line [2-3] and [5-6], there were 2 teeth pairs in mesh. In line [3-5], there was only 1 tooth pair in mesh. Point 3 refers to HPSTC and point 5 refers to LPSTC. Parameters of $r_{b1,2}$ and $r_{a1,2}$ refer to base radius and any radius in the mesh of pinion and gear.

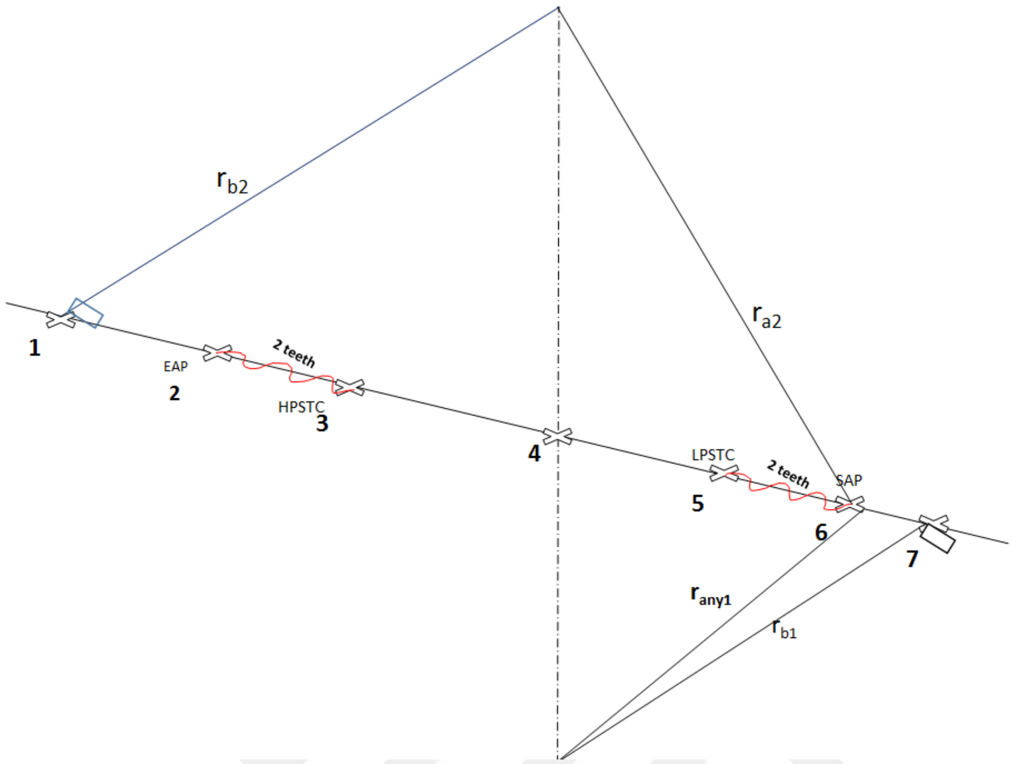

Figure 4.4 General Gear Mesh Diagram.

Gear mesh properties were summarised in Table 4.4. Specific sliding velocities are also stated in Table 4.4 as "Specific Sliding Gear" and "Specific Sliding Pinion". For a gear pair of 45/63, radius of contact points on contact line was calculated for pinion and gear and also stated in Table 4.4. Curvatures radius of pinion and gear were calculated for instant gear mesh points. Calculated radius values were used in contact pressure calculations.

Table 4.4 *Mesh Properties of Teeth Numbers of 45 and 63.*

CONTACT LENGTH																		
Pinion (r_{any}) (mm)	**Pinion Pressure Angle (Degree)**	**Curvature Radius Pinion (mm)**	**Pinion θany (Roll Angle) (Degree)**	**V pinion (m/s)**	**V base pinion (m/s)**	**V tangential pinion (m/s)**	**V relative sliding pinion (m/s)**	**Specific Sliding - Pinion**	**Gear (r_{any}) (mm)**	**Gear Pressure Angle (Degree)**	**Curvature Radius Gear (mm)**	**Gear θany (Roll Angle) (Degree)**	**V gear (m/s)**	**V base gear (m/s)**	**V tangenti al gear (m/s)**	**V relative sliding gear (m/s)**	**Specific Sliding - Gear**	**Length Path of Contact (mm)**
47.00	25.88	20.52	0.49	72.85	65.54	31.80	13.62	0.43	61.44	15.50	16.42	0.28	68.02	65.54	18.18	-13.62	-0.75	20.52
46.91	25.65	20.30	0.48	72.70	65.54	31.47	13.05	0.41	61.49	15.70	16.64	0.28	68.08	65.54	18.42	-13.05	-0.71	20.30
46.82	25.41	20.09	0.48	72.56	65.54	31.14	12.49	0.40	61.55	15.89	16.85	0.28	68.14	65.54	18.65	-12.49	-0.67	20.09
46.73	25.18	19.88	0.47	72.42	65.54	30.81	11.92	0.39	61.61	16.08	17.06	0.29	68.21	65.54	18.89	-11.92	-0.63	19.88
46.64	24.94	19.67	0.47	72.28	65.54	30.48	11.36	0.37	61.67	16.27	17.27	0.29	68.27	65.54	19.12	-11.36	-0.59	19.67
46.55	24.70	19.45	0.46	72.14	65.54	30.15	10.79	0.36	61.73	16.46	17.49	0.30	68.34	65.54	19.36	-10.79	-0.56	19.45
46.46	24.47	19.24	0.45	72.01	65.54	29.82	10.23	0.34	61.79	16.64	17.70	0.30	68.41	65.54	19.59	-10.23	-0.52	19.24
46.37	24.23	19.03	0.45	71.87	65.54	29.49	9.66	0.33	61.85	16.83	17.91	0.30	68.48	65.54	19.83	-9.66	-0.49	19.03
46.28	23.99	18.81	0.44	71.74	65.54	29.16	9.10	0.31	61.91	17.02	18.12	0.31	68.54	65.54	20.06	-9.10	-0.45	18.81
46.20	23.75	18.60	0.44	71.60	65.54	28.83	8.53	0.30	61.98	17.21	18.34	0.31	68.61	65.54	20.30	-8.53	-0.42	18.60
46.11	23.50	18.39	0.43	71.47	65.54	28.50	7.97	0.28	62.04	17.40	18.55	0.31	68.68	65.54	20.54	-7.97	-0.39	18.39
46.03	23.26	18.18	0.43	71.34	65.54	28.17	7.40	0.26	62.10	17.58	18.76	0.32	68.75	65.54	20.77	-7.40	-0.36	18.18
45.94	23.02	17.96	0.42	71.21	65.54	27.84	6.84	0.25	62.17	17.77	18.97	0.32	68.83	65.54	21.01	-6.84	-0.33	17.96
45.86	22.77	17.75	0.42	71.08	65.54	27.52	6.27	0.23	62.23	17.96	19.19	0.32	68.90	65.54	21.24	-6.27	-0.30	17.75
45.78	22.53	17.54	0.41	70.96	65.54	27.19	5.71	0.21	62.30	18.14	19.40	0.33	68.97	65.54	21.48	-5.71	-0.27	17.54
45.70	22.28	17.33	0.41	70.83	65.54	26.86	5.14	0.19	62.36	18.33	19.61	0.33	69.04	65.54	21.71	-5.14	-0.24	17.33
45.62	22.03	17.11	0.40	70.71	65.54	26.53	4.58	0.17	62.43	18.51	19.82	0.33	69.12	65.54	21.95	-4.58	-0.21	17.11
45.54	21.79	16.90	0.40	70.58	65.54	26.20	4.01	0.15	62.50	18.70	20.04	0.34	69.19	65.54	22.18	-4.01	-0.18	16.90
45.46	21.54	16.69	0.39	70.46	65.54	25.87	3.45	0.13	62.57	18.88	20.25	0.34	69.27	65.54	22.42	-3.45	-0.15	16.69
45.38	21.29	16.48	0.39	70.34	65.54	25.54	2.89	0.11	62.64	19.07	20.46	0.35	69.35	65.54	22.65	-2.89	-0.13	16.48
45.31	21.04	16.26	0.38	70.22	65.54	25.21	2.32	0.09	62.71	19.25	20.67	0.35	69.42	65.54	22.89	-2.32	-0.10	16.26
45.23	20.79	16.05	0.38	70.10	65.54	24.88	1.76	0.07	62.78	19.43	20.89	0.35	69.50	65.54	23.12	-1.76	-0.08	16.05
45.16	20.53	15.84	0.37	69.99	65.54	24.55	1.19	0.05	62.85	19.62	21.10	0.36	69.58	65.54	23.36	-1.19	-0.05	15.84
45.08	20.28	15.63	0.37	69.87	65.54	24.22	0.63	0.03	62.92	19.80	21.31	0.36	69.66	65.54	23.59	-0.63	-0.03	15.63
45.01	20.03	15.41	0.36	69.76	65.54	23.89	0.06	0.00	62.99	19.98	21.52	0.36	69.74	65.54	23.83	-0.06	0.00	15.41
44.94	19.77	15.20	0.36	69.65	65.54	23.56	-0.50	-0.02	63.07	20.16	21.74	0.37	69.82	65.54	24.07	0.50	0.02	15.20
44.86	19.52	14.99	0.35	69.54	65.54	23.23	-1.07	-0.05	63.14	20.34	21.95	0.37	69.90	65.54	24.30	1.07	0.04	14.99
44.79	19.26	14.78	0.35	69.43	65.54	22.90	-1.63	-0.07	63.21	20.52	22.16	0.37	69.98	65.54	24.54	1.63	0.07	14.78
44.72	19.00	14.56	0.34	69.32	65.54	22.57	-2.20	-0.10	63.29	20.70	22.37	0.38	70.07	65.54	24.77	2.20	0.09	14.56
44.66	18.75	14.35	0.34	69.21	65.54	22.24	-2.76	-0.12	63.36	20.88	22.59	0.38	70.15	65.54	25.01	2.76	0.11	14.35
44.59	18.49	14.14	0.33	69.11	65.54	21.91	-3.33	-0.15	63.44	21.06	22.80	0.39	70.23	65.54	25.24	3.33	0.13	14.14
44.52	18.23	13.93	0.33	69.00	65.54	21.58	-3.89	-0.18	63.52	21.24	23.01	0.39	70.32	65.54	25.48	3.89	0.15	13.93
44.45	17.97	13.71	0.32	68.90	65.54	21.26	-4.46	-0.21	63.59	21.42	23.22	0.39	70.40	65.54	25.71	4.46	0.17	13.71
44.39	17.71	13.50	0.32	68.80	65.54	20.93	-5.02	-0.24	63.67	21.60	23.44	0.40	70.49	65.54	25.95	5.02	0.19	13.50
44.32	17.45	13.29	0.31	68.70	65.54	20.60	-5.59	-0.27	63.75	21.78	23.65	0.40	70.58	65.54	26.18	5.59	0.21	13.29
44.26	17.18	13.08	0.31	68.60	65.54	20.27	-6.15	-0.30	63.83	21.95	23.86	0.40	70.67	65.54	26.42	6.15	0.23	13.08
44.20	16.92	12.86	0.30	68.51	65.54	19.94	-6.72	-0.34	63.91	22.13	24.07	0.41	70.75	65.54	26.65	6.72	0.25	12.86
44.14	16.66	12.65	0.30	68.41	65.54	19.61	-7.28	-0.37	63.99	22.31	24.29	0.41	70.84	65.54	26.89	7.28	0.27	12.65
44.08	16.39	12.44	0.29	68.32	65.54	19.28	-7.85	-0.41	64.07	22.48	24.50	0.41	70.93	65.54	27.12	7.85	0.29	12.44
44.02	16.13	12.23	0.29	68.23	65.54	18.95	-8.41	-0.44	64.15	22.66	24.71	0.42	71.02	65.54	27.36	8.41	0.31	12.23
43.96	15.86	12.01	0.28	68.14	65.54	18.62	-8.98	-0.48	64.23	22.83	24.93	0.42	71.11	65.54	27.59	8.98	0.33	12.01
43.90	15.59	11.80	0.28	68.05	65.54	18.29	-9.54	-0.52	64.32	23.01	25.14	0.42	71.21	65.54	27.83	9.54	0.34	11.80
43.85	15.32	11.59	0.27	67.96	65.54	17.96	-10.10	-0.56	64.40	23.18	25.35	0.43	71.30	65.54	28.07	10.10	0.36	11.59
43.79	15.06	11.38	0.27	67.87	65.54	17.63	-10.67	-0.61	64.48	23.35	25.56	0.43	71.39	65.54	28.30	10.67	0.38	11.38
43.73	14.79	11.16	0.26	67.79	65.54	17.30	-11.23	-0.65	64.57	23.53	25.78	0.44	71.48	65.54	28.54	11.23	0.39	11.16
43.68	14.52	10.95	0.26	67.70	65.54	16.97	-11.80	-0.70	64.65	23.70	25.99	0.44	71.58	65.54	28.77	11.80	0.41	10.95
43.63	14.25	10.74	0.25	67.62	65.54	16.64	-12.36	-0.74	64.74	23.87	26.20	0.44	71.67	65.54	29.01	12.36	0.43	10.74
43.58	13.98	10.53	0.25	67.54	65.54	16.31	-12.93	-0.79	64.83	24.04	26.41	0.45	71.77	65.54	29.24	12.93	0.44	10.53
43.53	13.71	10.31	0.24	67.46	65.54	15.98	-13.49	-0.84	64.91	24.22	26.63	0.45	71.87	65.54	29.48	13.49	0.46	10.31
43.48	13.43	10.10	0.24	67.39	65.54	15.65	-14.06	-0.90	65.00	24.39	26.84	0.45	71.96	65.54	29.71	14.06	0.47	10.10

For a given gear pair 45/63, spesific sliding velocities were found by the new analytical method as shown in Figure 4.5. KISSsoft programme was used to create the same gear pair geometry by using the same gear parameters as shown in Table 4.2 and the result was seen in Figure 4.6. It was found that contact ratio was the same as KISSsoft result that was 1.76. It means that the gear output parameters which are summarized in Table 4.4 are in line with KISSsoft program.

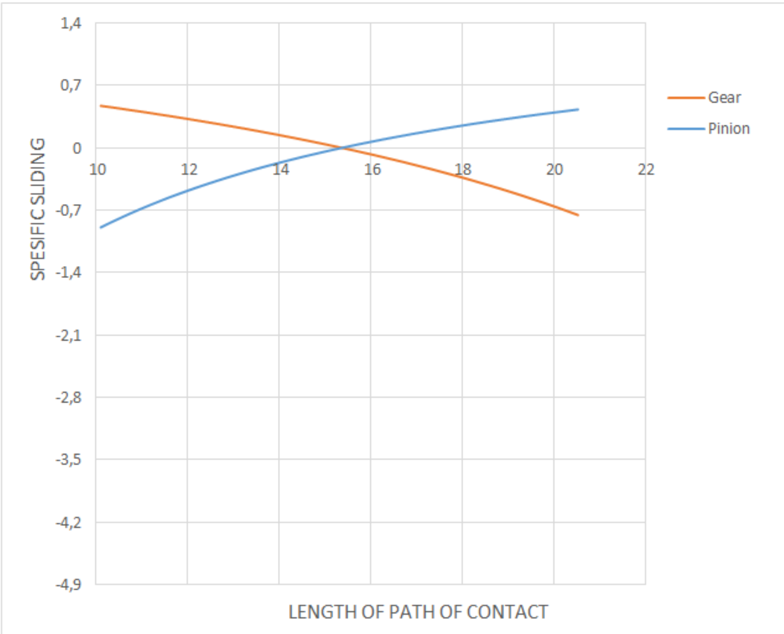

Figure 4.5 *Specific Sliding Velocities of Teeth Numbers of 45 and 63 by the New Analytical Method.*

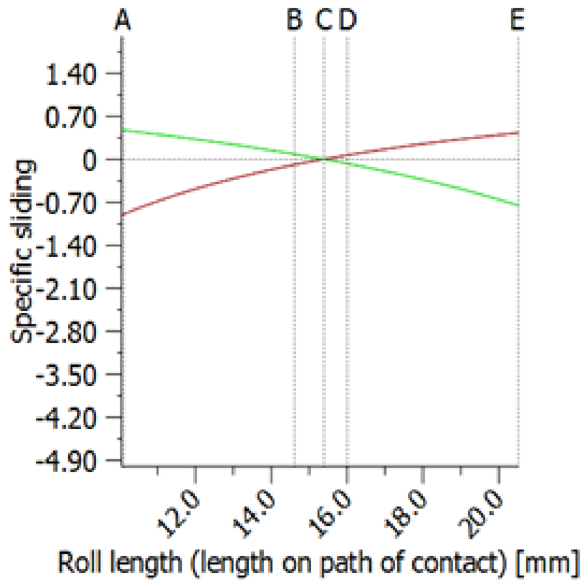

Figure 4.6 *Specific sliding Velocities of Teeth Numbers of 45 and 63 in KISSsoft.*

For the second gear pair, teeth numbers of 45/57, input ant output parameters were given in Table 4.5. Diagram shown in Figure 4.4 can be effectively used to create output data shown in Table 4.6.

Table 4.5 *Pinion and Gear Parameters of Teeth Numbers of 45 and 57.*

	Pinion	**Gear**
Module	2	2
Teeth Number	45	57
Pressure Angle (α)	20	20
Gear Width (mm)	13	14
v	0.3	0.3
E (N/m^2)	200000	200000
Base Output		
Base Radius (mm)	42.2	53.5
Addendum Factor	1	1
Dedendum Factor	1.25	1.25
Pitch Radius [Reference Radius] (mm)	45	57
Tip Radius (mm)	47	59
Root Radius (mm)	42.5	54.5
Center Distance of Gear Pair (mm)	102	
Working Pressure Angle	20	20
Length of Theoretical Line of Action (mm)	34.88	
Length of Actual Line of Action (mm)	10.36	
Contact Ratio [Ɛ]	**1.75**	

Table 4.6 *Geometrical Values of Gear Mesh of Teeth Numbers of 45 and 57.*

[1-7]: Length of Theroretical Line of Action	34.89
[1-6]	24.74
[6-7]	10.15
[2-7]	20.52
[1-2]	14.37
[2-6]	10.37
P_B = [3-6]=[2-5]	5.90
[5-6]	4.46
[2-3]	4.46
[1-5]	20.27
$r_{SAP1\ pinion}$	43.49
$r_{EAP1\ -\ pinion}$	47.00
$r_{SAP2\ -\ gear}$	59.00
$r_{EAP2\ -\ gear}$	55.46
$r_{HPSTC1\ -\ pinion}$	45.23
$r_{LPSTC1\ -\ pinion}$	44.74
$r_{HPSTC2\ -\ gear}$	57.27
$r_{LPSTC2\ -\ gear}$	56.78

Table 4.7 *Mesh Properties of Teeth Numbers of 45 and 57.*

CONTACT LENGTH																				
Pinion (r_{any}) (mm)	Pinion Pressure Angle (Degree)	Curvature Radius Pinion (mm)	Pinion θany (Roll Angle) (Degree)	V pinion (m/s)	V base pinion (m/s)	V tangential pinion (m/s)	V relative sliding pinion (m/s)	Specific Sliding - Pinion	Gear (r_{any}) (mm)	Gear Pressure Angle (Degree)	Curvature Radius Gear (mm)	Gear θany (Roll Angle) (Degree)	V gear (m/s)	V base gear (m/s)	V tangenti al gear (m/s)	V relative sliding gear (m/s)	Specific Sliding - Gear	Length Path of Contact (mm)
47.00	25.88	20.52	0.49	72.85	65.54	31.80	14.21	0.45	55.46	15.02	14.37	0.27	67.86	65.54	17.58	-14.21	-0.81	20.52
46.91	25.65	20.30	0.48	72.71	65.54	31.47	13.63	0.43	55.51	15.23	14.58	0.27	67.93	65.54	17.84	-13.63	-0.76	20.30
46.82	25.41	20.09	0.48	72.56	65.54	31.14	13.04	0.42	55.57	15.44	14.79	0.28	68.00	65.54	18.10	-13.04	-0.72	20.09
46.73	25.18	19.88	0.47	72.42	65.54	30.81	12.45	0.40	55.62	15.65	15.01	0.28	68.07	65.54	18.36	-12.45	-0.68	19.88
46.64	24.94	19.67	0.47	72.28	65.54	30.49	11.87	0.39	55.68	15.86	15.22	0.28	68.14	65.54	18.62	-11.87	-0.64	19.67
46.55	24.71	19.46	0.46	72.15	65.54	30.16	11.28	0.37	55.74	16.07	15.43	0.29	68.21	65.54	18.88	-11.28	-0.60	19.46
46.46	24.47	19.25	0.46	72.01	65.54	29.83	10.69	0.36	55.80	16.28	15.64	0.29	68.28	65.54	19.14	-10.69	-0.56	19.25
46.37	24.23	19.03	0.45	71.88	65.54	29.50	10.10	0.34	55.86	16.49	15.85	0.30	68.35	65.54	19.40	-10.10	-0.52	19.03
46.29	23.99	18.82	0.45	71.74	65.54	29.17	9.52	0.33	55.92	16.69	16.06	0.30	68.43	65.54	19.66	-9.52	-0.48	18.82
46.20	23.76	18.61	0.44	71.61	65.54	28.85	8.93	0.31	55.98	16.90	16.28	0.30	68.50	65.54	19.92	-8.93	-0.45	18.61
46.12	23.51	18.40	0.44	71.48	65.54	28.52	8.34	0.29	56.04	17.11	16.49	0.31	68.58	65.54	20.17	-8.34	-0.41	18.40
46.03	23.27	18.19	0.43	71.35	65.54	28.19	7.76	0.28	56.11	17.32	16.70	0.31	68.65	65.54	20.43	-7.76	-0.38	18.19
45.95	23.03	17.98	0.43	71.22	65.54	27.86	7.17	0.26	56.17	17.52	16.91	0.32	68.73	65.54	20.69	-7.17	-0.35	17.98
45.87	22.79	17.76	0.42	71.09	65.54	27.53	6.58	0.24	56.23	17.73	17.12	0.32	68.81	65.54	20.95	-6.58	-0.31	17.76
45.78	22.54	17.55	0.42	70.96	65.54	27.21	6.00	0.22	56.30	17.93	17.33	0.32	68.89	65.54	21.21	-6.00	-0.28	17.55
45.70	22.30	17.34	0.41	70.84	65.54	26.88	5.41	0.20	56.36	18.14	17.54	0.33	68.97	65.54	21.47	-5.41	-0.25	17.34
45.62	22.05	17.13	0.41	70.72	65.54	26.55	4.82	0.18	56.43	18.34	17.76	0.33	69.05	65.54	21.73	-4.82	-0.22	17.13
45.54	21.81	16.92	0.40	70.59	65.54	26.22	4.24	0.16	56.50	18.54	17.97	0.34	69.13	65.54	21.99	-4.24	-0.19	16.92
45.47	21.56	16.71	0.40	70.47	65.54	25.89	3.65	0.14	56.56	18.75	18.18	0.34	69.21	65.54	22.25	-3.65	-0.16	16.71
45.39	21.31	16.49	0.39	70.35	65.54	25.57	3.06	0.12	56.63	18.95	18.39	0.34	69.30	65.54	22.50	-3.06	-0.14	16.49
45.31	21.06	16.28	0.39	70.23	65.54	25.24	2.47	0.10	56.70	19.15	18.60	0.35	69.38	65.54	22.76	-2.47	-0.11	16.28
45.24	20.81	16.07	0.38	70.12	65.54	24.91	1.89	0.08	56.77	19.35	18.81	0.35	69.47	65.54	23.02	-1.89	-0.08	16.07
45.16	20.56	15.86	0.38	70.00	65.54	24.58	1.30	0.05	56.84	19.56	19.03	0.36	69.55	65.54	23.28	-1.30	-0.06	15.86
45.09	20.31	15.65	0.37	69.89	65.54	24.25	0.71	0.03	56.91	19.76	19.24	0.36	69.64	65.54	23.54	-0.71	-0.03	15.65
45.02	20.05	15.44	0.37	69.77	65.54	23.93	0.13	0.01	56.98	19.96	19.45	0.36	69.73	65.54	23.80	-0.13	-0.01	15.44
44.94	19.80	15.22	0.36	69.66	65.54	23.60	-0.46	-0.02	57.06	20.16	19.66	0.37	69.82	65.54	24.06	0.46	0.02	15.22
44.87	19.55	15.01	0.36	69.55	65.54	23.27	-1.05	-0.05	57.13	20.36	19.87	0.37	69.91	65.54	24.32	1.05	0.04	15.01
44.80	19.29	14.80	0.35	69.44	65.54	22.94	-1.63	-0.07	57.20	20.55	20.08	0.37	70.00	65.54	24.58	1.63	0.07	14.80
44.73	19.04	14.59	0.35	69.33	65.54	22.61	-2.22	-0.10	57.28	20.75	20.30	0.38	70.09	65.54	24.84	2.22	0.09	14.59
44.66	18.78	14.38	0.34	69.23	65.54	22.29	-2.81	-0.13	57.35	20.95	20.51	0.38	70.18	65.54	25.09	2.81	0.11	14.38
44.60	18.52	14.17	0.34	69.12	65.54	21.96	-3.39	-0.15	57.43	21.15	20.72	0.39	70.27	65.54	25.35	3.39	0.13	14.17
44.53	18.26	13.96	0.33	69.02	65.54	21.63	-3.98	-0.18	57.51	21.34	20.93	0.39	70.37	65.54	25.61	3.98	0.16	13.96
44.46	18.00	13.74	0.33	68.92	65.54	21.30	-4.57	-0.21	57.58	21.54	21.14	0.39	70.46	65.54	25.87	4.57	0.18	13.74
44.40	17.75	13.53	0.32	68.82	65.54	20.97	-5.16	-0.25	57.66	21.74	21.35	0.40	70.56	65.54	26.13	5.16	0.20	13.53
44.33	17.48	13.32	0.32	68.72	65.54	20.65	-5.74	-0.28	57.74	21.93	21.57	0.40	70.65	65.54	26.39	5.74	0.22	13.32
44.27	17.22	13.11	0.31	68.62	65.54	20.32	-6.33	-0.31	57.82	22.13	21.78	0.41	70.75	65.54	26.65	6.33	0.24	13.11
44.21	16.96	12.90	0.30	68.52	65.54	19.99	-6.92	-0.35	57.90	22.32	21.99	0.41	70.85	65.54	26.91	6.92	0.26	12.90
44.15	16.70	12.69	0.30	68.43	65.54	19.66	-7.50	-0.38	57.98	22.51	22.20	0.41	70.95	65.54	27.17	7.50	0.28	12.69
44.09	16.44	12.47	0.29	68.33	65.54	19.33	-8.09	-0.42	58.06	22.71	22.41	0.42	71.05	65.54	27.42	8.09	0.30	12.47
44.03	16.17	12.26	0.29	68.24	65.54	19.01	-8.68	-0.46	58.14	22.90	22.62	0.42	71.15	65.54	27.68	8.68	0.31	12.26
43.97	15.91	12.05	0.28	68.15	65.54	18.68	-9.26	-0.50	58.23	23.09	22.84	0.43	71.25	65.54	27.94	9.26	0.33	12.05
43.91	15.64	11.84	0.28	68.06	65.54	18.35	-9.85	-0.54	58.31	23.28	23.05	0.43	71.35	65.54	28.20	9.85	0.35	11.84
43.86	15.37	11.63	0.27	67.97	65.54	18.02	-10.44	-0.58	58.39	23.47	23.26	0.43	71.45	65.54	28.46	10.44	0.37	11.63
43.80	15.11	11.42	0.27	67.89	65.54	17.69	-11.03	-0.62	58.48	23.66	23.47	0.44	71.56	65.54	28.72	11.03	0.38	11.42
43.75	14.84	11.20	0.26	67.80	65.54	17.37	-11.61	-0.67	58.56	23.85	23.68	0.44	71.66	65.54	28.98	11.61	0.40	11.20
43.69	14.57	10.99	0.26	67.72	65.54	17.04	-12.20	-0.72	58.65	24.04	23.89	0.45	71.77	65.54	29.24	12.20	0.42	10.99
43.64	14.30	10.78	0.25	67.64	65.54	16.71	-12.79	-0.77	58.74	24.23	24.11	0.45	71.87	65.54	29.50	12.79	0.43	10.78
43.59	14.03	10.57	0.25	67.56	65.54	16.38	-13.37	-0.82	58.82	24.42	24.32	0.45	71.98	65.54	29.76	13.37	0.45	10.57
43.54	13.76	10.36	0.24	67.48	65.54	16.05	-13.96	-0.87	58.91	24.60	24.53	0.46	72.09	65.54	30.01	13.96	0.47	10.36
43.49	13.49	10.15	0.24	67.40	65.54	15.73	-14.55	-0.93	59.00	24.79	24.74	0.46	72.20	65.54	30.27	14.55	0.48	10.15

For a given gear pair of 45/57, spesific sliding velocities were found by the analytical method as shown in Figure 4.7. KISSsoft programme was used to create the same gear pair geometry by using the same gear parameters in Table 4.7 and the result is shown in Figure 4.8.

It was found that contact ratio was the same as KISSsoft result that was 1.75. It means that the gear output parameters which are summarized in Table 4.7 are in agreement with KISSsoft program.

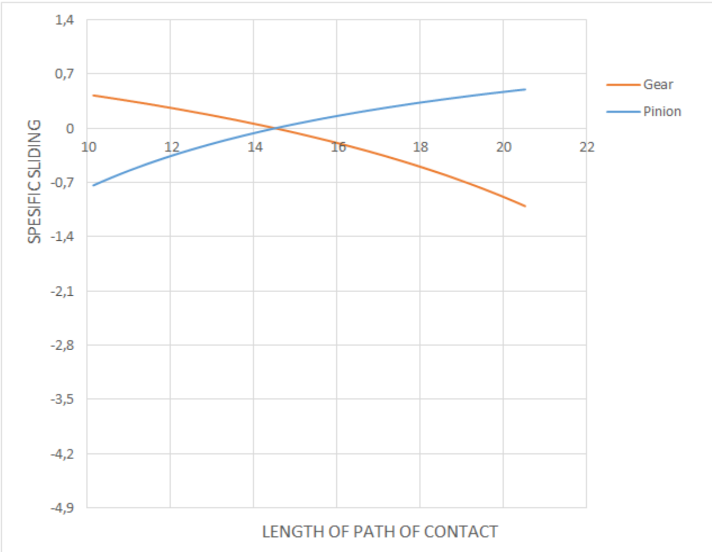

Figure 4.7 *Specific Sliding Velocities of Teeth Numbers of 45 and 57 by the Analytical Method.*

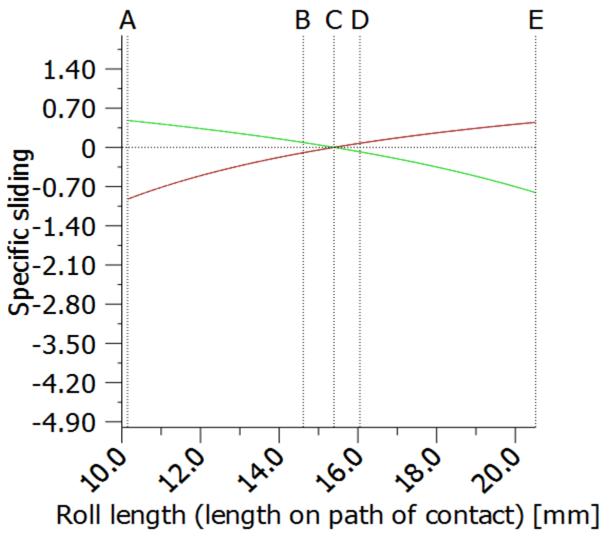

Figure 4.8 *Specific Sliding Velocities of Teeth Numbers of 45 and 57 in KISSsoft.*

For the third gear pair, teeth numbers of 29/49, input ant output parameters were given in Table 4.8. Diagram shown in Figure 4.4 was effectively used to create the output data shown in Table 4.9.

Table 4.8 *Pinion and Gear Parameters of Teeth Numbers of 29 and 49.*

	Pinion	**Gear**
Module	2	2
Teeth Number	29	49
Pressure Angle (α)	20	20
Gear Width (mm)	18	19
v	0.3	0.3
E (N/m^2)	200000	200000
Base Output		
Base Radius (mm)	27.2	46.0
Addendum Factor	1	1
Dedendum Factor	1.25	1.25
Pitch Radius [Reference Radius] (mm)	29	49
Tip Radius (mm)	31	51
Root Radius (mm)	26.5	46.5
Center Distance of Gear Pair (mm)	78	
Working Pressure Angle	20	20
Length of Theoretical Line of Action (mm)	26.67	
Length of Actual Line of Action (mm)	10.02	
Contact Ratio [Ɛ]	**1.69**	

Table 4.9 *Geometrical Values of Gear Mesh of Teeth Numbers of 29 and 49.*

[1-7]: Length of Theoretical Line of Action	26.68
[1-6]	21.93
[6-7]	4.75
[2-7]	14.78
[1-2]	11.90
[2-6]	10.03
P_B = [3-6]=[2-5]	5.90
[5-6]	4.12
[2-3]	4.12
[1-5]	17.80
$r_{SAP1\ pinion}$	27.66
$r_{EAP1\ -\ pinion}$	31.00
$r_{SAP2\ -\ gear}$	51.00
$r_{EAP2\ -\ gear}$	47.56
$r_{HPSTC1\ -\ pinion}$	29.26
$r_{LPSTC1\ -\ pinion}$	28.66
$r_{HPSTC2\ -\ gear}$	49.37
$r_{LPSTC2\ -\ gear}$	48.75

Geometrical values of gear mesh including specific sliding velocities were also given in Table 4.10. Specific sliding velocities were also stated in Table 4.10 as “Specific Sliding Gear” and “Specific Sliding Pinion”. For a gear pair of 29/49, radius of contact points on contact line was calculated for pinion and gear and also stated in Table 4.10. Curvatures radius of pinion and gear were calculated for instant gear mesh points.

Table 4.10 *Mesh Properties of Teeth Numbers of 29 and 49.*

CONTACT LENGTH																					
Pinion (r_{any}) (mm)	**Pinion Pressure Angle (Degree)**	**Curvature Radius Pinion (mm)**	**Pinion θany (Roll Angle) (Degree)**	**V pinion (m/s)**	**V base pinion (m/s)**	**V tangential pinion (m/s)**	**V relative sliding pinion (m/s)**	**Specific Sliding - Pinion**	**Gear (r_{any}) (mm)**	**Gear Pressure Angle (Degree)**	**Curvature Radius Gear (mm)**	**Gear θany (Roll Angle) (Degree)**	**V gear (m/s)**	**V base gear (m/s)**	**V tangential gear (m/s)**	**V relative sliding gear (m/s)**	**Specific Sliding - Gear**	**Length Path of Contact (mm)**			
31.00	28.47	14.78	0.54	48.05	42.24	22.90	11.99	0.52	47.56	14.49	11.90	0.26	43.63	42.24	10.92	-11.99	-1.10	14.78			
30.90	28.14	14.57	0.53	47.90	42.24	22.59	11.48	0.51	47.61	14.73	12.10	0.26	43.67	42.24	11.10	-11.48	-1.03	14.57			
30.81	27.80	14.37	0.53	47.75	42.24	22.27	10.98	0.49	47.66	14.97	12.31	0.27	43.72	42.24	11.29	-10.98	-0.97	14.37			
30.71	27.46	14.16	0.52	47.60	42.24	21.95	10.47	0.48	47.72	15.20	12.51	0.27	43.77	42.24	11.48	-10.47	-0.91	14.16			
30.62	27.12	13.96	0.51	47.46	42.24	21.64	9.97	0.46	47.77	15.44	12.72	0.28	43.82	42.24	11.67	-9.97	-0.85	13.96			
30.53	26.78	13.75	0.50	47.31	42.24	21.32	9.46	0.44	47.82	15.68	12.92	0.28	43.87	42.24	11.85	-9.46	-0.80	13.75			
30.43	26.44	13.55	0.50	47.17	42.24	21.00	8.96	0.43	47.88	15.91	13.13	0.29	43.92	42.24	12.04	-8.96	-0.74	13.55			
30.34	26.09	13.34	0.49	47.03	42.24	20.68	8.45	0.41	47.94	16.15	13.33	0.29	43.97	42.24	12.23	-8.45	-0.69	13.34			
30.25	25.74	13.14	0.48	46.89	42.24	20.37	7.95	0.39	47.99	16.38	13.54	0.29	44.03	42.24	12.42	-7.95	-0.64	13.14			
30.17	25.39	12.94	0.47	46.76	42.24	20.05	7.44	0.37	48.05	16.62	13.74	0.30	44.08	42.24	12.61	-7.44	-0.59	12.94			
30.08	25.04	12.73	0.47	46.62	42.24	19.73	6.94	0.35	48.11	16.85	13.95	0.30	44.13	42.24	12.79	-6.94	-0.54	12.73			
29.99	24.69	12.53	0.46	46.49	42.24	19.42	6.43	0.33	48.17	17.08	14.15	0.31	44.19	42.24	12.98	-6.43	-0.50	12.53			
29.91	24.33	12.32	0.45	46.35	42.24	19.10	5.93	0.31	48.23	17.32	14.36	0.31	44.24	42.24	13.17	-5.93	-0.45	12.32			
29.82	23.97	12.12	0.44	46.23	42.24	18.78	5.42	0.29	48.29	17.55	14.56	0.32	44.30	42.24	13.36	-5.42	-0.41	12.12			
29.74	23.61	11.91	0.44	46.10	42.24	18.46	4.92	0.27	48.35	17.78	14.77	0.32	44.36	42.24	13.54	-4.92	-0.36	11.91			
29.66	23.25	11.71	0.43	45.97	42.24	18.15	4.41	0.24	48.42	18.01	14.97	0.33	44.41	42.24	13.73	-4.41	-0.32	11.71			
29.58	22.89	11.50	0.42	45.85	42.24	17.83	3.91	0.22	48.48	18.24	15.17	0.33	44.47	42.24	13.92	-3.91	-0.28	11.50			
29.50	22.52	11.30	0.41	45.72	42.24	17.51	3.40	0.19	48.55	18.47	15.38	0.33	44.53	42.24	14.11	-3.40	-0.24	11.30			
29.42	22.15	11.09	0.41	45.60	42.24	17.19	2.90	0.17	48.61	18.70	15.58	0.34	44.59	42.24	14.30	-2.90	-0.20	11.09			
29.35	21.78	10.89	0.40	45.49	42.24	16.88	2.39	0.14	48.68	18.93	15.79	0.34	44.65	42.24	14.48	-2.39	-0.17	10.89			
29.27	21.41	10.68	0.39	45.37	42.24	16.56	1.89	0.11	48.74	19.15	15.99	0.35	44.71	42.24	14.67	-1.89	-0.13	10.68			
29.20	21.03	10.48	0.38	45.25	42.24	16.24	1.38	0.09	48.81	19.38	16.20	0.35	44.78	42.24	14.86	-1.38	-0.09	10.48			
29.12	20.66	10.27	0.38	45.14	42.24	15.93	0.88	0.06	48.88	19.61	16.40	0.36	44.84	42.24	15.05	-0.88	-0.06	10.27			
29.05	20.28	10.07	0.37	45.03	42.24	15.61	0.37	0.02	48.95	19.83	16.61	0.36	44.90	42.24	15.23	-0.37	-0.02	10.07			
28.98	19.90	9.87	0.36	44.92	42.24	15.29	-0.13	-0.01	49.02	20.06	16.81	0.37	44.97	42.24	15.42	0.13	0.01	9.87			
28.91	19.52	9.66	0.35	44.81	42.24	14.97	-0.64	-0.04	49.09	20.28	17.02	0.37	45.03	42.24	15.61	0.64	0.04	9.66			
28.85	19.14	9.46	0.35	44.71	42.24	14.66	-1.14	-0.08	49.16	20.51	17.22	0.37	45.10	42.24	15.80	1.14	0.07	9.46			
28.78	18.75	9.25	0.34	44.61	42.24	14.34	-1.65	-0.11	49.23	20.73	17.43	0.38	45.16	42.24	15.99	1.65	0.10	9.25			
28.71	18.37	9.05	0.33	44.50	42.24	14.02	-2.15	-0.15	49.30	20.95	17.63	0.38	45.23	42.24	16.17	2.15	0.13	9.05			
28.65	17.98	8.84	0.32	44.41	42.24	13.71	-2.66	-0.19	49.38	21.17	17.84	0.39	45.30	42.24	16.36	2.66	0.16	8.84			
28.59	17.59	8.64	0.32	44.31	42.24	13.39	-3.16	-0.24	49.45	21.39	18.04	0.39	45.36	42.24	16.55	3.16	0.19	8.64			
28.53	17.19	8.43	0.31	44.21	42.24	13.07	-3.67	-0.28	49.53	21.62	18.24	0.40	45.43	42.24	16.74	3.67	0.22	8.43			
28.47	16.80	8.23	0.30	44.12	42.24	12.75	-4.17	-0.33	49.60	21.83	18.45	0.40	45.50	42.24	16.92	4.17	0.25	8.23			
28.41	16.41	8.02	0.29	44.03	42.24	12.44	-4.68	-0.38	49.68	22.05	18.65	0.41	45.57	42.24	17.11	4.68	0.27	8.02			
28.35	16.01	7.82	0.29	43.94	42.24	12.12	-5.18	-0.43	49.76	22.27	18.86	0.41	45.64	42.24	17.30	5.18	0.30	7.82			
28.29	15.61	7.61	0.28	43.86	42.24	11.80	-5.69	-0.48	49.84	22.49	19.06	0.41	45.71	42.24	17.49	5.69	0.33	7.61			
28.24	15.21	7.41	0.27	43.77	42.24	11.48	-6.19	-0.54	49.91	22.71	19.27	0.42	45.79	42.24	17.67	6.19	0.35	7.41			
28.19	14.81	7.20	0.26	43.69	42.24	11.17	-6.70	-0.60	49.99	22.92	19.47	0.42	45.86	42.24	17.86	6.70	0.37	7.20			
28.14	14.41	7.00	0.26	43.61	42.24	10.85	-7.20	-0.66	50.07	23.14	19.68	0.43	45.93	42.24	18.05	7.20	0.40	7.00			
28.09	14.00	6.80	0.25	43.53	42.24	10.53	-7.71	-0.73	50.15	23.35	19.88	0.43	46.01	42.24	18.24	7.71	0.42	6.80			
28.04	13.60	6.59	0.24	43.46	42.24	10.22	-8.21	-0.80	50.24	23.57	20.09	0.44	46.08	42.24	18.43	8.21	0.45	6.59			
27.99	13.19	6.39	0.23	43.38	42.24	9.90	-8.72	-0.88	50.32	23.78	20.29	0.44	46.16	42.24	18.61	8.72	0.47	6.39			
27.94	12.78	6.18	0.23	43.31	42.24	9.58	-9.22	-0.96	50.40	24.00	20.50	0.45	46.23	42.24	18.80	9.22	0.49	6.18			
27.90	12.37	5.98	0.22	43.24	42.24	9.26	-9.73	-1.05	50.48	24.21	20.70	0.45	46.31	42.24	18.99	9.73	0.51	5.98			
27.86	11.96	5.77	0.21	43.18	42.24	8.95	-10.23	-1.14	50.57	24.42	20.91	0.45	46.39	42.24	19.18	10.23	0.53	5.77			
27.81	11.55	5.57	0.20	43.11	42.24	8.63	-10.74	-1.24	50.65	24.63	21.11	0.46	46.47	42.24	19.36	10.74	0.55	5.57			
27.77	11.13	5.36	0.20	43.05	42.24	8.31	-11.24	-1.35	50.74	24.84	21.31	0.46	46.54	42.24	19.55	11.24	0.57	5.36			
27.73	10.72	5.16	0.19	42.99	42.24	8.00	-11.74	-1.47	50.83	25.05	21.52	0.47	46.62	42.24	19.74	11.74	0.59	5.16			
27.70	10.30	4.95	0.18	42.93	42.24	7.68	-12.25	-1.60	50.91	25.26	21.72	0.47	46.70	42.24	19.93	12.25	0.61	4.95			
27.66	9.89	4.75	0.17	42.87	42.24	7.36	-12.75	-1.73	51.00	25.47	21.93	0.48	46.78	42.24	20.12	12.75	0.63	4.75			

For a given gear pair of 29/49, spesific sliding velocities were found by analytical method as shown in Figure 4.9. KISSsoft programme was used to create the same gear pair geometry by using the same gear parameters in Table 4.10 and the result was shown in Figure 4.10.

It was found that contact ratio was the same as KISSsoft result that was 1.69. It means that the gear output parameters which are summarized in Table 4.10 are in agreement with KISSsoft program.

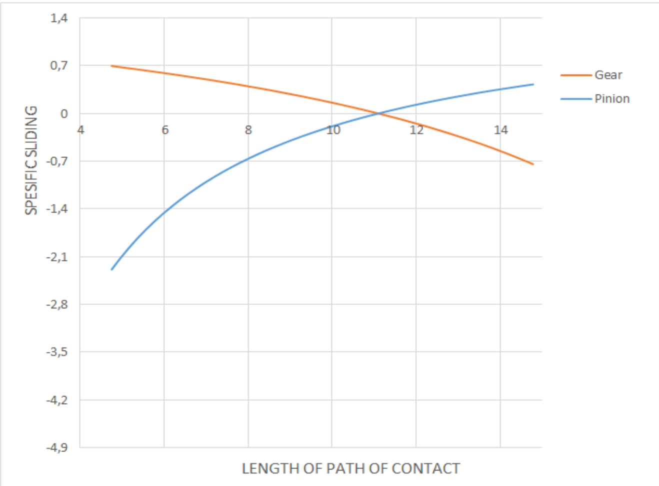

Figure 4.9 *Specific Sliding Velocities of Teeth Numbers of 29 and 49 by the Analytical Method.*

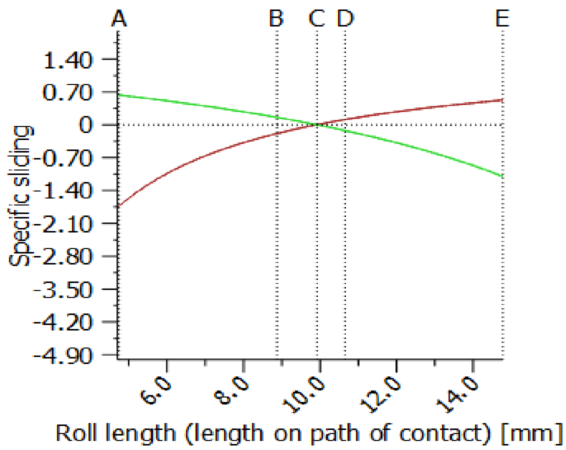

Figure 4.10 *Specific Sliding Velocities of Teeth Numbers of 29 and 49 in KISSsoft.*

4.2 Material Selection

Gear material is one of the most important parameters effecting durability under the high loading applications. In aerospace gearbox applications, SAE9310 steel is used due to its high mechanical properties. In this study, material effects on safety factors were investigated based on different alloys which are 20MnCr5, 18CrNiMo7-6 and SAE9310. The materials 16MnCr5, 18CrNiMo7-6 and SAE9310 correspond to Grades 1-3 respectively as given in Figure 4.11.

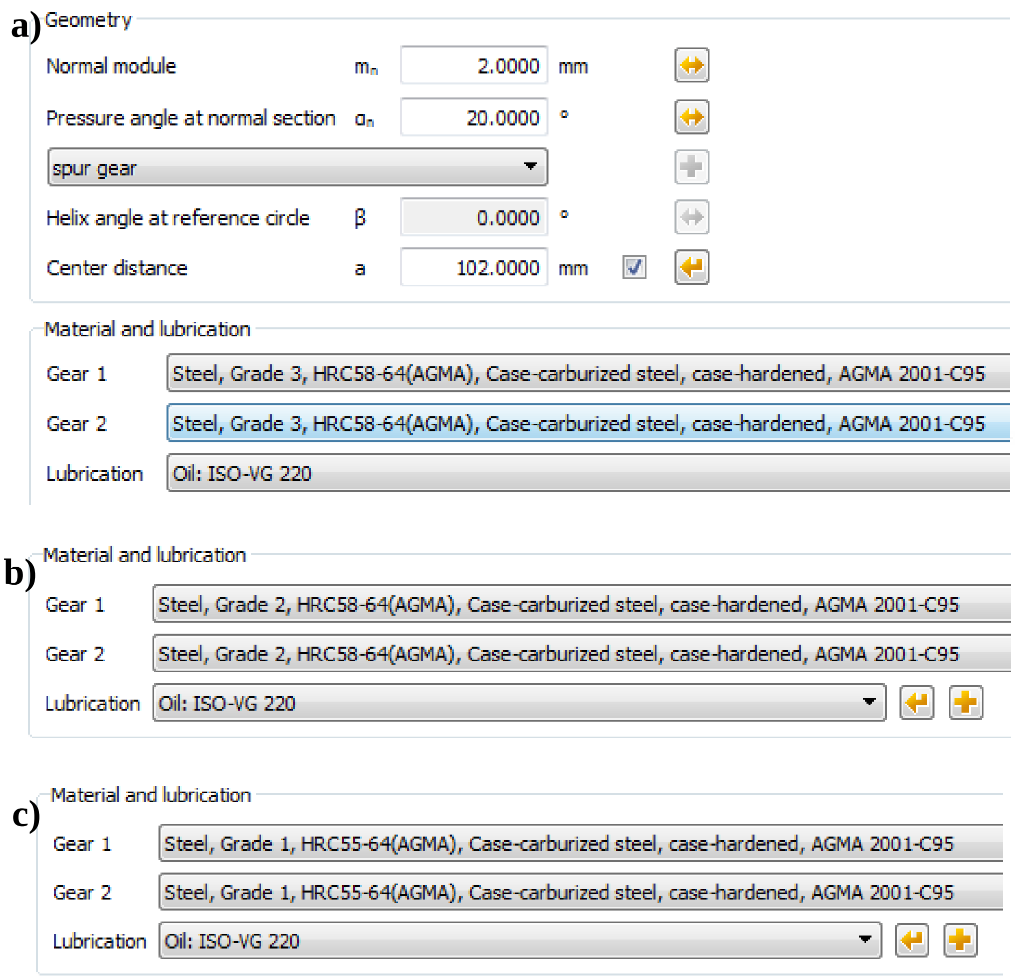

Figure 4.11 *Gear Material Selection (KISSsoft Programme): a) Grade 3 (SAE9310); b) Grade 2 (18CrNiMo7-6); c) Grade 1 (16MnCr5).*

4.3 Profile Modification Selection

Tip relief modifications are commonly carried out on gear geometry in aerospace applications. Tip relief modifications make powertrain system more efficient by decreasing transmission error. However, chosing the starting point for tip relief modification is critical for higher efficiency. HPSTC point could be chosen as starting point for lower transmission error and higher efficiency. Modification parameters are given in Figure 4.12. Related parameters are explained below.

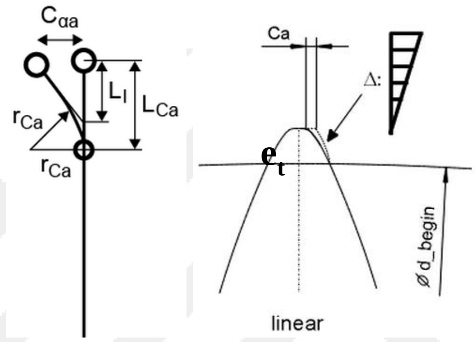

Figure 4.12 *Tip Relief Modification Parameters.*

L_{Ca} : Resulting tip relief length

C_{α_a} : Tip relief

r_{Ca} : Transition radius in the tip area

Hence, the equation can be expressed as:

$$\frac{L_I}{L_{Ca}} = \frac{e_t}{C\alpha_a} \tag{4.1}$$

CHAPTER 5

ANALYSIS AND RESULTS

5.1 Calculation of Mesh Stiffness

Calculations of mesh stiffness for gear pairs were carried out based on gear geometry. For the first gear pair of 45/63, 2D geometries of the gears are shown in Figure 5.1. Contact line during mesh is shown in Figure 5.2.

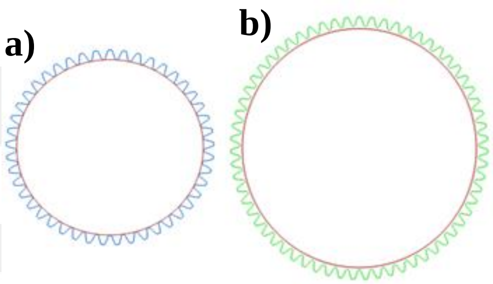

Figure 5.1 *2D Gear Geometry of Gear Pair of 45 and 63: a) Pinion; b) Gear.*

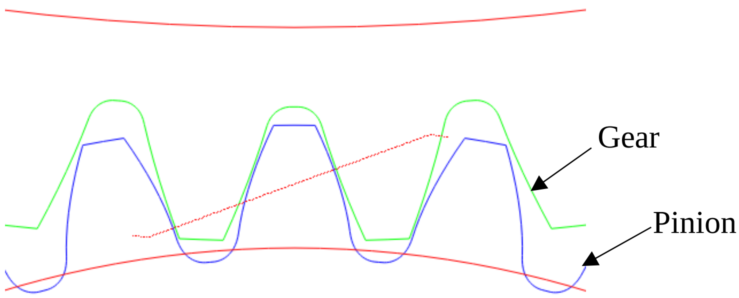

Figure 5.2 *Gear Mesh of Gear Pair of 45 and 63.*

,

3D geometries of the gears were also created and shown in Figure 5.3. Related gear parameters of first gear pair were used to create these geometries.

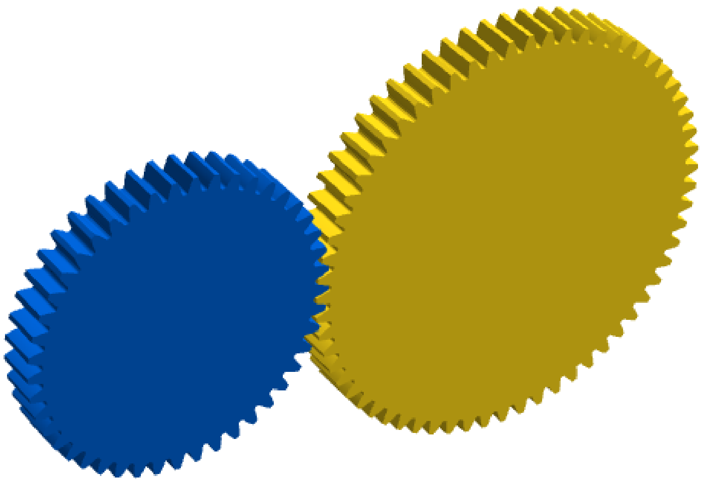

Figure 5.3 *Gear pairs of 3D (45 and 63).*

Calculated mesh stiffness values for the first gear pair of 45/63 are shown as graphs in Figure 5.4. Figure 5.4.a shows pinion stiffness according to length of contact and Figure 5.4.b shows gear stiffness versus length of path of contact.

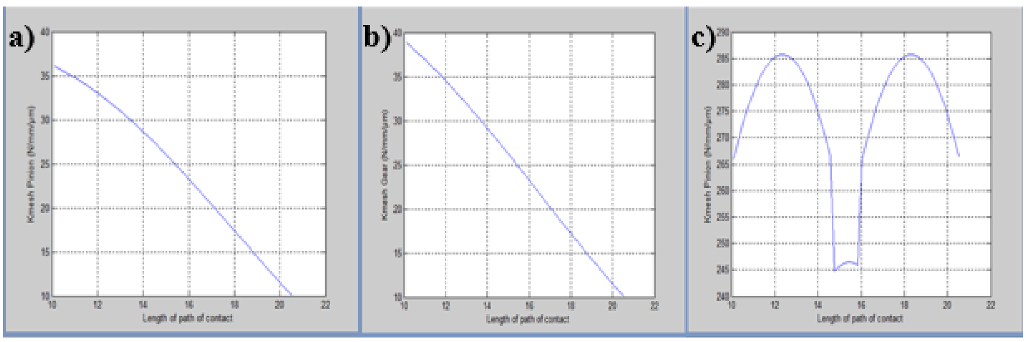

Figure 5.4 *Mesh Stiffness of Gear Pair of 45 and 63: a) Pinion Stiffness; b) Gear Stiffness; c) Mesh Stiffness.*

Figure 5.4.c shows the total mesh stiffness of gear pair. It can be seen that in Figure 5.4.c, stiffness values are decreased where single tooth pair contact occurs. Calculations in KISSsoft program were also run and given in Figure 5.5. It is seen that calculated stiffness values were in agreement with KISSsoft.

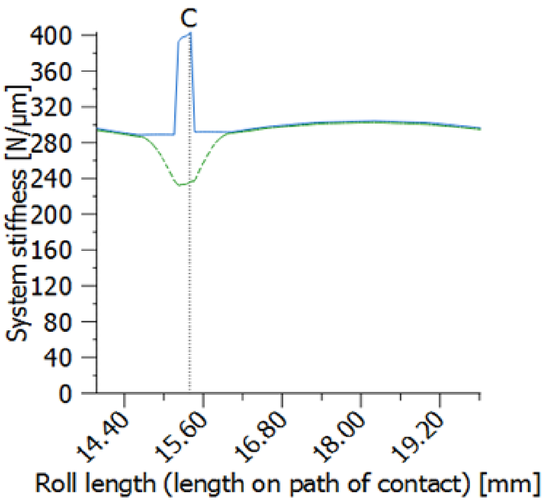

Figure 5.5 *Mesh Stiffness of Gear Pair of 45 and 63 in KISSsoft.*

For the second gear pair of 45/57, 2D geometries of the gears are shown in Figure 5.6. Contact line during mesh is shown in Figure 5.7.

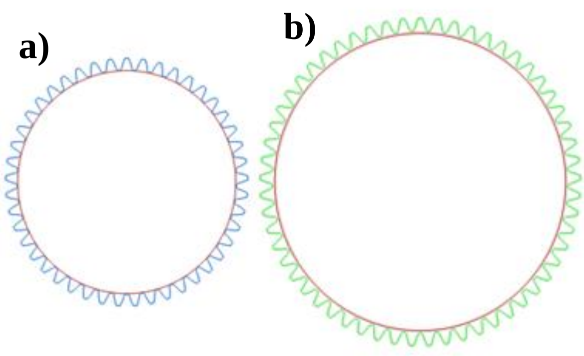

Figure 5.6 *2D Gear Geometry of Gear Pair of 45 and 57: a) Pinion; b) Gear.*

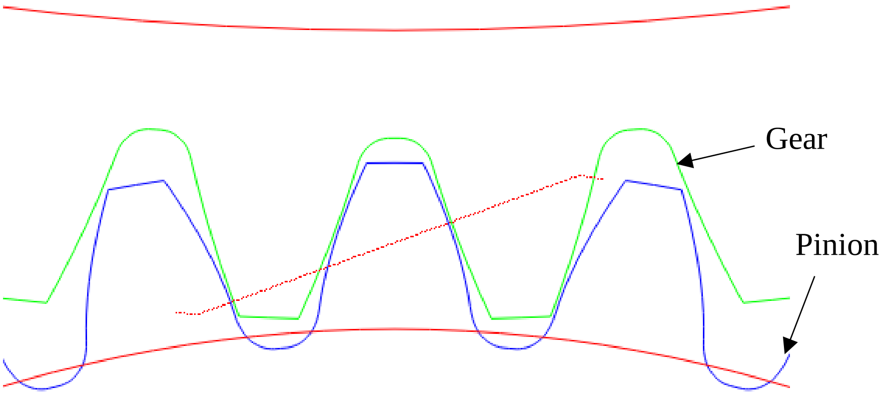

Figure 5.7 *Gear Mesh of Gear Pair of 45 and 57.*

3D geometries of the gears were also created and shown in Figure 5.8. Related gear parameters of second gear pair were used to create these geometries.

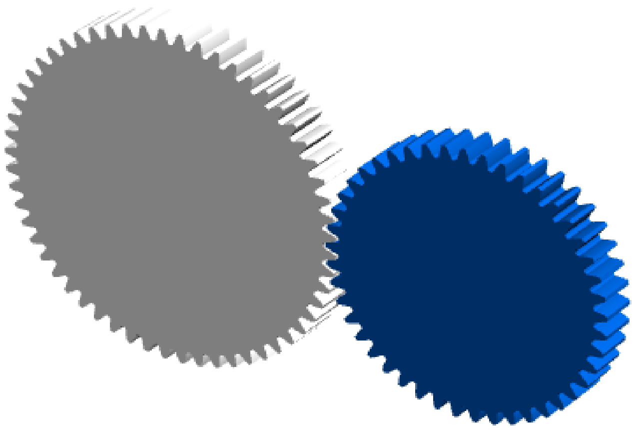

Figure 5.8 *Gear Pair of 3D (45 and 57).*

Calculated mesh stiffness vaules for the second gear pair of 45/57 are shown in Figure 5.9. Figure 5.9.a shows pinion stiffness according to length of contact and Figure 5.9.b shows gear stiffness versus length of path of contact.

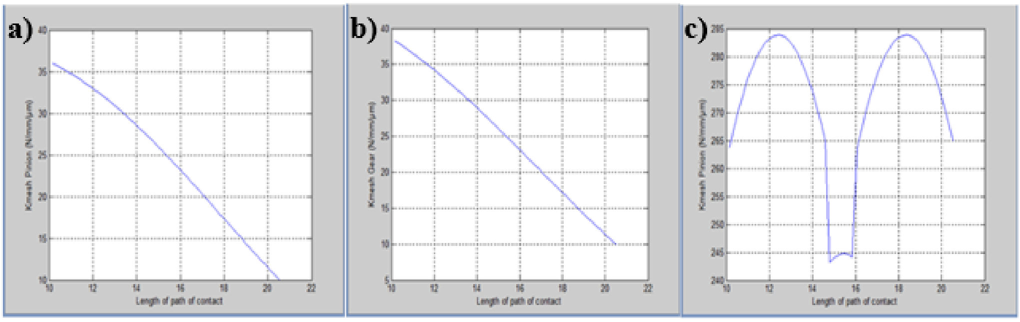

Figure 5.9 *Mesh Stiffness of Gear Pair of 45 and 57: a) Pinion Stiffness; b) Gear Stiffness; c) Mesh Stiffness.*

Figure 5.9.c shows the total mesh stiffness of gear pair. It can be seen that in Figure 5.9.c, the stiffness values were decreased where single tooth pair contact occurs. Calculations in KISSsoft program were also run and given in Figure 5.10. It is seen that calculated stiffness values were in agreement with KISSsoft results.

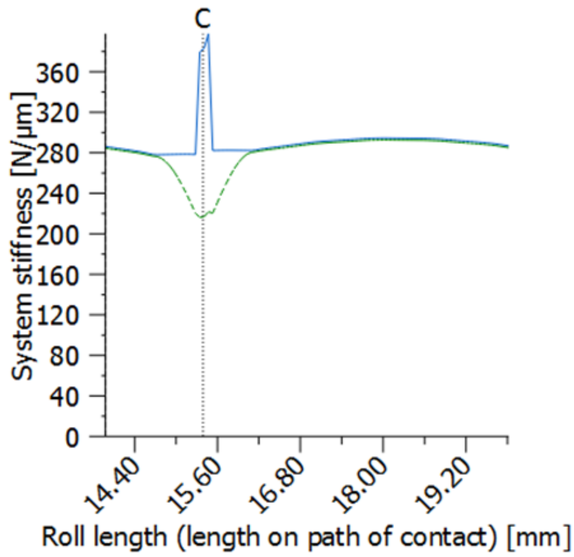

Figure 5.10 *Mesh Stiffness of Gear Pair of 4 and 57 in KISSsoft.*

For the third gear pair of 29/49, 2D geometries of the gears are shown in Figure 5.11. Contact line during mesh is shown in Figure 5.12.

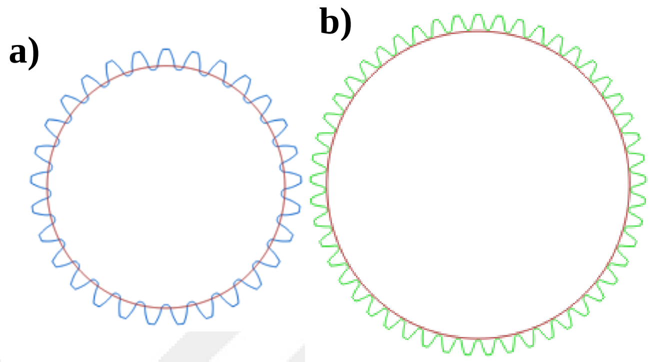

Figure 5.11 *2D Gear Geometry of Gear Pair of 29 and 49: a) Pinion; b) Gear.*

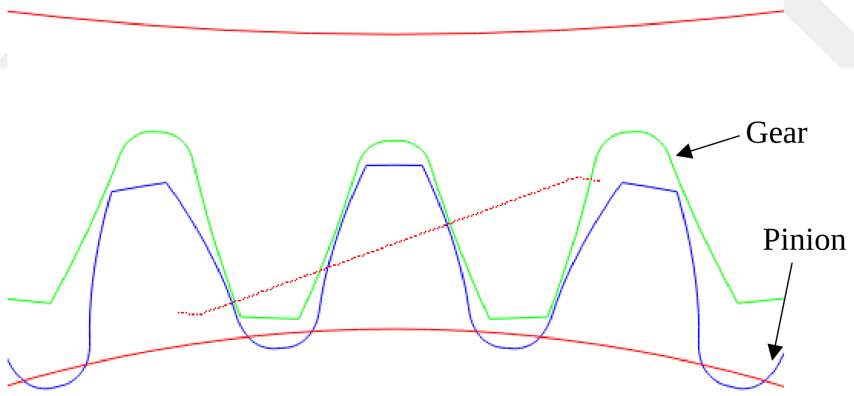

Figure 5.12 *Gear Mesh of Gear Pair of 29 and 49.*

3D geometries of the gears were also created and shown in Figure 5.13. Related gear parameters of third gear pair were used to create these geometries.

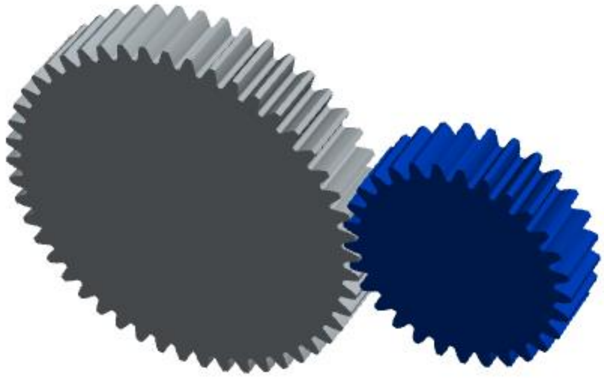

Figure 5.13 *Gear Pair of 3D (29 and 49).*

Calculated mesh stiffness values for the third gear pair of 29/49 are shown in Figure 5.14. Figure 5.14.a shows pinion stiffness according to length of contact and Figure 5.14.b shows gear stiffness versus length of path of contact.

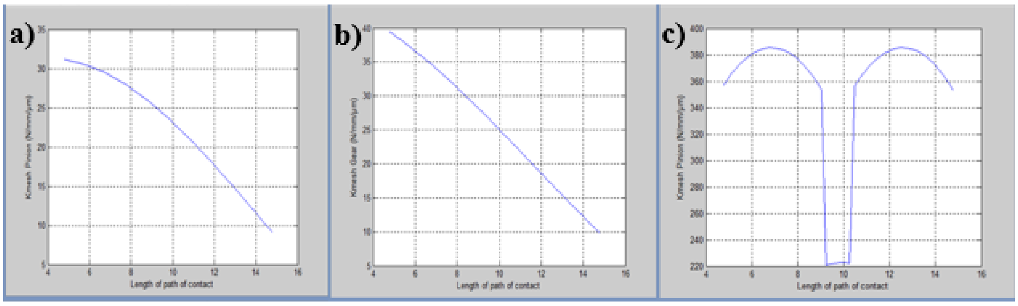

Figure 5.14 *Mesh Stiffness of a gear pair of (29,49): a) Pinion stiffness; b) Gear stiffness; c) Mesh stiffness.*

Figure 5.14.c shows the total mesh stiffness of gear pair. It can be seen that in Figure 5.14.c, stiffness values were decreased where single tooth pair contact occurs. Calculations in KISSsoft program were also run and given in Figure 5.15. It is seen that calculated stiffness values were in agreement with KISSsoft.

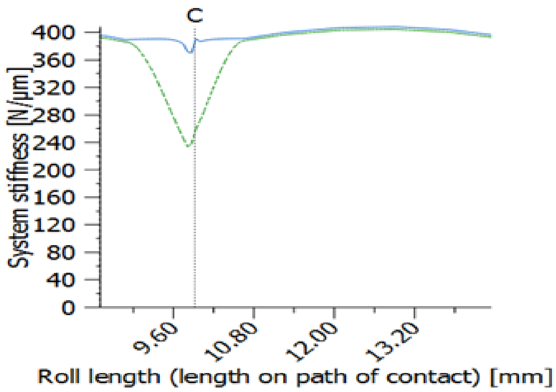

Figure 5.15 *Mesh Stiffness of Gear Pair of 29 and 49 in KISSsoft.*

5.2. Calculation of Contact Stress

Calculated load distribution values for the first gear pair of 45/63 are shown in Figure 5.16. It is seen that load on the gear flank increases in the area where single teeth contact occurs. It means that total load was transmitted through only one teeth pair in that area.

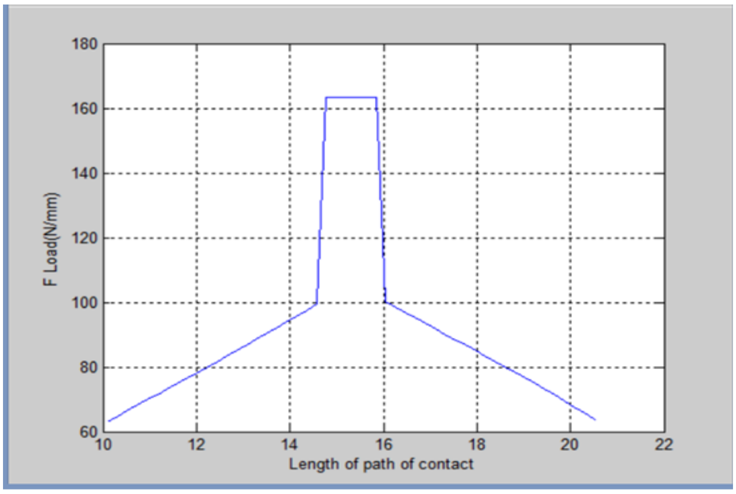

Figure 5.16 *Force Distribution of Gear Pair of 45 and 63.*

In order to analyze the situation through gear width, contact pressure values were calculated and ploted in 3D graph as shown in Figure 5.19. It is seen that through gear width pressure values do not change significantly. Also, peak point of contact pressure was reached where the single tooth pair in contact in 3D graph.

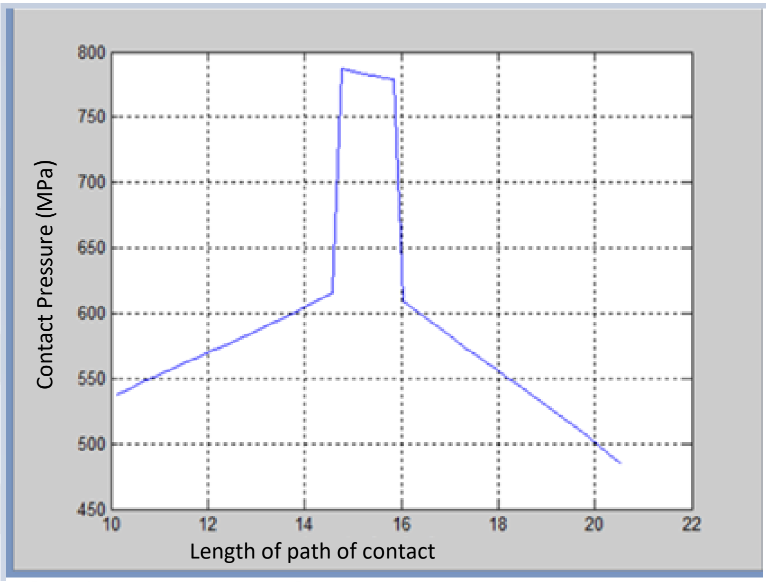

Figure 5.17 *Contact Pressure Distribution of Gear Pair of 45 and 63.*

Figure 5.17 shows the contact pressure distribution through contact line in gear mesh. Additionally, contact pressure distribution was calculated as seen in Figure 5.18 in KISSsoft. It can be seen that the contact pressure values were increased where single tooth pair contact occurs. It is also seen that calculated pressure values were in agreement with KISSsoft.

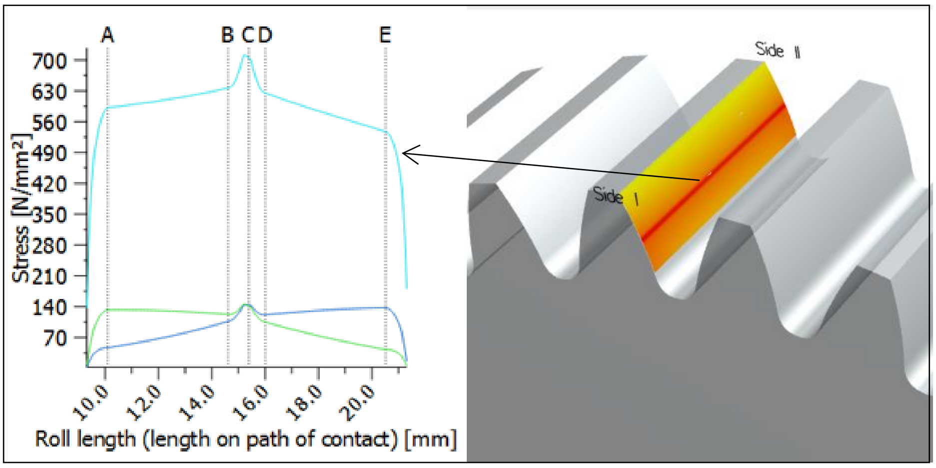

Figure 5.18 *Contact Pressure Distribution of Gear Pair of 45 and 63 in KISSsoft.*

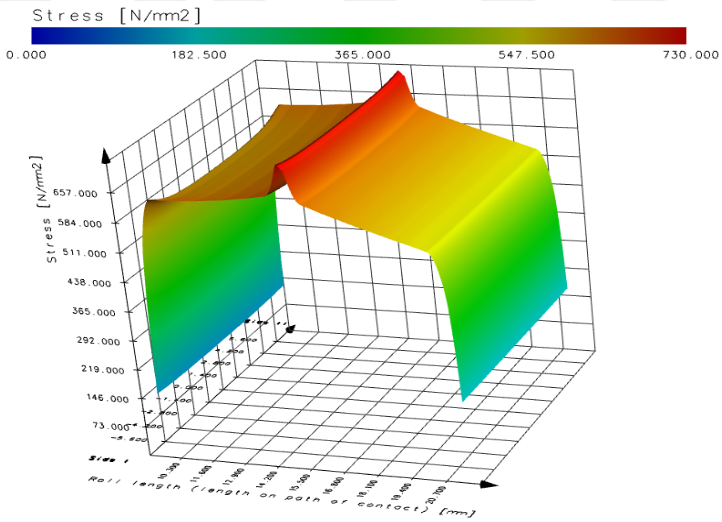

Figure 5.19 *3D Contact Pressure Distribution of Gear Pair of 45 and 63.*

In Figure 5.20, contact temperature distribution is given as a 3D graph. Since contact temperature was highly dependent on sliding velocities, the temperature values significantly decrease at the point where sliding velocity was zero. It is also seen that contact temperature through gear width does not change significantly.

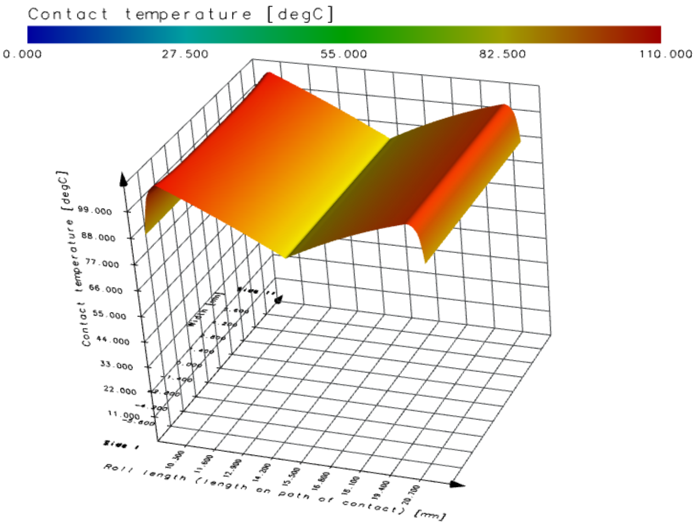

Figure 5.20 *3D Contact Temperature Distribution of Gear Pair of 45 and 63.*

Calculated load distribution vaules for the second gear pair of 45/57 are shown in Figure 5.21. It is seen that the load on the gear flank increases in the area where single teeth contact occurs. It means that total load was transmitted through only one teeth pair in that area.

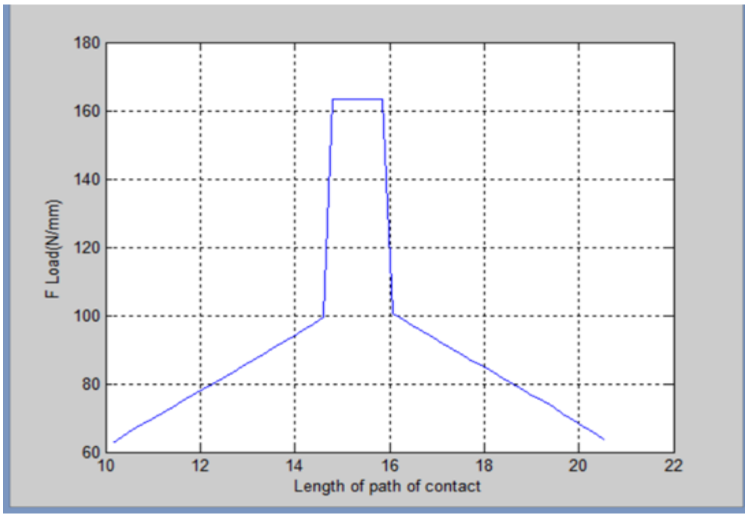

Figure 5.21 *Force Distribution of Gear Pair of 45 and 57.*

In order to analyze the situation through gear width, contact pressure values were calculated and ploted in 3D graph as shown in Figure 5.24. It is seen that through gear width pressure values do not change significantly. Also, peak point of contact pressure was reached where the single tooth pair was in contact in 3D graph.

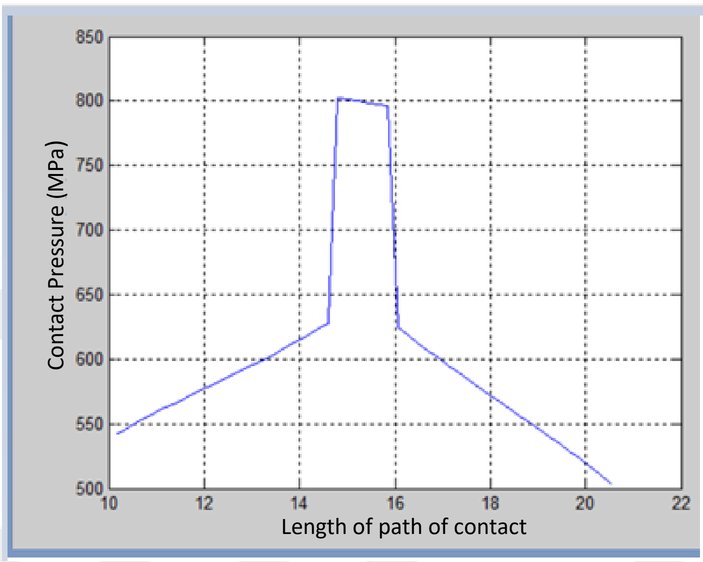

Figure 5.22 *Contact Pressure Distribution of Gear Pair of 45 and 57.*

Figure 5.22 shows contact pressure distribution through contact line in gear mesh. Additionally, contact pressure distribution was calculated as seen in Figure 5.23 in KISSsoft. It can be seen that the contact pressure values were increased where single tooth pair contact occurs. It is also seen that calculated pressure values were in agreement with KISSsoft.

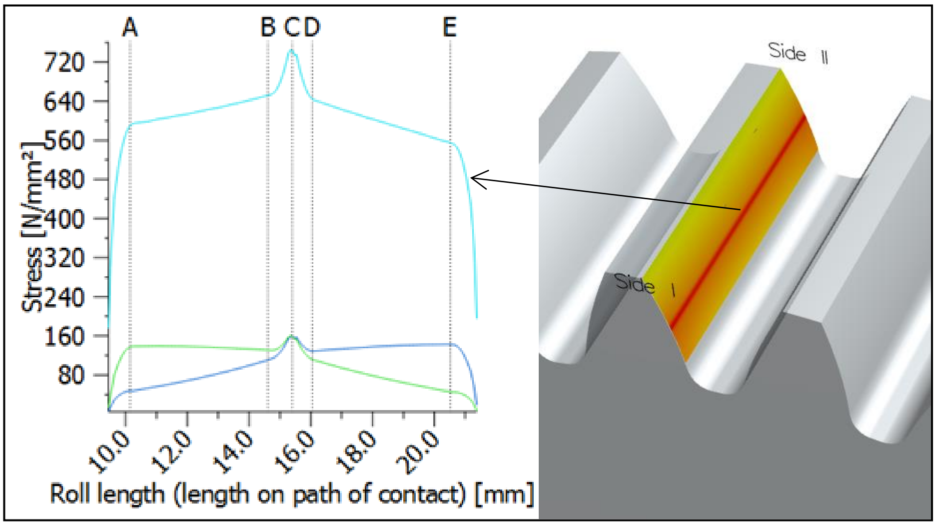

Figure 5.23 *Contact Pressure Distribution of Gear Pair of 45 and 57 in KISSsoft.*

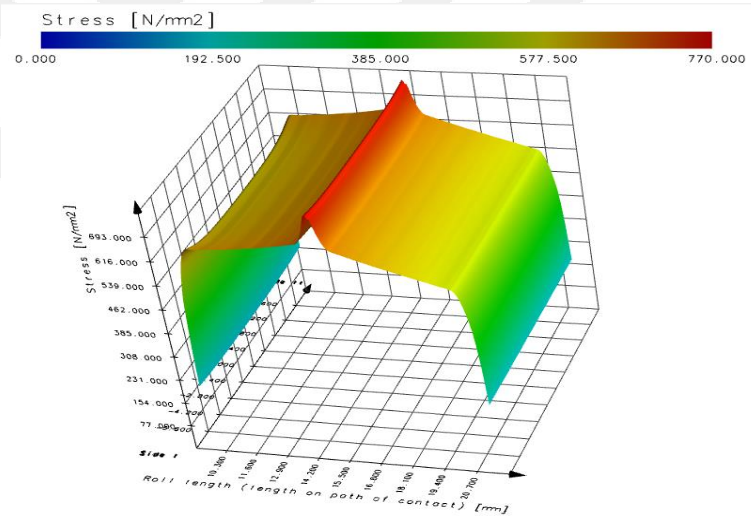

Figure 5.24 *3D Contact Pressure Distribution of Gear Pair of 45 and 57.*

Contact temperature distribution was shown in Figure 5.25. Since contact temperature was highly dependent on sliding velocities, the temperature values significantly decrease at the point where sliding velocity was zero. It was also seen that contact temperature through gear width do not change significantly.

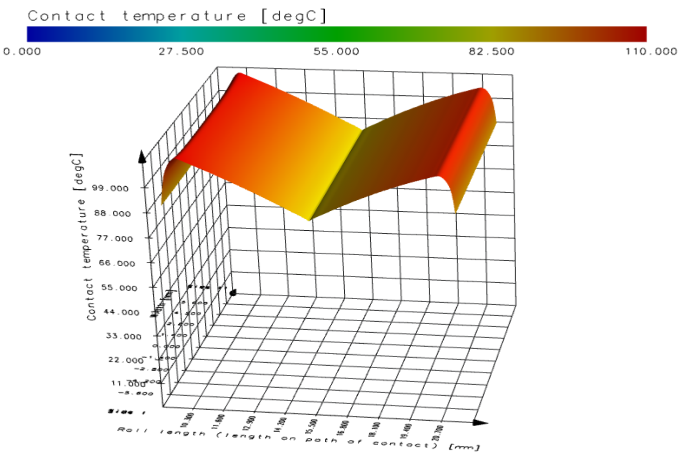

Figure 5.25 *3D Contact Temperature Distribution of Gear Pair of 45 and 57.*

Calculated load distribution values for the third gear pair of 29/49 were shown in Figure 5.26. It is seen that the load on the gear flank increases in the area where single teeth contact occurs. It means that total load was transmitted through only one teeth pair in that area.

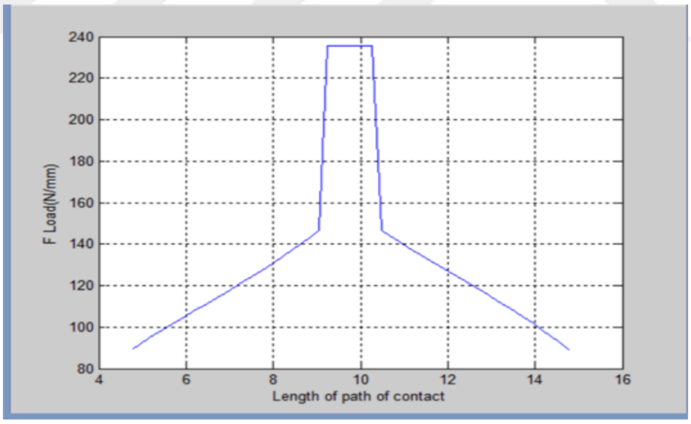

Figure 5.26 *Force Distribution of Gear Pair of 29 and 49.*

Figure 5.27 shows contact pressure distribution through contact line in gear mesh. Additionally, contact pressure distribution was calculated as seen in Figure 5.28 in KISSsoft.

It can be seen that the contact pressure values were increased where single tooth pair contact occurs. It is also seen that calculated pressure values were in agreement with KISSsoft.

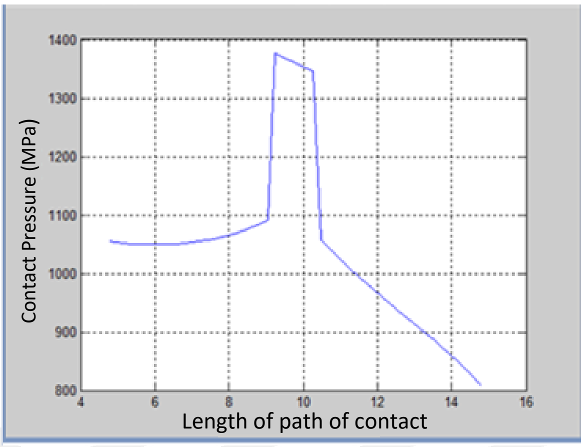

Figure 5.27 *Contact Pressure Distribution of Gear Pair of 29 and 49.*

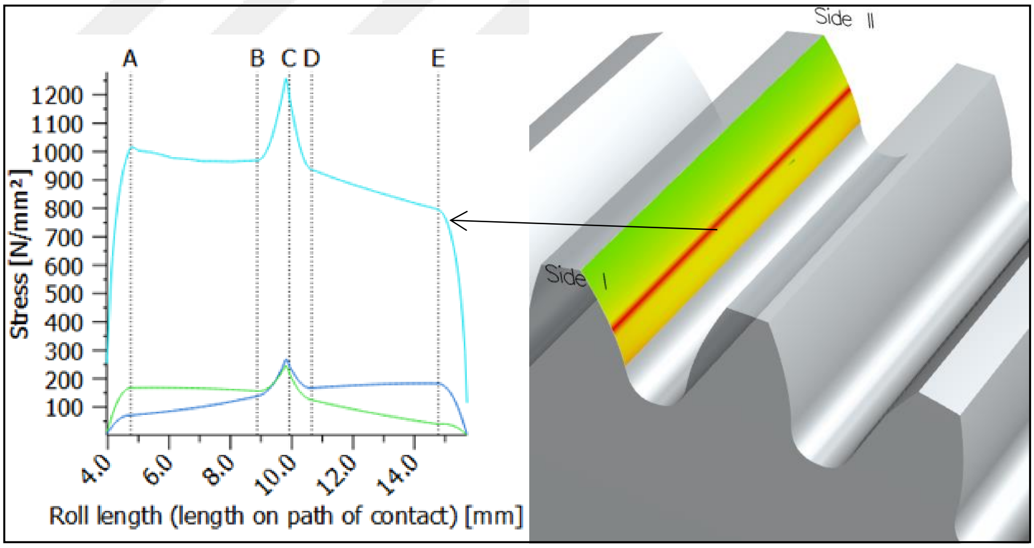

Figure 5.28 *Contact Pressure Distribution of Gear Pair of 29 and 49 in KISSsoft.*

In order to analyze the situation through gear width, contact pressure values were calculated and ploted in 3D graph in Figure 5.29. It is seen that through gear width pressure values do not change significantly. Also peak point of contact pressure was reached where the single tooth pair in contact occurs in 3D graph.

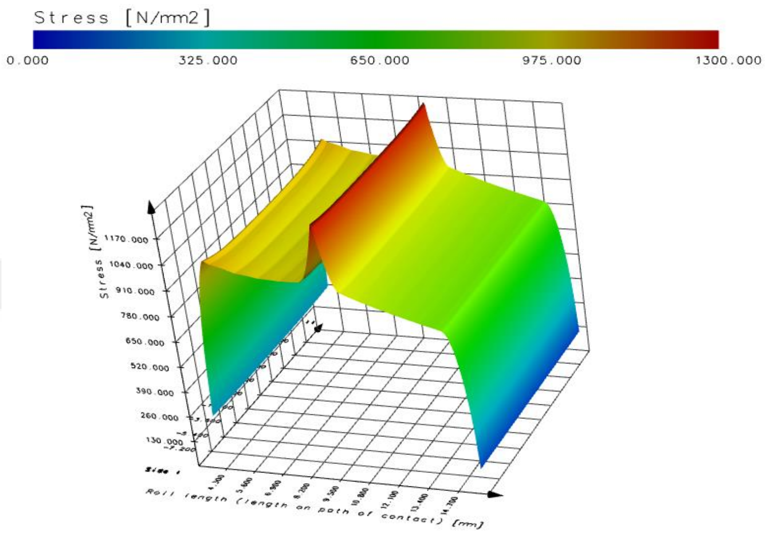

Figure 5.29 *3D Contact Pressure Distribution of Gear Pair of 29 and 49.*

In Figure 5.30, contact temperature distribution was given as a 3D graph. Since contact temperature was highly dependent on sliding velocities, the temperature values significantly decrease at the point where sliding velocity was zero. It is also seen that contact temperature through gear width does not change significantly.

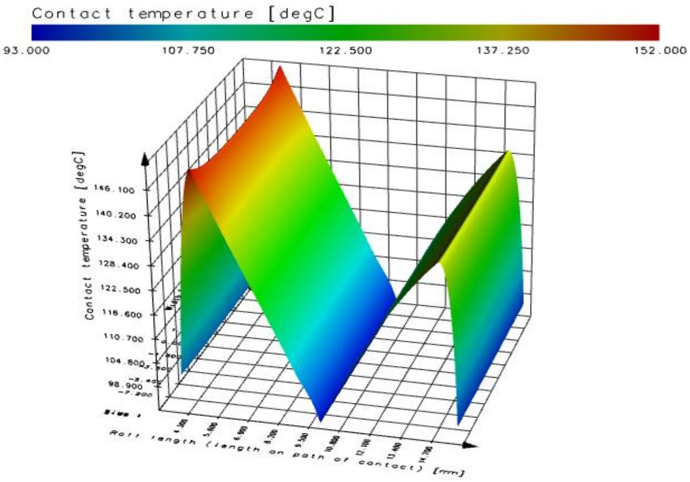

Figure 5.30 *3D Contact Temperature Distribution of Gear Pair of 29 and 49.*

5.3 Calculation of Transmission Errors

For the first gear pair of 45/63, second gear pair of 45/57 and third gear pair of 29/49, calculated transmission error graphs are given in Figure 5.31-5.33, respectively.

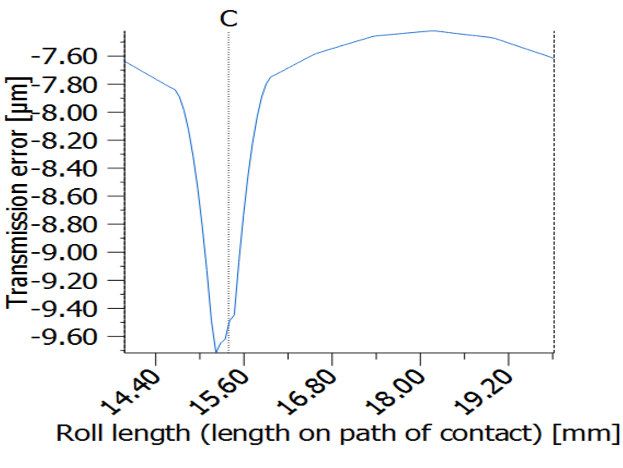

Figure 5.31 *Transmission Error of Gear Pair of 45 and 63.*

It is seen that transmission error magnitude ranges were higher for the gear meshes where higher sliding velocities occur. For the second gear pair of 45/57, transmission error range was smaller with than the other two pairs. However, third gear pair of 29/49 has transmission error range which was the highest among other gear pairs due to higher sliding velocities as shown in Figure 5.33.

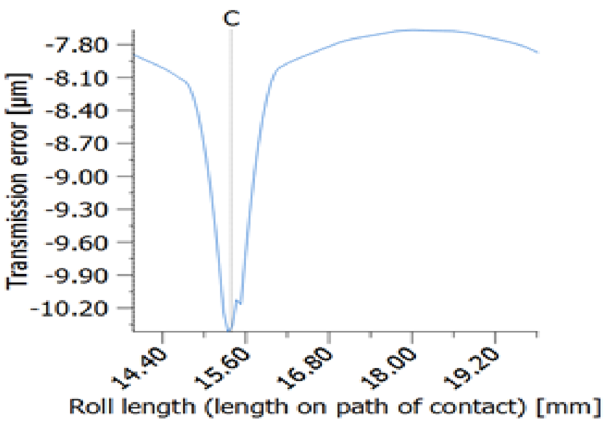

Figure 5.32 *Transmission Error of Gear Pair of 45 and 57.*

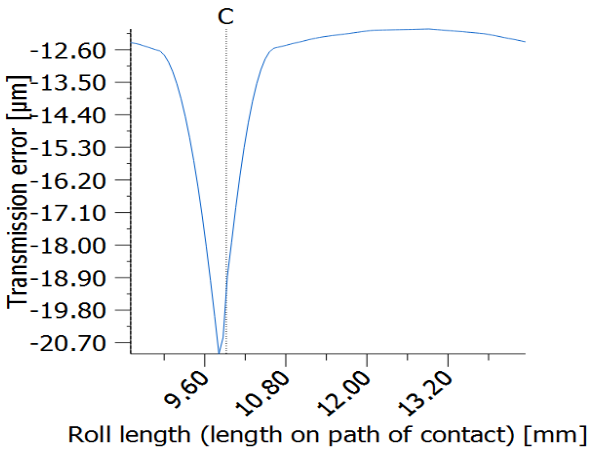

Figure 5.33 *Transmission Error of Gear Pair of 29 and 49.*

5.3.1 Profile Modifications Effects

Profile modifications are commonly used to decrease transmission error to have higher efficiency in transmission systems. In order to investigate the effect of tip relief, first gear pair of 45/63 was used to obtain transmission error quantities. To obtain lowest transmission error by tip relief modification, starting point should be aligned with HPSTC. In order to start modification from HPSTC, dCa was arranged by taking the factor as 2.2. Transmission error range that was around 2.02 µm divided into two and given as a value of tip relief to pinion and gear in order to have better efficiency. Transmission error graphs for firsth gear pair of 45/63 were given in Figure 5.34a and b respectively. It can be seen that magnitude of transmission error range was decreased and yielded in higher efficiency for the gear mesh. In Figure 5.35, tip relief modification was given as a 3D diagram. As it is seen in diagram, amount of modification was kept constant through gear face width.

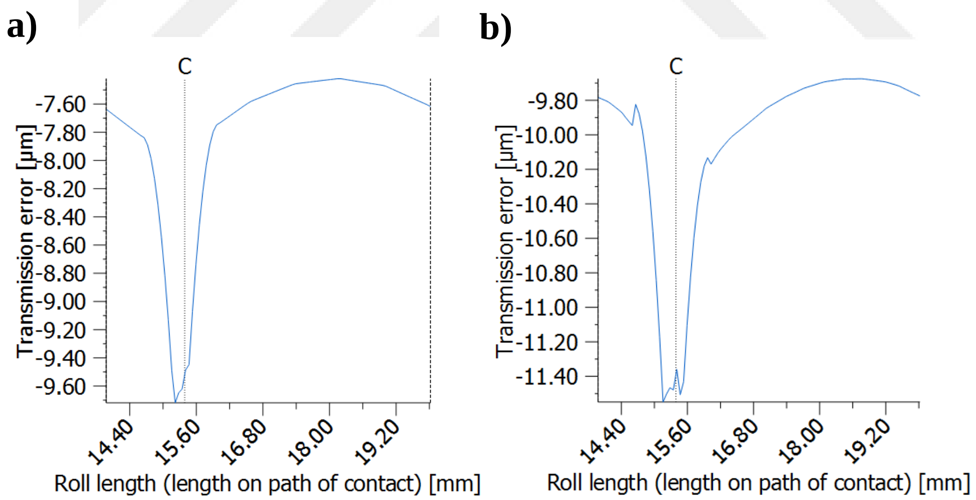

Figure 5.34 *Transmission Error of Gear Pair of 45 and 63: a) Transmission Error Without Tip Relief; b) Transmission Error With Tip Relief.*

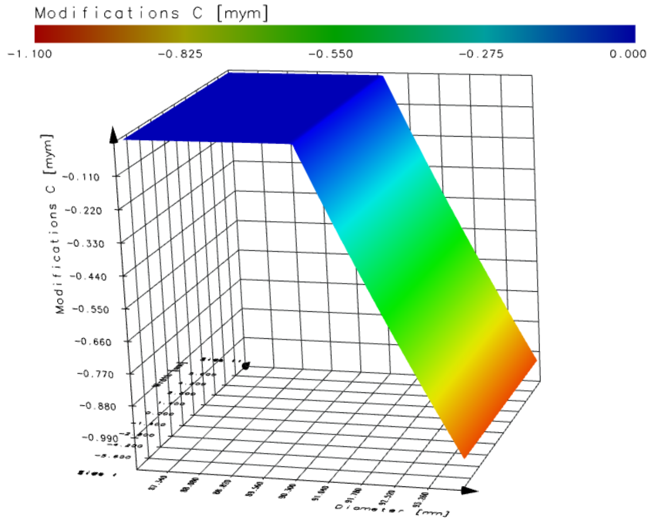

Figure 5.35 *Linear Tip Relief of Gear Pair of 45 and 63.*

In order to investigate the effect of tip relief, second gear pair of 45/57 was used to obtain transmission error quantities. To obtain lowest transmission error by tip relief modification, starting point should be aligned with HPSTC. In order to start modification from HPSTC, dCa was arranged by taking the factor as 2.2.

Maximum transmission error that was around 10.5 µm given as a value of tip relief to pinion and gear in order to have better efficiency. Transmission error graphs for second gear pair of 45/57 are given in Figure 5.36a and b. It can be seen that magnitude of transmission error range was decreased and yielded in higher efficiency for the gear mesh. In Figure 5.37, tip relief modification is given as a 3D diagram. As it is seen in diagram, amount of modification was kept constant through gear face width.

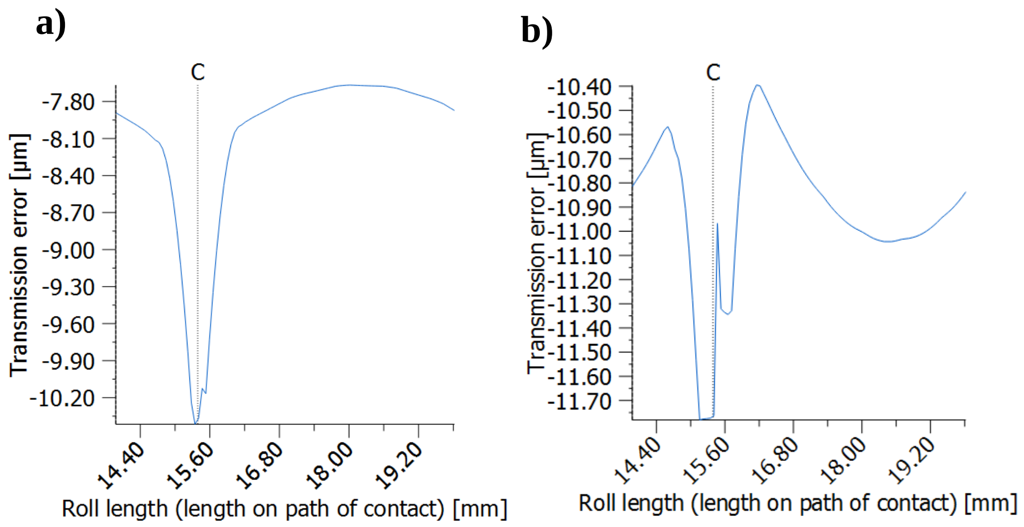

Figure 5.36 *Transmission Error of Gear Pair of 45 and 57: a) Transmission Error Without Tip Relief; b) Transmission Error With Tip Relief.*

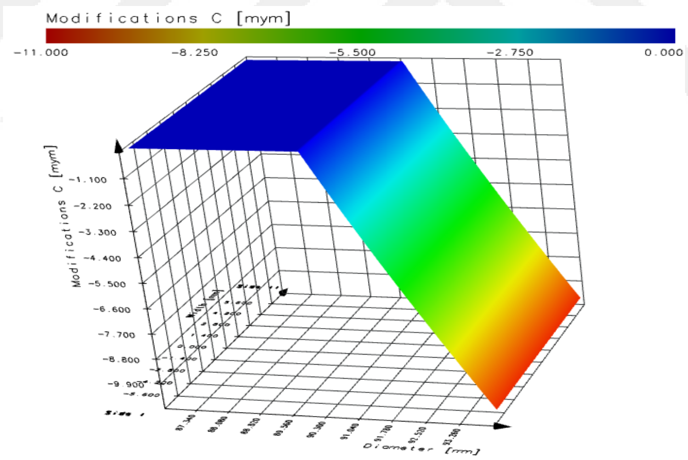

Figure 5.37 *Linear Tip Relief of Gear Pair of 45 and 57.*

In terms of transmission error, third gear pair had the most critical mesh in powertrain. In order to investigate the effect of tip relief, third gear pair of 29/49 was used to obtain transmission error quantities.

To obtain lowest transmission error by tip relief modification, starting point should be aligned with HPSTC. In order to start modification from HPSTC, dCa was arranged by taking the factor as 2.2.

Maximum transmission error that was around 20.7 µm given as a value of tip relief to pinion and gear in order to have better efficiency. Transmission error graphs for third gear pair of 29/49 are given in Figure 5.38a and b. It can be seen that magnitude of transmission error range was decreased significantly and yielded in higher efficiency for the gear mesh. In Figure 5.39, tip relief modification is given as a 3D diagram. As it is seen in diagram, amount of modification was kept constant through gear face width.

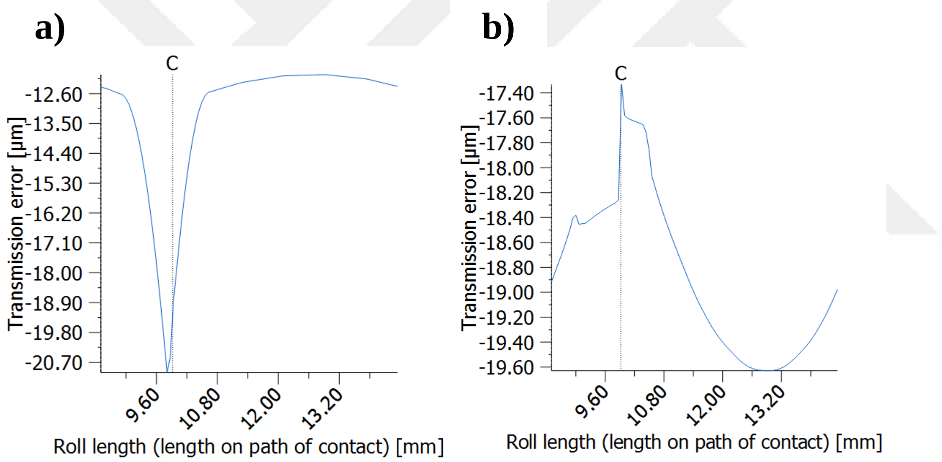

Figure 5.38 *Transmission Error of Gear Pair of 29 and 49: a) Transmission Error Without Tip Relief; b) Transmission Error With Tip Relief.*

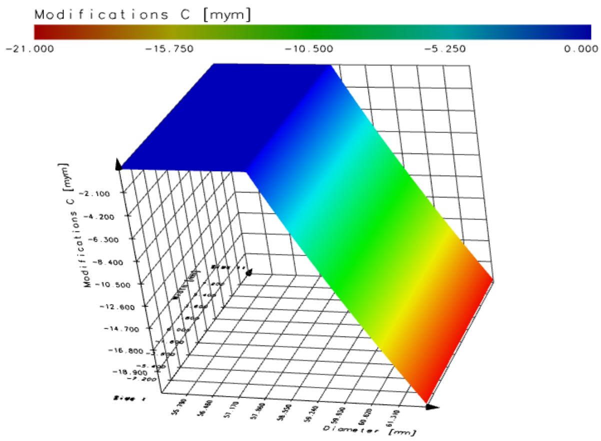

Figure 5.39 *Linear Tip Relief of Gear Pair of 29 and 49.*

5.4 Effects of Gear Materials

In Section 3, gear materials and their technical properties are summarised in Table 3.1. It is important to use high strength materials in aerospace applications. In order to investigate the effects of the materials, ISO 6336:2006 standard was used to carry out calculations in terms of root and flank safety of the gears.

Then safety factors are compared in order to obtain the results of different material usage. As a first case study, first gear pair was chosen and safety factors were obtained. Input datas are 100 kW power, 10000 rpm and 20000 working hours. All the input factors were taken as 1. Pinion was selected as driving gear and working flank was right side. Sense of rotation was chosen as clockwise. Obtained safety factors are summarised in Table 5.1.

Table 5.1 *Safety Factors of First Gear Pair of 45 and 63.*

	Grade 3		**Grade 2**		**Grade 1**	
	Pinion	Gear	Pinion	Gear	Pinion	Gear
Root Safety Factor	3.66	2.81	3.20	2.46	2.70	2.07
Flank Safety Factor	1.825	1.848	1.42	1.51	1.19	1.21
Contact Ratio	1.764					

As a second case study, second gear pair was chosen and safety factors were obtained. Input datas were 100 kW power, 10000 rpm and 20000 working hours. All the input factors were taken as 1. Pinion was selected as driving gear and working flank was right side. Sense of rotation was chosen as clockwise. Obtained safety factors are summarised in Table 5.2.

Table 5.2 *Safety Factors of Second Gear Pair of 45 and 57.*

	Grade 3		**Grade 2**		**Grade 1**	
	Pinion	Gear	Pinion	Gear	Pinion	Gear
Root Safety Factor	3.93	4.23	3.23	3.48	2.90	3.12
Flank Safety Factor	2.2	2.22	1.75	1.77	1.44	1.45
Contact Ratio	1.76					

As a third case study, third gear pair was chosen and safety factors were obtained. Input datas were100 kW power, 7142 rpm and 20000 working hours. All the input factors were taken as 1. Pinion was selected as driving gear and working flank was right side. Sense of rotation was chosen as clockwise. Obtained safety factors are summarised in Table 5.3.

Table 5.3 *Safety Factors of Third Gear Pair of 29 and 49.*

	Grade 3		**Grade 2**		**Grade 1**	
	Pinion	Gear	Pinion	Gear	Pinion	Gear
Root Safety Factor	2.3	2.5	2.02	2.18	1.70	1.84
Flank Safety Factor	1.34	1.4	1.10	1.14	1.06	1.09
Contact Ratio	1.699					

In Table 5.1 - Table 5.3, it is seen that safety factors decrease from Grade 3 to 1. Here grades 3-1 refer to SAE9310, 18CrNiMo7-6 and 16MnCr5, respectively.

Due to the high strength properties as discussed in Table 3.1, it is seen that SAE9310 is the most suitable to be used in aerospace gearboxes. However, higher safety factors may yield in increased mass for gearbox. Therefore these factors should be optimized with respect to the application area of gearbox. It is also observed that AGMA 2001-C95 standard gives more conservative results (Table 5.4 - Table 5.6) than ISO 6336.

Table 5.4 *Safety Factors of First Gear Pair of 45 and 63 According to AGMA 2001-C95.*

	Grade 3		**Grade 2**		**Grade 1**	
	Pinion	Gear	Pinion	Gear	Pinion	Gear
Root Safety Factor	1.81	1.87	1.57	1.62	1.33	1.37
Flank Safety Factor	1.57	1.58	1.28	1.29	1.03	1.04
Contact Ratio	1.76					

Table 5.5 *Safety Factors of First Gear Pair of 45 and 57 According to AGMA 2001-C95.*

	Grade 3		**Grade 2**		**Grade 1**	
	Pinion	Gear	Pinion	Gear	Pinion	Gear
Root Safety Factor	1.54	1.58	1.34	1.37	1.13	1.16
Flank Safety Factor	1.87	1.88	1.53	1.54	1.22	1.23
Contact Ratio	1.76					

Table 5.6 *Safety Factors of First Gear Pair of 29 and 49 According to AGMA 2001-C95.*

	Grade 3		**Grade 2**		**Grade 1**	
	Pinion	Gear	Pinion	Gear	Pinion	Gear
Root Safety Factor	1.35	1.46	1.17	1.20	0.99	1.07
Flank Safety Factor	1.18	1.19	0.96	0.97	0.77	0.78
Contact Ratio	1.699					

Safety factor comparison was also made and given in Figure 5.40 - 45 for gear pairs of 45/63, 45/57, and 29/49. In x axis, 1 and 2 correspond to Grade 3, 3 and 4 correspond to Grade 2 and finally 5 and 6 correspond to Grade 1. Even numbers correspond to pinion and odd numbers correspond to gears in x axis. It is seen that calculations according to ISO 6336 standard yields in higher safety factors. Hence, AGMA 2001- C95 standard gives considerably more conservative results than ISO 6336. As seen in Figures 5.40 and 5.41, the root safety factors were higher than the flank safety factors. The reason is that in the first gear pair, the gears were subjected to high power but also high speed resulting in lower load. It is also seen that flank safety factors get close to limit 1 in the calculations according to AGMA standard for a given first gear pair. As a result, according to AGMA 2001-C95, calculations result in higher stress values than ISO 6336.

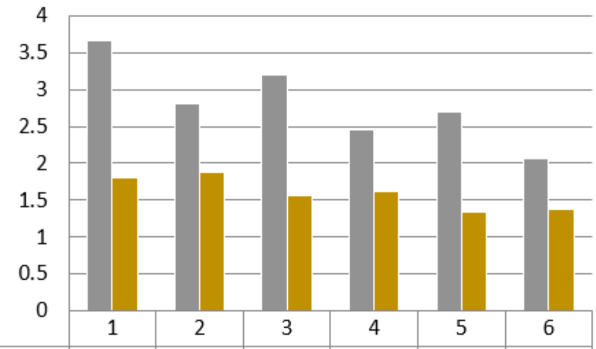

	1	2	3	4	5	6
ISO 6336 Root Safety Factor	3.66	2.81	3.20	2.46	2.70	2.07
AGMA 2001-C95 Root Safety Factor	1.81	1.87	1.57	1.62	1.33	1.37

Figure 5.40 *Root Safety Factor Comparison for ISO 6336 and AGMA 2001-C95 Standards for First Gear Pair of 45 and 63.*

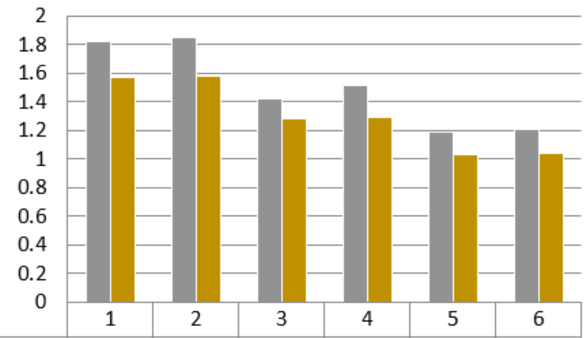

	1	2	3	4	5	6
ISO 6336 Flank Safety Factor	1.825	1.848	1.42	1.51	1.19	1.21
AGMA 2001-C95 Flank Safety Factor	1.57	1.58	1.28	1.29	1.03	1.04

Figure 5.41 *Flank Safety Factor Comparision for ISO 6336 and AGMA 2001-C95 Standards for First Gear Pair of 45 and 63.*

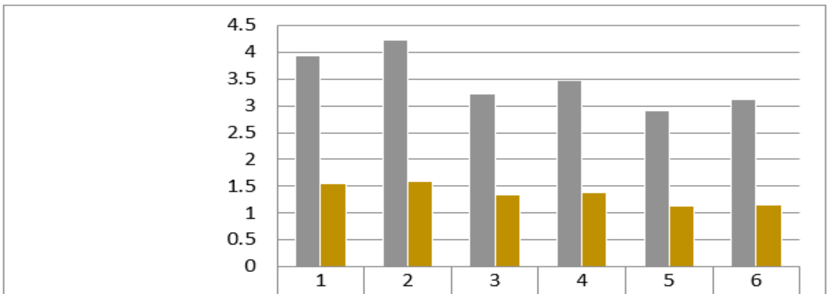

	1	2	3	4	5	6
ISO 6336 Root Safety Factor	3.93	4.23	3.23	3.48	2.90	3.12
AGMA 2001-C95 Root Safety Factor	1.54	1.58	1.34	1.37	1.13	1.16

Figure 5.42 *Root Safety Factor Comparision for ISO 6336 and AGMA 2001-C95 Standards for Second Gear Pair of 45 and 57.*

As seen in Figures 5.42 and 43, the root safety factors were higher than flank safety factors of second gear pair. It is also seen that flank safety factors get close to limit 1 in the calculations according to AGMA standard. However, flank safety factors were relatively higher than the first gear pair. Also, AGMA 2001-C95 yields in lower safety factors. Therefore, the calculations for AGMA 2001-C95 result in higher stress values than ISO 6336.

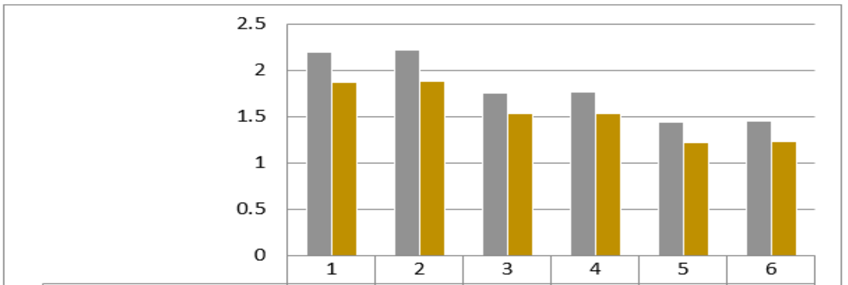

	1	2	3	4	5	6
ISO 6336 Flank Safety Factor	2.2	2.22	1.75	1.77	1.44	1.45
AGMA 2001-C95 Flank Safety Factor	1.87	1.88	1.53	1.54	1.22	1.23

Figure 5.43 *Flank Safety Factor Comparision for ISO 6336 and AGMA 2001-C95 Standards for Second Gear Pair of 45 and 57.*

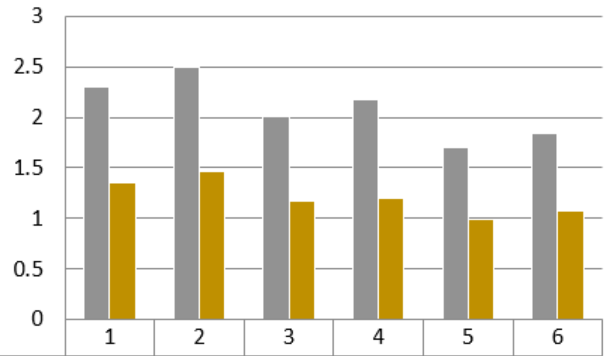

	1	2	3	4	5	6
ISO 6336 Root Safety Factor	2.3	2.5	2.02	2.18	1.70	1.84
AGMA 2001-C95 Root Safety Factor	1.35	1.46	1.17	1.20	0.99	1.07

Figure 5.44 *Root Safety Factor Comparision for ISO 6336 and AGMA 2001-C95 Standards for Third Gear Pair of 29 and 49.*

As seen in Figures 5.44 and 45, root safety factors were higher than flank safety factors of third gear pair. It is also seen that flank safety factors go under limit 1 in the calculations according to AGMA standard. Also, flank safety factors were relatively lower than other gear pairs because of higher loads on these gears.

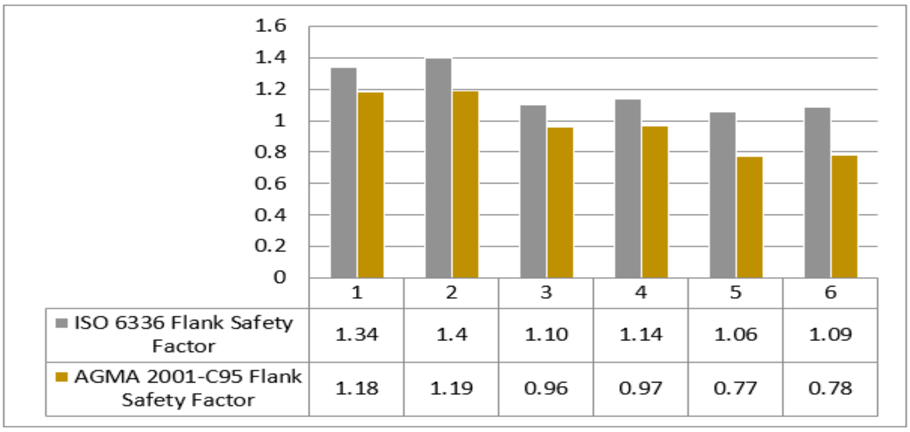

	1	2	3	4	5	6
ISO 6336 Flank Safety Factor	1.34	1.4	1.10	1.14	1.06	1.09
AGMA 2001-C95 Flank Safety Factor	1.18	1.19	0.96	0.97	0.77	0.78

Figure 5.45 *Flank Safety Factor Comparision for ISO 6336 and AGMA 2001-C95 Standards for Third Gear Pair of 29 and 49.*

5.5 Results of Calculations on FEM

In order to calculate maximum pressure values on gear flank by using finite element approach, all three gear meshes were modelled in MASTA software. For the first gear pair, 3D model was constructed as given in Figure 5.46. The same pinion and gear properties of the first gear pair were given to software in order to make comparasion between the results of analytical and FEM in the same basis.

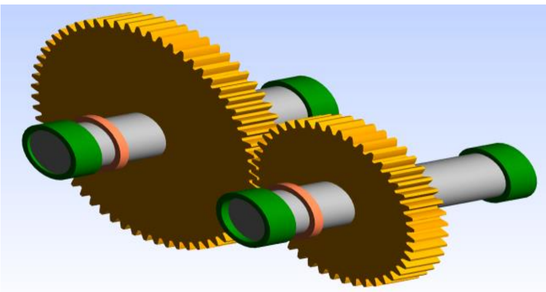

Figure 5.46 *First Gear Pair of 45 and 63 in MASTA Software.*

Meshing of the first gear pair was made as shown in Figure 5.47. Gear meshes were generated otomatically by using MASTA software. After meshing the gear and pinion teeth, tooth contact analysis was carried out by using detailed loaded tooth contact analysis module of MASTA.

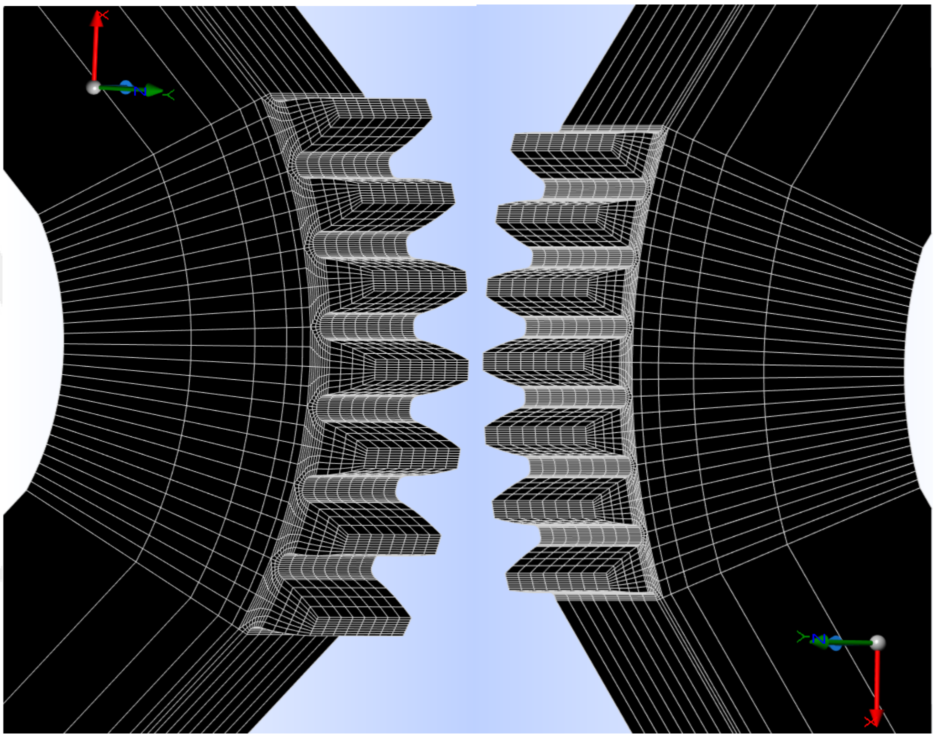

Figure 5.47 *FEM Mesh for First Gear Pair of 45 and 63.*

Gear meshes and obtained results are given in Figure 5.48. Pressure values on pinion flank was given through face width as seen in Figure 5.48a and b. For a given gear pair, calculated pressure values are shown as a chart in Figure 5.48c. It is observed that pressure values do not tend to differ through gear width.

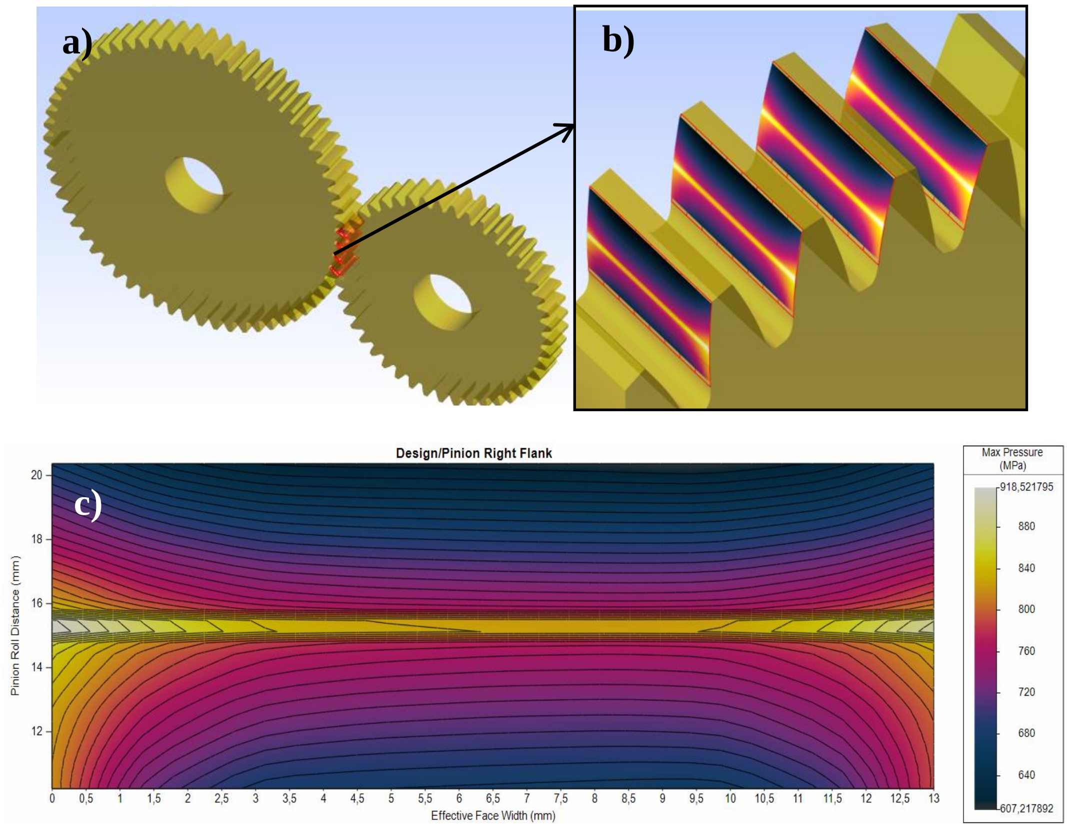

Figure 5.48 *FEM Tooth Contact Analysis for First Gear Pair of 45 and 63: a) Gear Mesh; b) Pressure Distribution on Pinion Flank; c) Contact Pressure.*

It is also observed that, pressure values reach its maximum where only one teeth pair was in contact. It means that maximum value of load distribution reached its peak where in single teeth pair contact occurs. Hence, it is concluded that maximum pressure value for the first gear pair of (45/63) was found as 918 MPa by using FEM.

For the second gear pair, 3D model was constructed as given in Figure 5.49. The same pinion and gear properties of the second gear pair were given to software in order to make comparision between the results of analytical and FEM in the same basis.

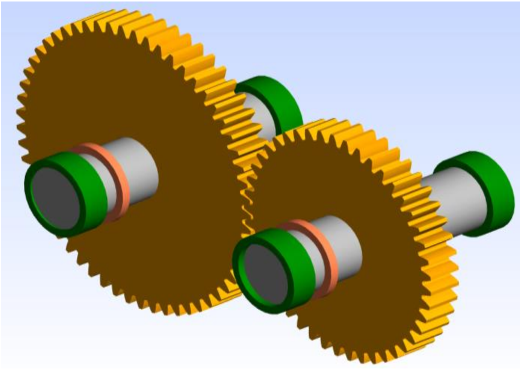

Figure 5.49 *Second Gear Pair of 45 and 57 in MASTA Software.*

Meshing of the second gear pair was made as shown in Figure 5.50. Gear meshes were generated otomatically by using MASTA software. After meshing the gear and pinion teeth, tooth contact analysis was carried out by using detailed loaded tooth contact analysis module of MASTA.

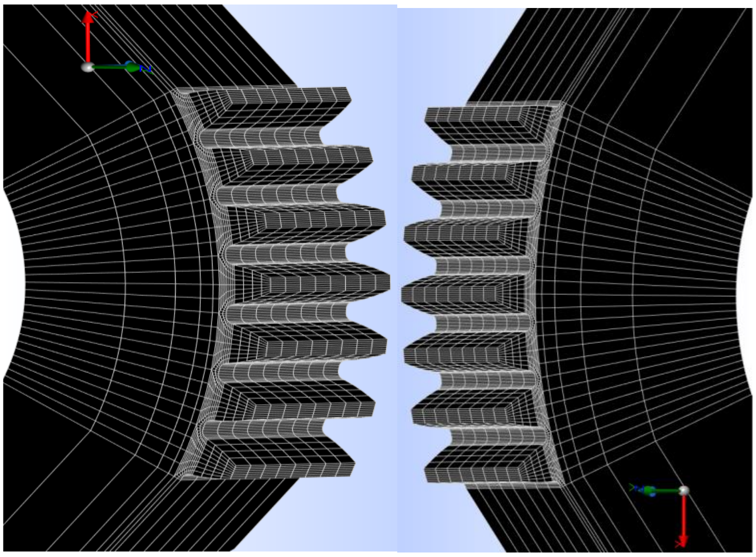

Figure 5.50 *FEM Mesh for Second Gear Pair of 45 and 57.*

Gear meshes and obtained results are given in Figure 5.51. Pressure values on pinion flank were given through face width as seen in Figure 5.51a and b. For a given gear pair, calculated pressure values are shown as a chart in Figure 5.51c. It is observed that pressure values do not tend to differ through gear width.

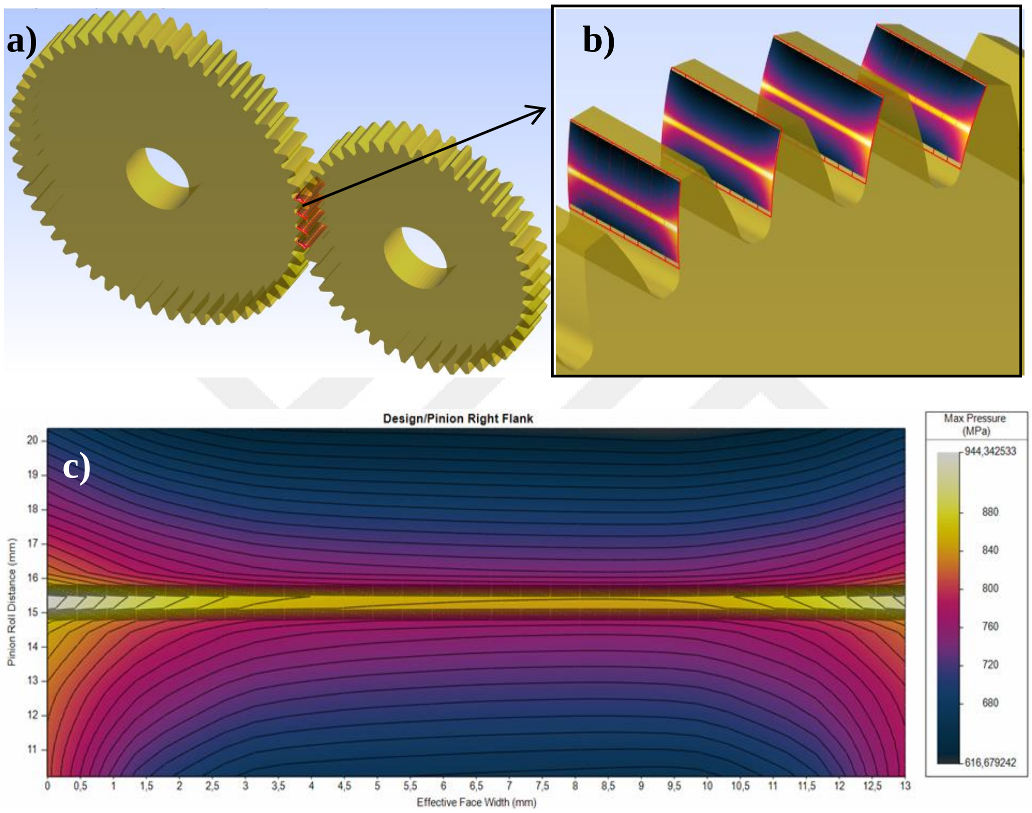

Figure 5.51 *FEM Tooth Contact Analysis for Second Gear Pair of 45 and 57: a) Gear Mesh; b)Pressure Distribution on Pinion Flank; c) Contact Pressure.*

It is also observed that, pressure values reach its maximum where only one teeth pair was in contact. It means that maximum value of load distribution reached its peak where in single teeth pair contact occurs. Hence, it is concluded that maximum pressure value for the first gear pair of (45/57) was found as 944 MPa by using FEM.

For the third gear pair, 3D model was constructed as given in Figure 5.52. The same pinion and gear properties of the second gear pair were given to software in order to make comparasion between the results of analytical and FEM in the same basis.

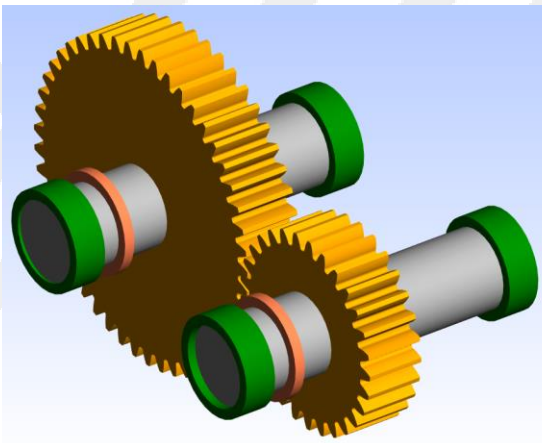

Figure 5.52 *Third Gear Pair of 29/49 in MASTA Software.*

Meshing of the third gear pair was made as shown in Figure 5.53. Gear meshes were generated otomatically by using MASTA software. After meshing the gear and pinion teeth, tooth contact analysis is carried out by using detailed loaded tooth contact analysis module of MASTA.

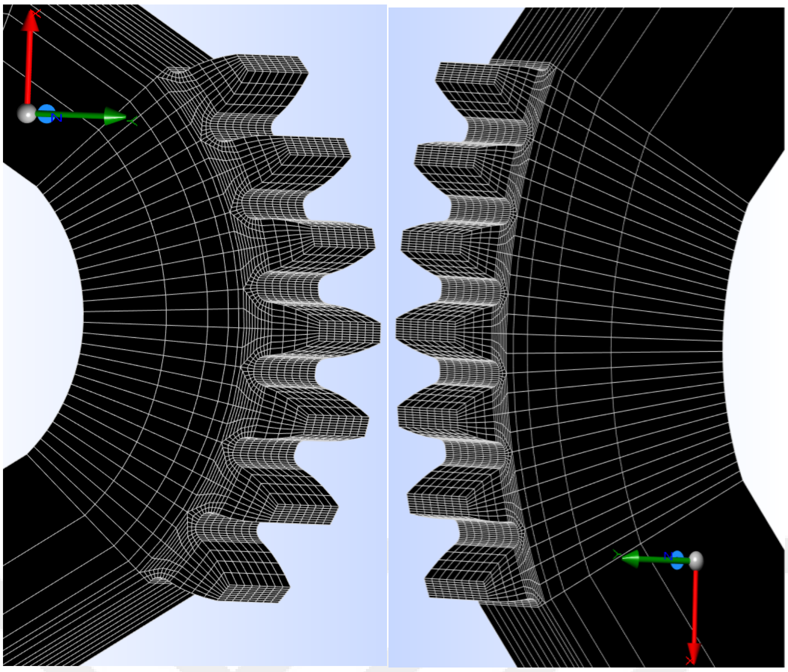

Figure 5.53 *FEM Mesh for Third Gear Pair of 29 and 49.*

Gear meshes and obtained results are given in Figure 5.54. Pressure values on pinion flank were given through face width as seen in Figure 5.54a and b. For a given gear pair, calculated pressure values are shown as a chart in Figure 5.54c. It is observed that pressure values do not tend to differ through gear width.

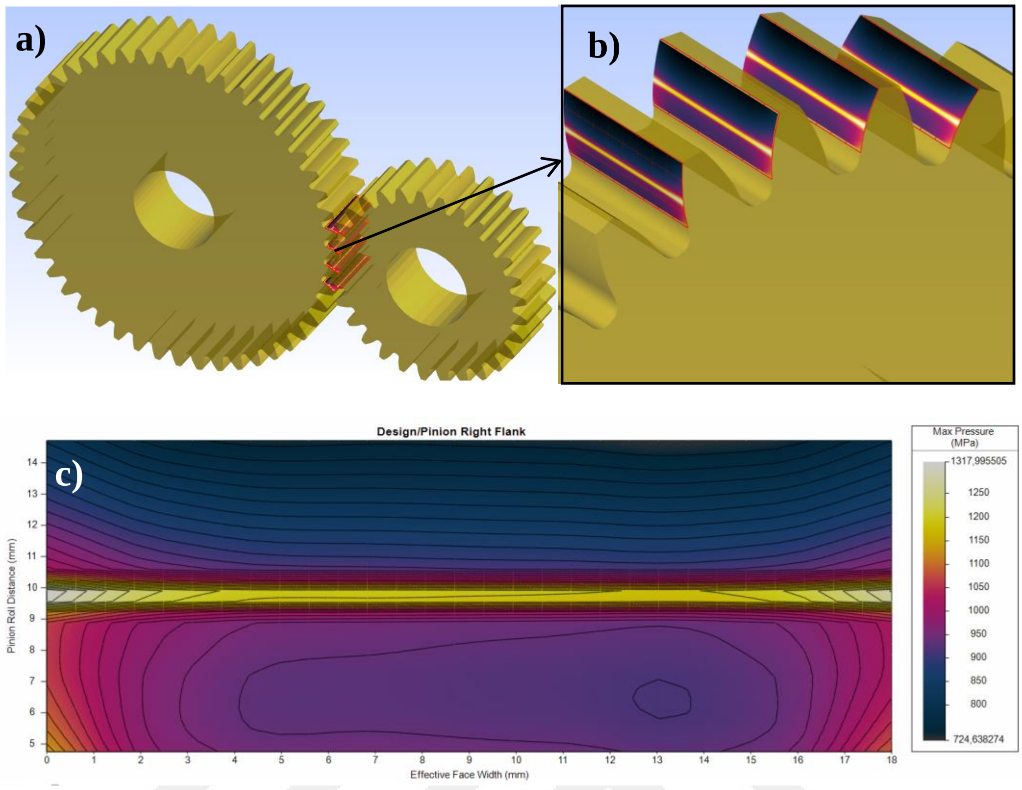

Figure 5.54 *FEM Tooth Contact Analysis for Third Gear Pair of 29 and 49: a) Gear Mesh; b) Pressure Distribution on Pinion Flank; c) Contact Pressure.*

It is also observed that pressure values reach its maximum where only one teeth pair is in contact. It means that maximum value of load distribution reached its peak where in single teeth pair contact occurs. Hence, it is concluded that maximum pressure value for the first gear pair of (29/49) was found as 1317 MPa by using FEM.

CHAPTER 6

DISCUSSION

Contact stress of gears has been under investigations for many years. Main contribution was Hertzian Contact Theory to calculate tooth contact stress by considering cylinders for instant gear meshes in contact. In the basis, Weber and Banaschek, 1949 made the major study regarding mesh stiffness calculation and it is accepted by other gear researchers for many years. From that time, many works have also been carried out on the calculation of gear mesh as stated in Table 2.1. Among these work, the study by Sainsot et al., 2004 made the crucial contribution to gear foundation as stated in Section 3.4. Time varying mesh stiffness of gears was calculated by Chaari et al., 2009 by considering bending, Hertzian and foundation stiffness. In addition to that, axial compressive and shear stiffness were also added in a study by Chen and Shao, 2011.

However, gear profile effects on gear mesh stiffness calculations were not studied. In a later study by Chen and Shao, 2013, effects of gear profile modifications including tip and root modifications on mesh stiffness were investigated. Besides the works on analytical solution, FEM methods were also used to calculate contact stress within the gears for many years in literature.

In the scope of mesh stiffness calculations, different methods were used in literature:

- FEM was used in the studies by Wu et al., 2012; Li, 2007a.
- Analytical methods used in the studies by Ma et al., 2013; Ma et al., 2015; Li et al., 2004; Wan et al., 2018; Liang et al., 2014; Chen and Shao, 2011; Ma et al., 2014; Fernandez del Rincon et al., 2013; Chang et al., 2015.
- Analytical-FEM combined methods used in the studies by Wang et al., 2018; Pedersen and Jørgensen, 2014.
- Experimental methods used in the studies by Pandya and Parey, 2013; Raghuwanshi and Parey, 2018.

Sun et al, 2018 proposed a revised time varying mesh stiffness model for spur gear. Hertzian contact stiffness calculations were combined with the correction factors obtained from FEM. It was shown that analytical solutions get close to FEM results by correction factor.

In an another study, Mengjiao et al., 2018, proposed an improved analytical method for TVMS of helical gears. Slice approach through gear width was used by including the gear foundation mesh stiffness formulation proposed by Sainsot et al., 2004. In this study, methods on the foundation of gear mesh stiffness proposed by Cai, 1995; Gu et al, 2015; Chang et al., 2015; Mengjiao et al., 2018 were discussed.

In order to compare the outcomes of these main proposed stiffness calculation methods with the analytical solution of this thesis, gear pair parameters were chosen as seen in Table 6.1.

Table 6.1 *Gear Parameters for Comparison of Methods.*

Parameters	***Gear Pair***
Teeth Number	*40*
Normal Module	*4*
Tooth Width	*30*
Pressure Angle	*20*
Helix Angle	*15*
v	*0.3*
E (GPa)	*210*

The comparison between mean stiffness values of different methods is given in Table 6.2. Table 6.2 was constructed based on the studies by Feng et al., 2018 in which Cai's Method, Gu's Method, Wang's Method, Wan's Method, Chang's Method were included. In order to compare the result of analytical solution in this thesis with these methods, obtained analytical solutions and results of KISSsoft program were added to the first two row, according to ISO standard as seen in Table 6.2.

Table 6.2 *Mean Stiffness Comparision of Different Methods.*

Methods	**Mean Stiffness (x 10^8 N/m)**
Obtained Solution by Analytical Method	5.56
KISSsoft - ISO-6336	5.08
FE Methods, study by Feng et al, 2018	5.38
Feng's Method, study by Feng et al, 2018	5.14
Cai's Method, study by Cai, 1995	6.18
Gu's Method, study by Gu et al., 2015	6.04
Wang's Method, study by Wang and Zhang, 2017	6.26
Wan's Method, study by Wan et al., 2015	6.58
Chang's Method, study by Chang et al., 2015	5.3

It was seen that obtained solution by analytical method with the given pairs in Table 6.1 were found to be close to the FEM and the ISO 6336 solutions. Results of the other studies were also parallel to each other. For the same gear pair, in order to make comparison, results obtained from these different methods are shown in Figure 6.1. Solutions of obtained analytical method in this thesis were illustrated with red line as seen in Figure 6.1.

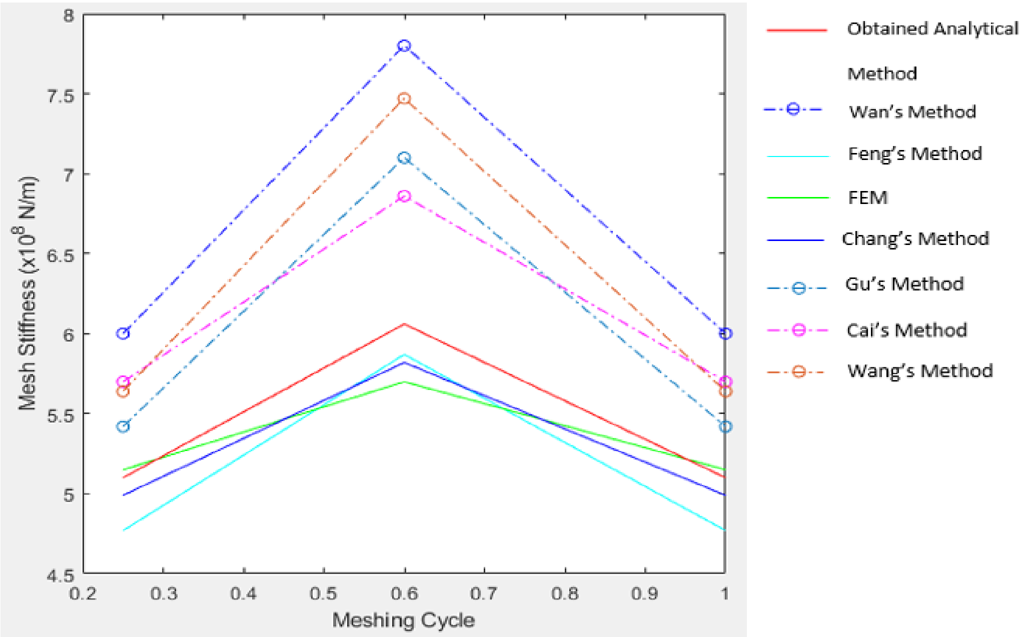

Figure 6.1 *Comparison of Mesh Stiffness Analytical Methods.*

In these comparative studies, regarding work has been done: In Gu's Method, helical gears were represented by thin spur gears, mesh stiffness of gear pairs calculated based on analytical approach and verified by Load Distribution Program (LDP) in a study by Gu et al., 2015. In Chang's Method, analytical-FE combination method was proposed for mesh stiffness and load distribution calculation for helical gear pairs. The effect of helix angle, face width, tooth number and module of gear were investigated in a study by Chang et al., 2015.

In the Wang's Method, helical gears were investigated based on based on slice method and effect of profile modifications on stiffness were investigated in a study by Wang and Zhang, 2017. In the Wan's Method, analytical method was proposed to determine mesh stiffness of helical gears with crack formation. Effect of helix angle, face width and module on mesh stiffness were investigated in a study by Wan et al., 2015. In Feng's Method, helical gears were regarded as spur gears along gear width and mesh stiffness of gear pair was calculated by sum of stiffness of these spur gear slices in a study by Feng et al, 2018.

Since helix angel was added in comparative studies, the difference between the results of obtained analytical method and these studies can not be correlated. It was seen that increasing the helix angle yields an increase in mesh stiffness. The reason for that, helix angle in gears change the contact ratio that directly affects mesh stiffness according to studies by Mengjiao et al., 2018, Wan et al., 2015, Chang et al., 2015. It seems that differences between results obtained from the newly developed method and the methods used by Wan's, Wang's, Gu's and Cai's were caused by helix angle and methodology difference. Since in these methods, different analytical methods used instead of the Weber-Banaschek formulations. However, in the newly developed method, the Weber-Banaschek formulations were used based on slice approach including gear foundation effects obtained from empirical formulas proposed in a study by Sainsot et al., 2004.

It was also seen that the obtained analytical solutions resulted close to Chang's Method and also FEM since Chang's Method use FE corrections in addition to analytical approach when calculating mesh stiffness. The obtained analytical method resulted close to Feng's Method which uses slice approach through gear mesh when calculating mesh stiffness. The reason seems to use the same approach for the newly developed method and Feng's Method. However, the difference between the stiffness curves occur due to helix angle used in Feng's Method.

For tip relief modifications, KISSsoft software was used and transmission error was minimised for given gear pairs. It was observed that tip relief modifications have crucial impact on transmission error. For the gear meshes it was found that in order to accomplish maximum efficiency through gear pair, maximum transmission error should be applied to pinion and gear as a tip relief.

It was also observed that start point of tip relief is also crucial for lower transmission error and higher efficiency. When chosing the starting point from HPSTC, transmission error tends to decrease. In that scope, proper tip relief amounts were found and transmission errors are stated in Table 6.3.

Table 6.3 *Effects of Profile Modification on Transmission Error.*

Parameters	**First Gear Pair**		**Second Gear Pair**		**Third Gear Pair**	
	Pinion	Gear	Pinion	Gear	Pinion	Gear
Tip Relief Amount (μm)	1.01	1	10.5	10.5	20.7	21
Tip Relief Start Diameter (mm)	90.5	127	90.43	115	58.32	99
Peak to Peak Transmission Error without tip relief (μm)	2		2.4		8.1	
Peak to Peak Transmission Error with tip relief (μm)	1.6		1.3		2.2	

From Table 6.3, it was seen that tip relief starting diameters were chosen as HPSTC points which were close to pitch diameters. For selected gear pairs, peak to peak transmission errors were significantly minimised by tip relief modifications.

In the scope of contact stress investigations, in a study by Hwang et al., 2013, contact stress analysis for a pair of mating gears was carried out with respect to the AGMA standard and the FEM. It was stated that for a given gear pair, the FEM results higher contact stress than the AGMA standard. Hence results obtained from this thesis were found to be parallel to the Hwang’s study. In addition to that, in this thesis, the ISO standard and the analytical solution were proposed and results were discussed in Table 6.1. In a study by Qin and Guan, 2014, contact stress in spur gears was investigated by the FEM and the analytical method by including crack initiation. von-Misses stress distribution on gear contact during mesh was simulated by FEM. Fine meshes were generated at the area of the contact surface on the gear in order to have accurate results. Calculation of von-Misses stress according to the FEM yielded in higher values than Hertzian Theory as it was the same as in this thesis.

In this scope, in a study by Shehata et al., 2019, the models were created by using ABAQUS, LDP and KISSsoft programmes to make comparision between results of contact stress for gear pairs. The same gear pairs were created to compare the results in the same baseline. The outcomes showed that LDP resulted lower contact stress than KISSsoft and ABAQUS. Also KISSsoft resulted in higher contact stress than ABAQUS. Hence, the results seem to be contrast for the study by Hwang et al., 2013 and also in this thesis. However, in a study by Shehata et al., 2019, the calculation method used in KISSsoft was not stated. Also, it is known that application factors, which were also not stated in study, have crucial effects on results. Moreover, it is known that different calculation standards yield in different results. Therefore, the difference between the studies can not be correlated. In addition, results from both the AGMA 2001-C95 and the ISO 6336 were not compared with the FEM results of MASTA in literature before.

In this thesis, it was found that calculations according to the AGMA standard yielded in higher contact stress values than the ISO standard. Namely, lower safety factors were obtained in the calculations based on the AGMA standard. Also, contact stress calculation according to the FEM resulted in higher values than both the ISO and the AGMA standards.

In order to calculate contact pressure, main FEM studies were carried out by Patil et al., 2014b, Perez and Aznar, 2017, Mehta et al., 2018 in literature. In the scope of transmission error calculations, static and dynamic transmission errors were studied by Bruyere et al., 2015; Ma et al., 2016; Bozca, 2018; Shweiki et al., 2019; Sanchez, et al., 2019. From literature review, it was observed that analytical solutions give more accurate results on contact stress in less time.

The main aim of this thesis was to derive analytical approach and compare the results with existing softwares. Another aspect of this thesis was to compare the results of KISSsoft and MASTA (FEM Module) solutions. In literature review, it was observed that analytical formulations differ and the accuracy of available transmission softwares were not compared. Therefore, results of known transmission softwares were also investigated in this thesis. In addition to that, comparison of results from ISO and AGMA standards was also made. In this scope, for the calculation of meshes, the Weber-Banaschek formulation was used in the sense of summation of the matrices. Deformation matrices were created and instant gear meshes were found. The contribution of gear foundation was also considered in the mesh calculations by using Sainsot's Method. The results of mesh calculations were found similar to KISSsoft results as summarized in Table 6.4. For the calculation of contact pressure, created stiffness values were used. Load distribution was also found and given as graphs. The Hertzian contact theory was successfully applied to calculate contact pressure by using radius of curvatures of pinion and gear at instant angles. As a result, the comparision was given to see the difference between results as shown in Table 6.4.

***Table 6.4** Comparison of the Analytical Method and Transmission Tools.*

Gear Pair	Teeth	Analytical Result	KISSsoft Result				MASTA Result (FEM Module)		
		Maximum Contact Stress (MPa)	Max. Contact Stress (MPa)		Max.Root Stress (MPa)		Maximum Contact Stress (MPa)	Maximum Root Stress (MPa)	
			ISO	AGMA	Pinion	Gear		Pinion	Gear
First Gear Pair	45/63	770	730	824	252	235	918	220	202
Second Gear Pair	45/57	800	742	858	215	200	944	209	198
Third Gear Pair	29/49	1360	1280	1312	343	322	1317	320	301

In the scope of calculation of contact pressures, the comparision between the ISO 6336 and the AGMA 2001-C95 was also made and results were shown as graphs from Figure 5.40 to 45. It was seen that the AGMA 2001-C95 standard gave relatively more higher contact pressure results than the ISO 6336, since these two standards use different application factors during calculations. These factors related to dynamic loading, overload and sizing of gears tend to differ according to application in these two standards.

However, for the root stress, the FEM methods give relatively lower stress values. The reason for that is the differentiation in application factors from software to software. In addition to that, meshes of the root area are easy to be applied in more accurate way rather than contact flank of the gear meshes.

From Table 6.4, it is observed that results obtained from MASTA programme (FEM Module) tend to be higher than analytical solutions in the calculations of contact pressure. The reason for that the difference between the results are highly dependent on mesh sensitivity and load distribution factors. Meshes in contact area are otomatically developed by MASTA program within loaded tooth contact analysis module. Results obtained from developed method in this thesis were found close to outcomes obtained from the ISO standard which is commonly known calculation standard. Difference between maximum contact pressure obtained from the newly developed analytical method and the ISO-6336 standard that is based on experimental datas found as 5% ((770MPa-730 MPa)/730 MPa) for the first gear pair, 8% ((800 MPa -742 MPa)/742 MPa) for the second gear pair and 6% ((1360 MPa -1280 MPa MPa)/1280 MPa) for the third gear pair.

In order compare the results obtained from the newly developed method with experimental results, parameters established in a study by Patil et al, 2016, were used as summarized in Table 6.5.

Table 6.5 *Parameters Used for Comparative Study.*

	Pinion	Gear
Number of Teeth	20	20
Module (mm)	5	5
Center Distance (mm)	100	100
Torque (Nm)	45	
Speed (rpm)	30	

For these parameters stated in Table 6.5, experimental maximum contact stress was found as 735 MPa in a study by Patil et al, 2016. Calculations according to the newly developed method resulted 768 MPa as shown in Figure 6.2.

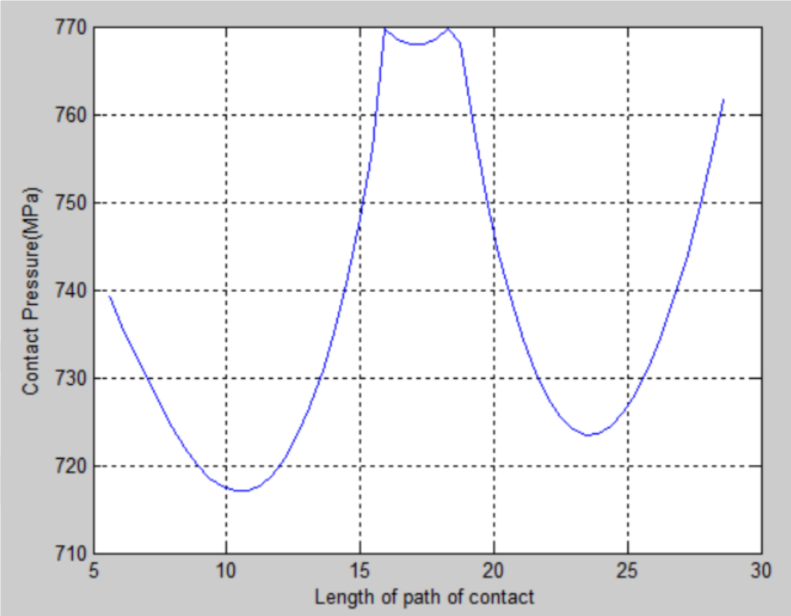

Figure 6.2 *Results Obtained from the Analytical Method.*

The difference between results obtained from the newly developed method and experimental results found as 4%.

CHAPTER 7

FUTURE WORKS

The following areas are worthy of further research that can be carried out beyond the scope of this thesis:

- Gear mesh stiffness foundation can be expanded to cover high contact ratio gears in which load sharing differ significantly through gear mesh.
- Mesh stiffness foundation was limited to symmetrical gear profile in this thesis so that can be expanded to cover gear mesh calculations of asymmetrical spur gears.
- In terms of profile modification, in addition to tip relief, crowning and tooth contact pattern optimization can be further studied by including misalignment effects.
- The study can be expanded to cover helical and bevel gears considering the system effects on gear mesh stiffness including bearings, misalignment, housing stiffness.
- Experimental study can be added to verify obtained analytical and MASTA(FEM) results.

CHAPTER 8

CONCLUSION

After investigating the contact pressure and transmission errors on the gear contact analysis for high speed gears, following results were drawn:

- Results obtained from the newly developed analytical method that is combination of the Weber-Banaschek and the Sainsot's methods for contact pressure were found close to the experimental results.
- Results obtained from the new analytical method of gear mesh calculations differ significantly where helix angle was added.
- MASTA solutions tend to be higher for gear contact pressure than analytical solutions obtained from the newly developed method and KISSsoft results.
- MASTA solutions tend to be lower for root contact pressure than the analytical solutions obtained from the newly developed method and KISSsoft results.
- MASTA solutions take larger computational time compared to the analytical solutions.
- The AGMA2001-C95 standard gives relatively higher results than the ISO 6336 standard.
- Transmission design software's give different results for the same gear parameters due to different application factors.
- Tip relief modifications yields in reduction of transmission errors for high power gears. Besides that, starting point for tip relief has crucial place for the modification in order to minimize transmission error.

REFERENCES

Bozca M., “Transmission error model-based optimization of the geometric design parameters of an automotive transmission gearbox to reduce gear-rattle noise”, Applied Acoustics 130 (2018), pp. 247-259.

Bruyere J., Gu X., Velex P., “On the analytical definition of profile modifications minimising transmission error variations in narrow-faced spur helical gears”, Mechanism and Machine Theory 92 (2015), pp. 257-272.

Bruyere J., Velex P., Guilbert B., Houser D.R., “An analytical study on the combination of profile relief and lead crown minimizing transmission error in narrow-faced helical gears”, Mechanism and Machine Theory 97 (2019), pp. 224-243.

Cai Y., “Simulation on the rotational vibration of helical gears in consideration of the tooth separation phenomenon (a new stiffness function of helical involute tooth pair)”, Journal of Mechanical Design 117(3) (1995), pp. 460-469.

Chaari F., Fakhfakh T., Haddar M., “Analytical modelling of spur gear tooth crack and influence on gearmesh stiffness.”, European Journal of Mechanics-A/Solids 28 (2009), pp. 461-468.

Chang L., Liu G., Wu L., “A robust model for determining the mesh stiffness ofcylindrical gears”, Mechanism and Machine Theory 87 (2015), pp. 93-114.

Chen Z., Shao Y., “Dynamic simulation of spur gear with tooth root crack propagating along tooth width and crack depth”, Engineering Failure Analysis 18 (2011), pp. 2149-2164.

Chen Z., Shao Y., “Mesh stiffness calculation of a spur gear pair with tooth profile modification and tooth root crack”, Mechanism and Machine Theory 62 (2013), pp. 63-74.

Dudley, Darle. W., Handbook of Practical Gear Design, McGraw-Hill, New York, (1984).

Feng M., Ma H., Li Z., Wang Q., Wen B., “An improved analytical method for calculating time-varying mesh stiffness of helical gears.”, Meccanica (2018) 53, pp.1131-1145.

Fernandez del Rincon A., Viadero F., Iglesias M., García P., de-Juan A., Sancibrian R., “A model for the study of meshing stiffness in spur gear transmissions”, Mechanism and Machine Theory 61 (2013), pp. 30-58.

Gu X., Velex P., Sainsot P., Bruye`re J., “Analytical investigations on the mesh stiffness function of solid spur and helical gears”, ASME Journal of Mechanical Design 137 (6): 063301 (2015).

Guan Y., Fang Z., Yang X., Chen G., “Tooth contact analysis of crown gear coupling with misalignment”, Mechanism and Machine Theory 126 (2018), pp. 295-311.

Guan Y., Yang X., Fang Z., Chen G., “Comparative analysis of three geometric models for crown gear coupling”, Mechanism and Machine Theory 136 (2019), pp. 269-283.

Hwang S. C., Lee J. H., Lee D. H., Hana S. H., Lee K. H., “Contact stress analysis for a pair of mating gears”, Mathematical and Computer Modelling 57 (2013), pp. 40-49.

Jia C., Fang Z., “Design and analysis of double-crowned high-contact-ratio cylindrical gears considering the load sharing of the multi-pair contact”, Mechanism and Machine Theory 131 (2019), pp. 92-114.

Jyothirmai S., Ramesh R., Swarnalatha T., Renuka D., “A finite element approach to bending, contact and fatigue stress distribution in helical gear systems”, Procedia Materials Science 6 (2014), pp. 907 - 918.

Kim S., Moon S., Sohn J., Park Y., Choi C., Lee G., “Macro geometry optimization of a helical gear pair for mass, efficiency, and transmission error”, Mechanism and Machine Theory 144 (2020), 103634.

Li R., Yang C., Lin T., Chen X., Wang L., “Finite element simulation of the dynamical behaviour of a speed-increase gearbox”, Journal of Materials Processing Technology 150 (2004), pp. 170-174.

Li S., “Effects of machining errors, assembly errors and tooth modifications on loading capacity, load-sharing ratio and transmission error of a pair of spur gears”, Mechanism and Machine Theory 42 (2007a), pp. 698-726.

Li S., “Finite element analyses for contact strength and bending strength of a pair of spur gears with machining errors, assembly errors and tooth modifications”, Mechanism and Machine Theory 42 (2007b), pp. 88-114.

Liang X., Zuo M., Pandey M., “Analytically evaluating the influence of crack on the mesh stiffness of a planetary gear set”, Mechanism and Machine Theory 76 (2014), pp. 20-38.

Lin T., Ou H., Li R., “A finite element method for 3D static and dynamic contact/impact analysis of gear drives”, Computer Methods in Applied Mechanics Engineering. 196 (2007), pp. 1716-1728.

Litvin F. L. and Fuentes A., *Gear Geometry and Applied Theory.* (2004).

Ma H., Pang X., Feng R., Song R., Wen B., “Fault features analysis of cracked gear considering the effects of the extended tooth contact”, Engineering Failure Analysis 48 (2015), pp. 105-120.

Ma H., Song R., Pang X., Wen B., “Time-varying mesh stiffness calculation of cracked spur gears”, Engineering Failure Analysis 44 (2014), pp. 179-194.

Ma H., Yang J., Song R., Zhang S. and Wen B., “Effects of tip relief on vibration responses of a geared rotor system”, Mechanical Engineering Science 228(7) (2013), pp. 1132-1154.

Ma H., Zeng J., Feng R., Panga X., Wen B., “An improved analytical method for mesh stiffness calculation of spur gears with tip relief”, Mechanism and Machine Theory 98 (2016), pp. 64-80.

Mao K., “Gear tooth contact analysis and its application in the reduction of fatigue wear”, Wear 262 (2007), pp. 1281-1288.

Mehta G., Somani M., Babu N., Watts T., “Contact stress analysis on composite spur gear using finite element method”, Materials Today: Proceedings 5 (2018), pp. 13585-13592.

Mengjiao F., Wang Q., Ma H., Li Z, “An improved analytical method for calculating time-varying mesh stiffness of helical gears”, Meccanica (2018) 53, pp. 1131-1145.

Pandya Y., Parey A., “Experimental investigation of spur gear tooth mesh stiffness in the presence of crack using photoelasticity technique”, Engineering Failure Analysis 34 (2013), pp. 488-500.

Patil S.S., Karuppanan S., Atanasovska I., Wahab A. A., “Contact stress analysis of helical gear pairs, including frictional coefficients”, International Journal of Mechanical Sciences 85 (2014a), pp. 205-211.

Patil S.S., Karuppanan S., Atanasovska I., "Frictional tooth contact analysis along line of action of a spur gear using finite element method", Procedia Materials Science 5 (2014b), pp. 1801-1809.

Patil S.S., Karuppanan S., Atanasovska I., "Experimental measuremenet of strain and stress state at the contacting helical gear pairs", Mesaurement 82 (2016), pp. 313-322.

Pedersen N.L., M. Jørgensen F., "On gear tooth stiffness evaluation", Computers and Structures 135 (2014), pp. 109-117.

Perez I.G., Aznar A.F., "Implementation of a finite element model for stress analysis of gear drives based on multi-point constraints", Mechanism and Machine Theory 117 (2017), pp. 35-47.

Perez I.G., Iserte J. L., Fuentes A., "Implementation of Hertz theory and validation of a finite element model for stress analysis of gear drives with localized bearing contact", Mechanism and Machine Theory 46 (2011), pp. 765-783.

Qin W.J., Guan C.Y., "An investigation of contact stresses and crack initiation in spur gears based on finite element dynamics analysis", International Journal of Mechanical Sciences 83 (2014), pp. 96-103.

Raghuwanshi K., Parey A., "Experimental measurement of mesh stiffness by laser displacement sensor technique", Measurement 128 (2018), pp. 63-70.

Sainsot P, Velex P, Duverger O., "Contribution of gear body to tooth deflections - A new bidimensional analytical formula", Journal of Mechanical Design 126 (2004), pp. 748-752.

Sánchez M. B., Pleguezuelos M., Pedrero J., "Influence of profile modifications on meshing stiffness, load sharing, and trasnsmission error of involute spur gears", Mechanism and Machine Theory 139 (2019), pp. 506-525.

Seol I.H., Kim D.H., "The kinematic and dynamic analysis of crowned spur gear drive", Comput. Methods Appl. Mech. Engrg. 167 (1998), pp. 109-118.

Shehata A., Adnan M. A., Mohammed O., "Modeling the effect of misalignment and tooth microgeometry on helical gear pair in mesh", Engineering Failure Analysis 106 (2019) 104190.

Shinde S.P., Nikam A.A., Mulla T.S., "Static analysis of spur gear using finite element analysis", IOSR Journal of Mechanical and Civil Engineering (IOSR-JMCE) (2009), pp. 26-31.

Shweiki S., Rezayat A., Tamarozzi T., Mundo D., “Transmission error and strain analysis of lightweight gears by using a hybrid FE-analytical gear contact model”, Mechanical Systems and Signal Processing 123 (2019), pp. 573-590.

Sirichai S., Howard I., Morgan L. and Teh K., “Finite element analysis of gears in mesh”, Fifth International Congress on Sound and Vibration (1997), Australia, pp. 869-876.

Sun Y., Ma H., Huangfu Y., Chen K., Che L., “A revised time-varying mesh stiffness model of spur gear pairs with tooth modifications”, Mechanism and Machine Theory 129 (2018), pp. 261-278.

Tobie T., Hippenstiel F., Mohrbacher H., “Optimizing gear performance by alloy modification of carburizing steels”, Metals 7(415) (2017).

Tran V.T., Hsu R.H., Tsay C.B., “Tooth contact analysis of double-crowned involute helical pairs shaved by a crowning mechanism with parallel shaving cutters”, Mechanism and Machine Theory 79 (2014), pp. 198-216.

Wan Z., Cao H., Zi Y., He W., Chen Y., “Mesh stiffness calculation using an accumulated integral potential energy method and dynamic analysis of helical gears”, Mechanism and Machine Theory (2015) 92, pp.447-463.

Wan Z., Cao H., Zi Y., He W., He Z., “An improved time-varying mesh stiffness algorithm and dynamic modelling of gear-rotor system with tooth root crack”, Engineering Failure Analysis 94 (2018), pp. 339-353.

Wang Q., Zhang Y., “A model for analyzing stiffness and stress in a helical gear pair with tooth profile errors”, Journal of Vibration and Control 23 (2) (2017), pp.272-289.

Wang Q., Chen K., Zhao B., Ma H., Kong X., “An analytical-finite-element method for calculating mesh stiffness of spur gear pairs with complicated foundation and crack”, Engineering Failure Analysis 94 (2018), pp. 339-353.

Weber C., Banaschek K., “The deformation of loaded gears and the effect on their load-carrying capacity.” London: DSIR(1949), Part 5.

Wen Q., Du Q., Zhai X., “An analytical method for calculating the tooth surface contact stress of spur gears with tip relief”, International Journal of Mechanical Sciences 151 (2019), pp. 170-180.

Wu Y., Wang J., Han Q., “Contact finite element method for dynamic meshing characteristics analysis of continuous engaged gear drives”, Journal of Mechanical Science and Technology 26 (6) (2012), pp. 1681-1685.

Wu Y.R., Tran V.T., “Transmission and load analysis for a crowned helical gear pair with twist-free tooth flanks generated by an external gear honing machine”, Mechanism and Machine Theory 98 (2016), pp. 36-47.

Ye S.Y., Tsai S.J., “A computerized method for loaded tooth contact analysis of high-contact-ratio spur gears with or without flank modification considering tip corner contact and shaft misalignment”, Mechanism and Machine Theory 97 (2016), pp. 190-214.